Dissertation

Water Treatment Residual and Vegetative Filter Strip Effects on Phosphorus Transport Dynamics

Submitted by

Colleen Heather Green

Department of Soil and Crop Sciences

In partial fulfillment of the requirements

for the degree of Doctor of Philosophy

Colorado State University

Spring 2004

Colorado State University

February 3, 2004

WE HEREBY RECOMMEND THAT THE DISSERTATION PREPARED UNDER OUR SUPERVISION BY COLLEEN H. GREEN ENTITLED WATER TREATMENT RESIDUAL AND VEGETATIVE FILTER STRIP EFFECTS ON PHOSPHORUS TRANSPORT DYNAMICS BE ACCEPTED AS FULFILLING IN PART REQUIREMENTS FOR THE DEGREE OF DOCTOR OF PHILOSOPHY.

Committee on Graduate Work

Department Head

Abstract of Dissertation

Water Treatment Residual and Vegetative Filter Strip Effects on Phosphorus Transport Dynamics

Agricultural practices are regarded as being sources of water and soil contamination. As a result, attention has been directed to management techniques of agricultural waste to minimize environmental impacts. Phosphorus (P) is recognized as a contaminant that causes adverse conditions in surface water bodies.

Alum is a coagulant that municipalities use in the water treatment process to remove turbidity, color, taste, and odor from raw water while augmenting sedimentation rates. Water treatment residuals (WTRs) are the waste material from water treatment facilities. They generally consist of sand, silt, clay, organic substances, and coagulated aluminum compounds. Previous research has found that WTRs directly added to soil lessened the threat of non-point source pollution due to reduction in available P. Sorption isotherms indicated the WTR P partitioning coefficient is 185 L kg^{-1} versus 27 L kg^{-1} for the unnamed Aridic Argiustoll soil. These results indicate that WTR application may be used beneficially as a best management practice to control P availability.

Experiments were conducted to determine i) if a WTR application rate for maximum P sorption could be identified, ii) if WTR applied to the soil surface would retain more P and leach less P than the soil alone, iii) if HYDRUS-1D model could predict total soil and WTR P transport, iv) if electron microprobe analysis using wavelength dispersive spectroscopy (EMPA-WDS) would identify Al-P complexes differently for various P concentrations, and v) if the Opus2Z model could elucidate how

vegetative filter strips (VFSs) and WTRs impact TP transport in the interaction of surface water and soil water.

A greenhouse experiment's MRP concentrations and Opus2Z model simulations indicated that a continuous layer of WTR over the soil with a depth of at least 5-6 mm was found to significantly reduce TP surface transport. Column experiments demonstrated that TP was mostly retained in the region of the WTR; this result was verified by the HYDRUS-1D model. The EMPA-WDS images illustrated P predominantly sorbed to the perimeter of a particle while P permeated the particle's interior as well as the interior at high P concentrations.

Colleen H. Green
Colorado State University
Fort Collins, Colorado
Spring 2004

Acknowledgements

I would like to thank Dr. Dean Heil for his contributions and mentorship in my pursuit of a career in soil chemistry. His unlimited support and assistance during my degree programs at Colorado State University are greatly appreciated. He has greatly impacted my life and provided me with tremendous opportunities for professional growth.

I would like to extend my love and gratitude to my family because without them I would not be who I am today. My parents, Sheryl and Allen Crawford, have been especially supportive throughout my education and for that I am grateful. Finally, I would like to thank my grandmother, Tina Machado Graham, because without her endurance in this country I would not have had the opportunity to pursue my dreams.

Table of Contents

List of Tables

List of Figures

Abbreviations

VFS, vegetative filter strip

WTR, water treatment residual

TP, total phosphorus (mg L^{-1})

TDP, total dissolved phosphorus (mg L^{-1})

MRP, molybdate reactive phosphorus (mg L^{-1})

STP, soil test phosphorus (mg kg^{-1})

p, probability level

EC, electrical conductivity (dS m^{-1})

CEC, cation exchange capacity ($cmol_c$ kg^{-1})

CCE, calcium carbonate equivalent (g kg^{-1})

DI, deionized water

EMPA-WDS, electron microprobe analysis using wavelength dispersive spectroscopy

SEM-EDS, scanning electron microscopy-electron dispersive spectroscopy

ICP-AES, inductively coupled plasma-atomic emission spectroscopy

USEPA, US Environmental Protection Agency

Chapter I

Introduction

Introduction

Agricultural practices are commonly regarded as being sources of water and soil contamination (Sharpley, 1995; Abbozzo et al., 1996; Burkholder et al., 1997). As a result, attention has been directed to management techniques for agricultural waste to minimize environmental impacts (Abbozzo et al., 1996; Gburek and Sharpley, 1998). Phosphorus (P) is recognized as a contaminant which causes adverse conditions in surface water bodies (Sharpley et al., 1994; Grobbelaar and House, 1995; Sims et al., 1998, Daniel et al., 1998; Parry, 1998). Public concern regarding the water quality impact of animal wastes that contain P (Satchell, 1996; 1997) has driven policy regulators to scrutinize its application on agricultural land. Stimulation of algal blooms by toxic dinoflagellates *Pfiesteria* has resulted in fish kills. Increased populations of this organism, due to increased nutrient concentrations in surface water bodies, have inspired environmental concerns (Burkholder et al., 1992).

Public awareness of environmental pollution has stimulated regulatory efforts to minimize water quality degradation. Environmental regulation has caused agricultural producers to design and implement more environmentally suitable practices. As a result, producers must comply with new fertilizer and animal waste application regulations to avoid over-application of P to cropland. Duda and Finan (1983) state that watersheds with intensive animal manure production have the greatest potential to pollute adjacent surface waters. Other sources of P include erosion and runoff from manure that has been land-applied and from uncovered livestock holding and manure stacking areas that has been applied to soil in rates excess of crop requirements (Sims, 1992).

Progress in controlling point source pollution has occurred since the passage of the Clean Water Act (CWA) in 1972. The CWA defines concentrated animal feeding operations (CAFO) as point sources of pollution and all other agricultural operations as non-point sources. Currently, the definition of a CAFO is undergoing review and may be changed so

that smaller operations and farms are required to implement water-quality programs that may be cost-prohibitive. Controlling and identifying non-point sources of pollution is an ongoing dilemma. Agricultural non-point source pollution is the major source of stream and lake contamination that has prohibited the Clean Water Act from accomplishing the USEPA's stated goals (Daniel et al., 1998). In order to effectively manage non-point sources of P, the origins and magnitude of P and the impacts that the hydrology of the area and land use have on the transport and export of P need to be identified (Dorioz et al., 1998). For example, a feedlot cattle study conducted by Erickson et al. (2002) demonstrated that supplementation of inorganic mineral P to typical grain-based diets is unnecessary. Their observations are pertinent because with less P intake by finishing feedlot calves, there can be less P released through animal wastes to the environment.

Cattle feedlots have been documented as important sources of runoff P from agricultural land (Dillaha et al., 1988). The impact of livestock waste on the physical and chemical states of soil has been published by Heckrath et al. (1995), Pote et al. (1999) and Edwards and Daniel (1993). The U.S. Environmental Protection Agency (USEPA, 2001) stated that approximately 132,000 Mg of dried manure were produced via the beef, dairy, swine and poultry industries. The number of animal units in the U.S. increased by 4.5 million (approximately three percent) between 1987 and 1992. During this time, the number of animal feeding operations decreased, indicating the trend of fewer producers with larger animal feeding operations.

In order to establish if a P water quality problem existed in northern Colorado, six samples were taken from various places and depths from a lagoon and measured for molybdate reactive P (MRP). The MRP in lagoon water ranged from 0.45 to 2.7 mg L^{-1}, indicating a high soluble P content. The water from this lagoon is used for irrigation purposes and is considered to be a P-fertilizer source. Soil P concentrations have not been tested to

determine if P has accumulated on the soil surface. The relationship of soil and soluble P is important because a small increase in surface water's P concentration (0.02 mg L^{-1}) can lessen its dissolved oxygen concentration while a change of the same magnitude would not impact soil because average total soil P levels in the western U.S. are approximately 600 mg kg^{-1} (Shackellette and Boerngen, 1984). The discrepancy between sensitive lake and soil P concentrations underscores the importance of determining how terrestrial P transport, storage and export mechanisms can be minimized so that the quality of surface water can be preserved. Evaluating whether the combination of vegetative filter strips (VFS) and water treatment residuals (WTR) can effectively reduce runoff P could help in finding a solution to non-point source P pollution.

Shreve et al. (1995) found that soluble P in field runoff can be reduced by the application of commercial alum. Basta and Storm (1997) stated that nutrient runoff from agricultural land treated with animal manures was reduced due to the land application of alum residuals. They found that when alum residuals were added directly to the soil, the threat of non-point source pollution was lessened due the reduction in available P. These results indicate that the application of WTRs may be used beneficially as a best management practice. Currently, federal guidelines do not exist for WTRs; however, its application may be limited by the USEPA or individual states (AWWA, 1987).

There is a need to identify critical P sources as well as balance the inputs and outputs. Identification of these areas will allow for routine soil tests and information regarding site susceptibility to P loss. The P index will aid in the assessment of site vulnerability (Lemunyon and Gilbert, 1993). The overall goal of effectively balancing P inputs and outputs while ultimately reducing P losses from agriculture to surface waters will include additional research and the education of agricultural producers. Site-specific P management strategies will best serve the public's and agricultural communities interests. Establishing strict

measures to reduce P transport to surface water bodies will affect smaller agricultural communities due to the expense to clean and monitor water quality.

The Colorado Legislature is trying to aid farmers and the related agricultural industries by allowing best management practices (BMP) to be voluntarily adopted as stated in the Agricultural Chemicals and Groundwater Protection Act (SB 90-126). This act promotes education and training the agricultural community in regards to more efficient usage of pesticides and fertilizers. With the voluntary adoption of BMPs, the State of Colorado is encouraging the prevention of water resource contamination while minimizing the need for mandatory regulations that may be too severe. Many agricultural sites need site-specific attention for pollution attenuation rather than compliance with overly strict laws.

Environmental regulation has expedited the necessity of agricultural producers to design and implement more environmentally suitable practices. An example of an environmental practice is applying P at crop requirement levels. Phosphorus is often the limiting constituent in eutrophication because nitrogen for algal growth can be obtained through atmospheric inputs. As a result, regulatory efforts are focused on reducing P inputs to surface waters.

In many soils, P content is greatest in the surface horizons, when compared to subsoil, due to greater biological activity, fixation of P, and most organic material residing in the surface layers. Soil parent material, texture, and management practices, structure, organic matter, clay type, and type of fertilizer source contribute to soil P content variation. Most soils contain approximately 50-75% inorganic P, but it can range from 10-90% (Chapman and Coombe, 1997). However, as organic P identification techniques improve more of this average value may be attributed to organic P. Vyas (1964), Gaur (1969), Nair et al. (1998), and Atalay (2001) have demonstrated P sorption by soils in the company of organic residues.

King et al. (1990) found that surface soil P concentration (0-0.5 m depth) was greater after effluent application at a field site versus a laboratory sorption experiment. Mansell et al. (1991), Nair et al. (1998), and He et al. (1999) have reported that P sorption occurs with soil depth for several soils. Phosphorus is more susceptible to movement through sandy soils with low P sorption capacities and with preferential flow through macropores and earthworm holes (Bengston et al., 1992; Sharpley and Syers, 1979); capacity for P leaching may be low due to predominately negatively charged surfaces and the complexing of Al and Fe by organic matter (Duxbury and Peverly, 1978; Miller, 1979). Phosphorus has been observed to move from soils high in P to subsurface waters, from which the P can reach surface water bodies (Sims, 1997).

The soil contains P in both organic and inorganic forms. Crop residues, manure, and humus are organic P forms. Manure can release P held in organic sources that can then dissolve and be transported more readily in runoff when improperly managed. Organic fertilizers are usually applied based on N recommendations, therefore P is commonly applied in excess of crop requirements. Dissolved P forms are considered immediately available for biological uptake (Nurnberg and Peters, 1984). Plants absorb inorganic P once it has been mineralized by microorganisms from organic matter. This conversion process begins with the break down of organic matter to the $H_2PO_4^-$ and HPO_4^{2-} ions. Phosphorus can also easily move when sediment-containing P is transported from agricultural land via runoff and erosion. This transport of P is the reason why agricultural industries are being targeted as areas in need of immediate attention, and regulation, for better nutrient management practices. The soil minerals that contain P are relatively insoluble but the P is not indefinitely fixed. The P held by soil minerals becomes available to plants over long periods of time.

Figure 1.1 illustrates the complexities of P transport. The increased focus on P has increased the need for environmentally relevant methods of P analysis in soil, water and other

materials. Sediment P can be a long-term source of P for aquatic biota (Carignan and Kalff, 1980). This research focused on runoff and soil P concentrations. The constituents determined include total P (TP), total dissolved P (TDP), molybdate reactive P (MRP) and soil test P (STP).

In this work, the term "sorption" rather than adsorption is used because the processes of chemisorption and precipitation cannot be distinguished by the methods used. Sorption is any process that removes ions from solution to a solid phase. The sorption of phosphate to hydrous aluminum oxides is termed chemisorption. It is defined as the process in which singly coordinated hydroxyl groups are replaced with phosphate after which the complex restructures into a stable double bridge between cations (Bohn et al., 1985). Precipitation is considered to be the removal of ions from solution to form a new solid phase. Both chemisorption and precipitation processes can occur at the interface between solution and a solid phase. The literature lacks clarity in how to differentiate adsorption and precipitation processes and current analytical methods do not distinguish between them.

The following chapters identify the impact of VFSs and WTRs on surface transport of soluble P. Experiments were conducted to determine i) if a WTR application rate for maximum P sorption could be identified, ii) if WTR applied to the soil surface at a potentially beneficial rate would retain more P and leach less P than the soil alone, iii) if the HYDRUS-1D model can predict total soil and WTR P transport, iv) if electron microprobe analysis using wavelength dispersive spectroscopy (EMPA-WDS) could identify P-Al complexes differently for various soluble P concentrations and, v) if the Opus2Z model could improve the understanding of how VFSs and WTRs impact TP transport in the interaction of surface water and soil water.

The greenhouse experiment incorporates the effects of WTR and VFS on soluble P surface transport while a laboratory column experiment analyzes effluent and soil P

concentrations from a vertical perspective. With model components fit to the conditions under which the column experiment occurred, the HYDRUS-1D model prediction was measured against experimental data. Additional soil and WTR characterizations in conjunction with soluble P provided insight as to what can be expected from their interactions. The EMPA-WDS images elucidated how P associates with a soil particle at varying soluble P concentrations. Finally, a sensitivity analysis of the Opus2Z model was performed to improve the understanding of how VFSs and WTRs impact TP surface transport including the interaction of soil water and surface water. Altogether, greenhouse and laboratory experiments and model simulations provided an understanding of how VFSs and WTRs affect P transport.

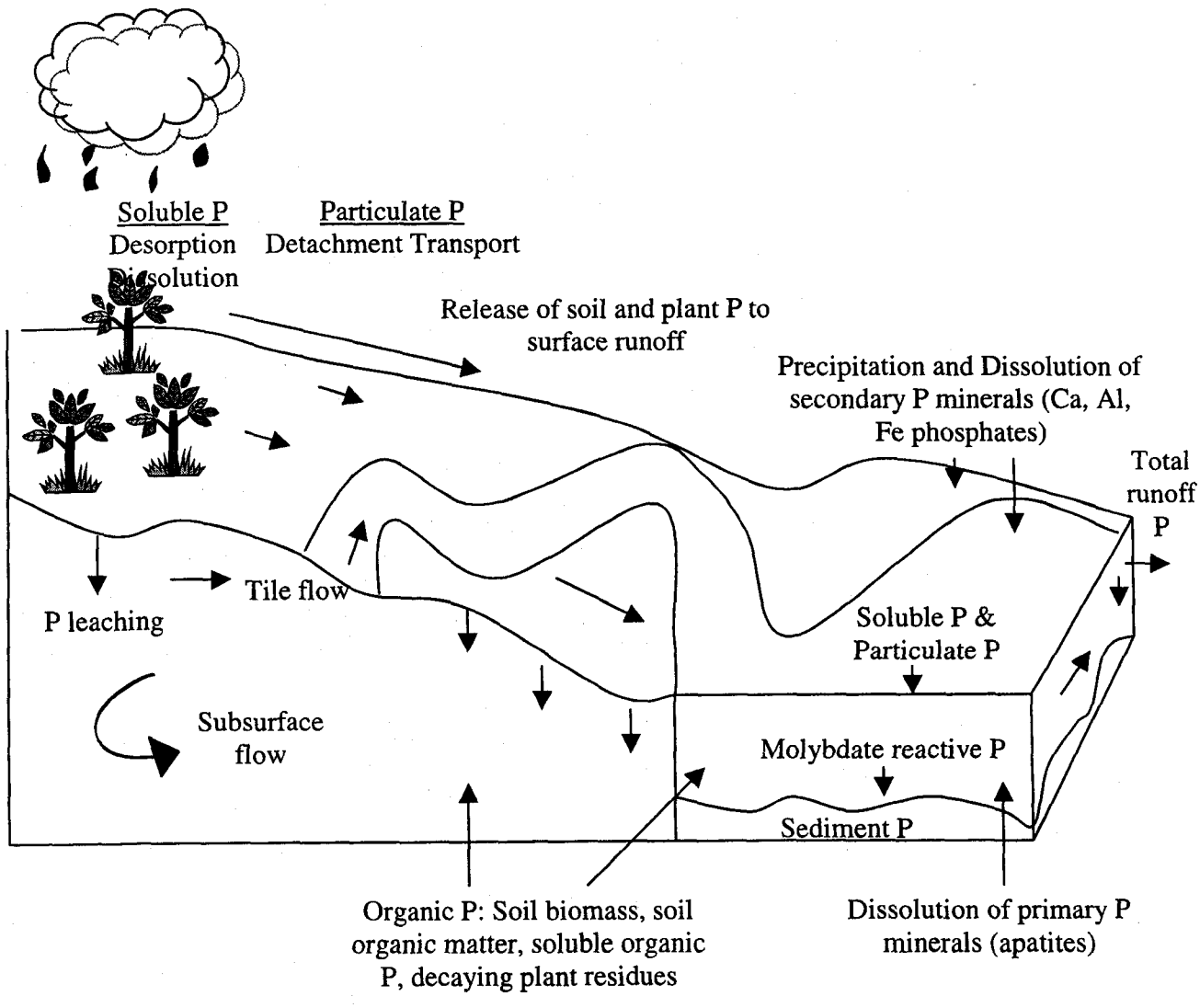

Figure 1.1. Phosphorus transport system (adapted from Sharpley and Halvorson, 1994).

Chapter II

Water Treatment Residual and Vegetative Filter Strip Effects on Phosphorus Runoff: A Greenhouse Study

Introduction

Agriculture is the main contributor of nonpoint source P. Phosphorus is considered to be a contaminant when it is applied in excess to crop requirements because it can be transported by sediment or water to nearby surface water bodies. Eutrophication can occur when P concentrates in water and encourages algal growth. As a result, management programs are being designed to minimize P transport to surface waters. This chapter focuses on the utilization of vegetative filter strips and water treatment residuals to minimize surface transfer of P.

Vegetative Filter Strips

Increasing interest in P-based nutrient management emphasizes the importance of understanding P behavior in soils with vegetative filter strips (VFS) and using water treatment residuals (WTR), the coagulant-sediment waste from a fresh-water treatment plant. Vegetated filter strips are widths of vegetation that can act as a filter for sediment and nutrient retention (Dillaha et al., 1989). They reduce contaminants in surface runoff from agricultural land (Schmitt et al., 1999; Gallimore et al., 1999; Magette et al., 1989; Dillaha et al., 1988). The USDA-NRCS began the National Buffer Initiative in 1997, which constituted establishing two million miles of conservation buffers in the U.S. by 2002. In the past, VFS efficacy focused on the removal of solids from agricultural areas, including feedlot runoff (Dillaha et al., 1989; Dillaha et al., 1988; Young et al., 1980; Magette et al., 1986). The design of a VFS is usually site specific and based on experience and limited data; therefore, the dimensions of the VFS for effective retention and removal of nutrients and sediments are not definitive (Fasching and Bauder, 2001).

There are few references that provide VFS data for minimally irrigated conditions in semi-arid and arid environments (less than 30-35 cm precipitation; Fasching and Bauder, 2001). We need more data on how VFS design, vegetation, and management impacts P transport and the effect that WTR have on P sorption and subsequent reduction of dissolved solid transport and P runoff in these environments. Due to changing USEPA regulations (2001) for confined animal feeding operations, it is imperative that the regulations are based on data that relates to regions with similar climates since these best management practices are site specific.

Due to the numerous P fractions that could be measured, the components selected for analysis for this research are shown in Figure 2.1. Phosphorus can move as soluble P ($H_2PO_4^-$ or HPO_4^{2-}) in surface (runoff) or groundwater (leaching). It can become sorbed to sediment (measured by soil test P analysis). Phosphorus can be leached or become desorbed, however, it typically remains in the top 15 cm of soil. Plants can absorb soluble P that can be released later when plants or organic amendments (i.e. manure) decompose.

Water treatment residuals are a waste product of water treatment flocculation processes. They are disposed in landfills or are stored on site unless a beneficial use is identified. Therefore, applying it at an optimum rate to sorb more P within the VFS will benefit the agricultural operations that contribute P to the environment as well as economically benefiting municipalities. The application of environmentally safe materials that can reduce the non-point P source threat to watersheds may be a practical approach to effectively limiting available soil P. Water treatment residual utilization to reduce P loading appears hopeful, but additional characterization is required to identify

the impact of WTR on soil and runoff water quality. Ippolito et al. (1999) found that WTR application to soils high in P could beneficially sorb excess soluble P.

The potential for sediment and dissolved P transport in runoff increases as soil P content increases. Sources of sediment P include eroding surface soil, streambanks, and channel beds. Therefore, these sources of sediment also control sediment P transport. Preferential transport of clay-sized particles means that the P content and sorption capacity of eroded particulate matter is greater than the overall soil P would indicate. Phosphorus transport can occur as particulate or dissolved P. Most of the P transported from cultivated land occurs as particulate P while most of the P in runoff from non-cultivated lands is in the dissolved form (USDA-SCS, 1994).

Water Treatment Residual and Alum

Alum [aluminum sulfate: $Al_2(SO_4)_3 \bullet 14H_2O$] is the precursor to the WTR byproduct. Alum is a coagulant that municipalities use in the water treatment process to remove turbidity, color, taste, and odor from raw water while augmenting sedimentation rates. The WTR waste material can contain colloids from the raw water and the products of coagulation including amorphous aluminum oxides (ASCE and AWWA, 1996) from when the alum is combined with lime during the water treatment process. Water treatment residuals can contribute to soil aggregation due to the presence of aluminum and iron oxides and contribute to an increased water holding capacity because of a total organic carbon content of approximately 30 g kg^{-1} (Elliott and Dempsey, 1991).

Water treatment residuals generally consist of sand, silt, clay, organic substances, and coagulated aluminum compounds. They have low nutrient contents and metal

concentrations that are similar to natural soils (Dayton and Basta, 2001; Fortenberry et al., 1994). Elliott and Singer (1988) stated that WTRs do not have an adverse impact on the environment unless the source itself is contaminated. However, since WTR sources vary, the WTR should always be analyzed before being used. With the application of WTR to land, no increases in dissolved solids or extractable Al have been observed in surface runoff (Gallimore et al., 1999) nor have increases in salinity or heavy metals in soils been noted (Peters and Basta, 1996; Basta and Storm, 1997).

The potential benefits of applying WTR to the soil include increased soil moisture retention and aeration (Bugbee and Frink, 1985) and greater soil aggregation and soil water holding capacity (Rengasamy et al., 1980). Shreve et al. (1995) found that soluble P in field runoff can be reduced by the application of commercial alum. Basta and Storm (1997) stated that nutrient runoff from agricultural land treated with animal manures was reduced due to the land application of alum residuals. They found that when alum residuals were added directly to the soil, the threat of non-point source pollution was lessened due to the reduction in available P. These results indicate that the application of WTRs may be used beneficially as a best management practice.

The addition of WTRs to land can reduce the movement of soluble P due to the binding of soluble P by aluminum oxides present in the WTR (Gallimore et al., 1999; Peters and Basta, 1996). Since alum is the precursor to the WTR by-product, it obviously contains a sufficient amount of Al that can bind P. Aluminum content is positively correlated with the P fixation capacity in soils (Freese et al., 1992). Ippolito et al. (2003) stated that P was bound by Al as determined by SEM-EDS images of a mixture of biosolids and WTR. If micropores are present within WTR aggregates, this would impact

the rate of sorption and desorption of P. Phosphorus sorption to a particle's exterior is faster than its sorption to a particle's interior (Selim, 1998). Therefore, P held within a particle would take longer to desorb than P bound to the exterior. Scanning electron microscopy-electron dispersive spectroscopy images can distinguish whether P lies within the particle's interior and/or exterior. Occlusion of P to the particles may occur accounting for an additional mechanism of P sorption to the particle's exterior.

Moore and Miller (1994) established that insoluble Al-phosphate minerals or stable surface complexes are formed by the complexation of Al and orthophosphate ions. Soil or sediment that contains Al, Fe or Ca can readily adsorb or precipitate soluble P (Hsu, 1964; 1976). Phosphorus in solution can be adsorbed and precipitated by iron and aluminum oxides or hydrous oxides (Stumm and Morgan, 1981; Tisdale et al., 1985). Insoluble P compounds are formed between calcium and soluble P (Lindsay, 1979). Since the unnamed Aridic Argiustoll being used for this research is basic, Al solubility is not of concern in this study (Sparks, 1996). The soil being used for this study is also calcareous and, therefore, P removal from solution may also occur due to adsorption and precipitation reactions induced by Ca^{2+} ions in solution. A study conducted by Tunesi et al. (1999) demonstrated that Ca-ion activity in solution is primarily accountable for the formation of insoluble Ca-P phases. Pote et al. (1996) confirmed that there is a linear relationship between soil test P and runoff P. Therefore, in order to minimize P loading either the source of the P must be lessened or the sorption capacity of the material through which the P moves must be increased. Freese et al. (1992) suggested increasing the surface area onto which the P comes in contact with by using Al-bearing materials, such as WTRs.

The United States annually produces approximately 0.35 million dry Mg of WTR. This by-product can be released to sanitary sewers, lagooned or dewatered and disposed in landfills (Elliott et al., 1990) at great expense to municipalities. The requirement for disposal space alone suggests the need for identifying a beneficial use for WTRs. Currently, federal guidelines do not exist for WTR application to agricultural lands; however, its application eventually may be limited by the USEPA or individual states (AWWA, 1987).

Potential disadvantages of WTR application include P deficiency in plants due to labile-P sorption by the amorphous aluminum oxides in WTR. When WTRs were applied at 10 g kg^{-1} soil, Rengasamy et al. (1980), found that P uptake was reduced but at lower rates corn (*Zea mays*) yields were increased and soil properties improved. Bugbee and Frink (1985) determined that P availability was reduced and lettuce (*Lactuca sativa*) yields were decreased as a result of using WTR as an amendment to potting soil at rates of 0 to 670 g kg^{-1}. Heil and Barbarick (1989) found that WTR fixation of P resulted in decreased yields of sorghum-sudangrass (*Sorghum bicolor* sudanense) when WTR additions were greater than 15 g kg^{-1}. Skene et al. (1995) surficially applied WTRs to sand at rates of 20, 40 and 100 g kg^{-1} resulting in the decreased growth of broad beans (*Vicia faba*). Dayton and Basta (2001) found that alum that contained water soluble P greater than 580 ug L^{-1} supported growth but produced inadequate tissue P in tomatoes. Elliott and Singer (1988) showed that WTRs could increase the soil pH resulting in a decrease in metal (Al and Mn) toxicity allowing for increased tomato (*Lycopersicon esculentum*) growth. Ippolito et al. (1999) did not observe P deficiency symptoms in conjunction with WTR application to blue gramma (*Bouteloua gracilis* H.B.K. Lag) and

western wheatgrass [*Pascopyrum smithii* (Rydb.) A. Love]. After one year of alum- and polymer-WTR application to a forest at rates of 0.8 to 2.5 g kg^{-1}, Bugbee and Frink (1985) and Novak et al. (1995), found that the amendments did not impact the growth or nutrient content. Geertsema et al. (1994) state that by determining an optimum WTR application rate, P plant deficiencies can be avoided.

By applying WTR for manure P retention to inhibit P movement into waterways, the WTR would be beneficially used instead of going to landfills. While WTR beneficial use decreases the amount of landfill space, it must also function within ecosystem and land use constraints. Plant availability of P should be considered when applying a material based on plant-N requirements to avoid excessive P application. Therefore, it is important to characterize a specific WTR to determine its limitations and potential applications relative to the soil's chemical and physical characteristics.

A study conducted by Tate et al. (2000) characterized total P and total suspended solids (TSS) in runoff from 10-m buffer strips on irrigated pastures in the Sierra Nevada foothills. Their results indicate that 15% and 69% of irrigation water applied to sprinkler and flood irrigated pastures became runoff. The buffer strips reduced total P and TSS loads with flood irrigation scheme but failed to reduce total P concentration.

The main concept presented here is that the VFS and WTR would remove solution-phase and sediment-sorbed P from the lagoon water that may serve as a potential irrigation source. With the nutrients reduced to an acceptable level, the water would not be saturating the surface sediments with P, over fertilization would be less likely to occur, and excess P would not be transported to nearby waterways when water flow was

sufficient. When runoff occurs, having the WTR and VFS *in situ* could minimize P transport in overland flow.

Since previous research has shown that WTR can be used effectively for P retention, with all conditions being equal I speculate that increasing the WTR rate will sorb more P to a certain extent. The effective depth of interaction between the surface material and runoff will limit the addition of WTR. Any topographical variation such as an accumulation of vegetative residue on the surface or mass of WTR (due to its alum coagulation properties) not evenly distributed on the surface will impact runoff flow paths thereby impacting the ability of the WTR to retain P from the runoff. The flow velocity and VFS box slope will also affect runoff dynamics and the WTR's P retention ability. Another sampling aspect to consider is that only 1.0 g of soil or 1.0 to 2.0 mL of water was analyzed per sample. Since soil was collected in a manner to have minimal effects on flow, a 100% of the cross sectional area was not sampled. The same is true for the runoff. It was collected at one location that was 2.5 cm in diameter. The portion of the sample that was analyzed for P came from a composite of the runoff collected from the one sampling location.

Objectives

The objectives to be addressed in this chapter are:

- Determine if a WTR rate that allows for maximum P sorption can be identified through MRP surface runoff analysis from a greenhouse experiment.
- Use Opus2Z model simulations to improve the understanding of how VFSs and WTRs impact surface water and soil water interaction in relation to TP transport.

Model Simulation of the VFS System

Previous research has provided understanding of mechanisms controlling soil P. The hydrologic controls linking spatially variable P sources, sinks, and transport processes within a watershed are not as well understood. Within a watershed runoff is usually generated from a limited number of source areas. These source areas are a function of antecedent moisture conditions, topography, duration and intensity of water input, temperature, and soils (Gburek and Pionke, 1993). Inclusion of hydrologic controls is imperative to the understanding of P export from agricultural watersheds (Smith, 1992).

Opus is a long-term simulation model that was originally developed for small agricultural areas to simulate a crop growth, root-zone soil, heat flow in soil and chemical additives on small, homogeneous catchments. Opus is an option for scientists interested in agricultural hydrology in that it has relatively advanced approaches to water movement and chemical transport simulations. Opus simulates infiltration and runoff by using the Smith-Parlange infiltration model (Parlange and Smith, 1978). Hortonian flow is estimated whenever surface boundary conditions turn into ponding.

This model has been adapted for this research and is now referred to as Opus2Z. This model simulates soil water and transport dynamics impacted by overland flow with a temporal and spatial distribution that is not addressed by any other model. The Opus2Z model allows the simulation of the interaction of adjacent soil/crop areas so that we have the ability to determine the impact of buffer strips. The weather simulation requires daily maximum and minimum temperatures, daily radiation and rainfall.

Opus uses Richards' (1931) equation to describe flow in the unsaturated soil profile [eq. 2.1]. Richards' equation [2.1] is solved for positive and negative surface flux boundary conditions.

$$\frac{\partial \theta}{\partial t} = \frac{\partial}{\partial x}\left[K\left(\frac{\partial h}{\partial x} + \cos\alpha \right)\right] - s \qquad [2.1]$$

where

θ is the volumetric water content ($L^3\ L^{-3}$),

t is time (T),

x is the soil spatial coordinate (L),

K is the unsaturated hydraulic conductivity function ($L\ T^{-1}$),

h is the water pressure head (L),

α is the angle between the flow direction and the vertical axis, and

s is the sink term ($L^3\ L^{-3}\ T^{-1}$).

This model allows for multiple soil horizons, different crops, a slope, and a P Langmuir sorption isotherm [eq. 2.2]. The Langmuir sorption equation is (Atalay, 2001; Pierzynski, 2000):

$$\frac{C_l}{C_s} = \frac{1}{kS_{max}} + \frac{C_l}{S_{max}} \qquad [2.2]$$

where

C_l is the concentration of soluble P after 24 h equilibration (mg L^{-1}),

C_s $=S'+S_o$, the total amount of P retained (mg kg^{-1}),

S'=P retained by the solid phase (mg kg^{-1}),

S_o = P originally sorbed on the solid phase (previously adsorbed P (mg kg^{-1})),

k is the Langmuir partitioning coefficient (mL g^{-1}), and

S_{max} is the P sorption maximum (mg kg^{-1}).

A linear regression analysis may be performed between C and C/C_s to derive the values for k and S_{max} as the slope and the intercept, respectively (Atalay, 2001).

The parameters in eqs. [2.3] and [2.4] must be estimated from the experimental data in most cases (Butters and Duchateau, 2002). However, the parameter values used were selected to yield the correct water content and flux as observed during the experiment. The van Genuchten (1980) model of pressure-saturation requires the residual (θ_r) and saturated volumetric water contents (θ_s). Figures 2.2 and 2.3 illustrate the plant available water range as determined from eq. [2.3] The mathematical expression used to graph plant available water is:

$$\Theta = \frac{\theta - \theta_r}{\theta_s - \theta_r} = \left[1 + (\beta h)^n\right]^m \qquad [2.3]$$

where

Θ is the degree of saturation,

β is the curvature parameter in the soil-water characteristic function

h is the pressure head,

n is a fitting parameter related to the tortuosity and connectivity of the capillary tubes, and

m is a fitting parameter.

The exponents in eq. 2.3 are related in the manner:

$$m = 1 - 1/n \qquad [2.4]$$

The strong surface tension of water that is locally continuous through the soil at a particular water content, the lower the water content, the smaller the effective radii of the water surface at granular interfaces. It is this gradient that causes water to move in the soil. Most models today treat soil-water movement using concepts of storage filling and draining. Opus describes the relation of water content to matric potential by using an expression similar to that of van Genuchten (1980) but relates directly to the Brooks and Corey relation (1966).

The Opus model requires five parameters to describe the hydraulic properties a soil horizon including: λ (a pore-size distribution parameter that is the log slope of the soil hydraulic characteristic), θ_s (the content of natural saturated water), θ_r (the content of residual soil water), ψ_b (the air-entry parameter for soil capillary characteristic function in mm) and K_s (which is the effective saturated hydraulic conductivity in mm min^{-1}) (Smith, 1992).

Material transport of labile P in the soil and on the surface is included in this model. Plant growth and response to radiation, temperature, nutrient and water availability are simulated mechanistically. Other hillslope models limit the range of interactions, especially in relation to transport simulation and the interaction of unsaturarated and saturated flow (Smith, 1992).

In Opus2Z, the surface water transport of nutrients is treated with a dynamic convective transport solution (Havis et al., 1992), parallel with the solution of convective transport of sediment, if any. Material may be leached from plants and surface residue; this is then added to surface water or to soil water influx. Because this research's focus was overland flow dynamics, surface water interacts dynamically along its flow path with

chemicals that have been selected to be transported. This interaction includes suspended particles and those that lie on the surface soil. The chemical outflow is summed at the end of the runoff event for both of the sorbed and dissolved forms. The equation for the surface transport of the dissolved solute is (Smith, 1992):

$$\frac{\partial(AC_R)}{\partial t}+\frac{\partial(QC_R)}{\partial x}=w[\omega(C_R-C_B)-f(C_R)+RC_w] \qquad [2.5]$$

in which

A is the cross sectional area of flow,

x is the distance along the flow path,

w is the width of flow,

f is the infiltration rate,

Q is the discharge [$L^3 t^{-1}$],

R is the rainfall rate,

C_R is the concentration in the surface water,

C_B is the concentration in the surface soil,

C_w is the concentration of the solute in liquid soil water [kg L^{-1}], and

ω is the film diffusion coefficient (mm min^{-1}).

The corresponding equation for the sorbed solute is (Smith, 1992):

$$\frac{\partial(AC_sC_{aR})}{\partial t}+\frac{\partial(QC_sC_{aR})}{\partial x}=w(\beta dC_{as}-e_DC_{aR})+q_sC_e \qquad [2.6]$$

in which

C_s is the concentration of particle size class in surface water,

C_{aR} is the concentration of sorbed chemical on suspended sediment,

C_{as} is the concentration of sorbed chemical in soil,

β is the relative particle class weighting based on particle specific surface,

d is the gross splash and erosion detachment rate of particle class,

e_D is gross deposition rate for particle size class (negative for erosion), and

q_sC_e is an external supply (if any) of sorbed material.

The equation [2.6] is applied to each of a range of particle size classes that cover the distribution of particles in the surface soil and sediment. Sediment particle size distribution in space and time is from the sediment transport equation (Bennett, 1974):

$$q_s(x,t)_k = \frac{\partial}{\partial t}(aC_{sk}) + \frac{\partial}{\partial x}(qC_{sk}) - d(x,t)_k \qquad [2.7]$$

in which

C_s is the sediment concentration,

a is the cross sectional area of flow (m^2)

q is water discharge per unit width ($m^2\ min^{-1}$)

d is the rate of erosion or deposition at the bed ($m\ min^{-1}$)

q_s is the local input of sediment ($m^3\ m^{-2}\ min^{-1}$), and

k is the subscript that refers to a particle size class.

With practically no erosion in my experiments, this part of the model was not used.

The surface water convective transport equation is numerically solved during runoff for each time step after which the flow velocity and its mean depth are available at the present and past time step. In order to accommodate the injected overland flow in this experiment, the plot experiments were treated like border irrigation plots, with a given P in the irrigation water.

Within the program, the flow length of each element is divided into 10 computational increments. The number of segments is $\sqrt{2L}$, with L in m. Opus divides

the soil profile into three sectors for the dynamics of residue and nutrients: a litter layer at the surface, a microbiologically active soil layer, and the deepest layer (Smith, 1992).

Leaching allows for the downward movement of solution while dispersion processes transport solution through the surface and subsurface materials. Macropore flow is considered to be the solution that is transported due to the presence of interconnected pores or channels in the soil subsurface created by vegetation (roots) or inherent as a physical property of a material matrix. Figure 2.4 illustrates the phosphorus processes that were preferred to occur in the model simulations.

Usually in Opus2Z, hillslope geometry is interpolated between any input points resulting in an input profile description at any location where the rate of change of slope changes. For this research, the entire profile is the same with a constant slope and depth because a single specification was made resulting in a uniform slope and the soil depth does not change spatially.

Materials and Methods

Soil Collection Site

The soil used is an unnamed Aridic Argiustoll that was collected from the top 15 cm adjacent to a feedlot in northern Colorado (Table 2.1). The site where the soil was collected did not have prior manure applications and had not received runoff from cattle areas. The WTR (Table 2.1) was collected in fall, 2001 from the Fort Collins Water Treatment Facility.

Greenhouse Experiment Solution

Distilled water was spiked with 10 mg L^{-1} P because it was considered to provide observable differences between runoff events and the soil/WTR concentrations. The soluble P source was concentrated phosphoric acid. I decided to use an amount that could provide observable differences. In a study comparing aluminum-containing residuals and their influence on P, Haustein et al. (2000) found that more than 85% of the runoff P was in the dissolved form. Therefore, it seemed reasonable that the P used for this greenhouse study be immediately available.

Greenhouse Vegetative Filter Strip (Soil) Box

Although an indoor soil box is a small-scale imitation of the field, in the protocol for the National Research Project for Simulated Rainfall-Surface Runoff Studies (SERA17, 2001), it is stated that an indoor soil box runoff will have a similar relationship between soil P and surface runoff P when compared to a field site that is extensively tilled. Two box designs were originally configured. This was in an effort to minimize the amount of soil that would be needed. The two boxes differed in length by 1 m; a 1 m by 1 m x 15 cm box and a 2 m by 1 m by 15 cm box were constructed. Two weeks were allowed as a settling time for the soil before runoff events took place to determine which was the better design. Because the inflow concentration equaled the outflow concentration more quickly with the shorter box, the longer box was selected for further runoff events.

The longer experimental box was constructed of two main pieces and two different layers of soil retaining materials. The base piece was a 2 m by 1 m frame

constructed of pine (Figure 2.5). The frame had cross members approximately every 50.8 cm. Attached to this frame was 14 gauge, welded wire field fencing. This wire had gap spacing of 5 cm by 10 cm. The wire was attached to the frame with staples. The wire served as a support for soil retention (Figure 2.5).

The upper piece was a 1 m by 2 m box constructed of 5 cm by 15 cm pine. The upper box was attached to the lower frame. Once the two boxes were securely joined, a 0.2 m by 0.12 m piece of PolyPro 55 weed barrier was laid into the box, resting on top of the field fencing. The weed barrier was then secured to the upper box with galvanized poultry staples. The weed barrier was for soil retention while allowing soil solution to drain freely. The weed barrier was made from woven needle punched polypropylene, was 28 mils thick, and had a permeability of 23.5 L min^{-1} cm^{-2}.

Three divets were cut onto the surface of the box at the bottom. Two of the holes were 3.8 cm in diameter and were approximately 7.6 cm from either side of the box. These holes were cut so overflow would not occur and they helped prevent contamination of the sample from the middle of the box. A hole 5 cm in diameter was placed in the center at the bottom of the box where runoff sample collection occurred. A 5-cm diameter polyethylene funnel was secured with silicone sealant into the groove so that the runoff could be collected into a bottle. Figure 2.5 shows the box and its components.

Six VFS boxes (2 m by 1 m by 15 cm) were divided in half (2 m by 0.5 m by 15 cm) leaving the water transport path as long as possible while minimizing the amount of soil required per box (Figure 2.5). Within the 2 m by 0.5 m by 15 cm box an inner area partition was formed by installing metal dividers on the sides pushed 2.5 cm into the soil surface so that only the surface flow is restricted; they were 23 cm apart, 1.8 m long, and

were approximately 12.7 cm from the wood frame. The head barrier was placed at the top of the two side barriers. This divider was also pushed 2.5 cm into the soil surface. With the surface flow barriers in place, the manifold rested on top of the barrier near the top of the box and was checked for balance to ensure that the water was distributed evenly.

The WTR was not sieved before being applied to the soil surface therefore, rocks and coagulated colloids were present when the WTR was distributed potentially resulting in topographical variations. The WTR rates differed in their depth (discussed above) and distribution. The WTR rates above 16 Mg ha^{-1} covered the soil surface entirely. The WTR used was collected from the Fort Collins Water Treatment facility.

Overland Flow Manifold

An overland flow design was desired for this study because northern Colorado is considered a semi-arid area in which less than 30 cm of rain are received annually so rainfall simulation would not produce adequate runoff for continual P evaluation. Also, in an effort to remediate lagoon water effectively and cost-efficiently, a manifold system would best disperse the water that contains sediment versus a sprinkler system. With contact-time greater with the sediment and vegetation, more P can be removed from the water.

An overland flow manifold system was designed so that surface sheet flow could be introduced at the upper end of the VFS. The manifold system had 11 holes that were 0.28 cm in diameter drilled into 3.8 cm schedule 40 PVC pipe with capped ends. A port for the pump-hose connection to the manifold was located in the middle of the manifold

so that water flowed equally to either side. An adjustable hose clamp controlled the water flow rate into the manifold. During overland flow runoff simulation, three holes on either side of the manifold, that were closest to the edges of the box, were plugged with rubber stoppers so that the flow was concentrated to the middle of the VFS. Five holes released the water into the 23-cm swath of VFS. This inner section application was necessary so that the water would not be lost through the wood frame:soil interface (i.e. to avoid edge-effects). A runoff event flow rate of 0.1 L sec^{-1} was selected because water could reach the end of the box with this rate.

Greenhouse Experiment Vegetation

Crested wheatgrass *(Agropyron cristatum* Ephraim), western wheatgrass *(Pascopyrum smithii* Rosanna), and streambank wheatgrass *(Elymus lanceolatus ssp. psammophilus* Sodar) were planted in each box. These species were selected because they are cool season, long-lived, drought tolerant, perennial grasses. The crested wheatgrass is a bunch grass while the streambank and western wheatgrasses are strongly rhizomatous sod-formers.

The VFS boxes were seeded with two times the recommended seeding rate for each of the three wheatgrasses. The seeds were broadcast and then the applicable WTR rate was randomly applied in replicate (0, 16, 32, 64, 128, and 256 Mg ha^{-1}) to 2 m x 0.5 m areas representing depths of 0, 1.4, 3.8, 7.5, 15, and 30 mm with the 1.4 and 3.8 cm not covering the soil surface continuously. The controls were seeded and then 1.2 cm of soil was placed on top of the seed. The grasses in the VFS boxes were established with a general use Miracle-Gro® Nutriblend water soluble fertilizer from the Scotts-Sierra

Horticultural Products Company applied with a 1:18 dilution. This amount of fertilizer was commensurate with typical P fertilization rates for establishing wheatgrasses. The irrigation water that contained fertilizer was sprinkled on the boxes with a watering can. After applying diluted fertilizer two times per week for four weeks, the boxes were irrigated one time per week for three weeks. By this time the wheatgrasses were at least 15 cm tall, which is typical for grazed land vegetation.

Phosphorus Analyses

Total P is considered to be the total amount of P in dissolved and particulate phases. The samples were not filtered. For this method the soil (1 g) and water (1 mL) samples were digested with perchloric and nitric acids in a 200°C heating block until 2.0 to 3.0 mL was left in the digestion tube. The samples were then placed in a 100°C heating block for two hours after which they were left to cool and then brought to volume. The samples then were shaken and left to settle for 12 hours. A portion of the sample was poured off into smaller tubes after which they were ready for inductively coupled plasma-atomic emission spectroscopy (ICP-AES) analysis.

Total dissolved P applies to the soil solution and refers to the dissolved inorganic (MRP) and the organic fractions. Total dissolved P differs from TP in that it is not digested however it is still a "total" analysis because when the samples are analyzed by ICP-AES they are combusted. The ICP-AES is considered to provide the complete inorganic P fraction in addition to some of the organic fraction. Both TP and TDP analysis are standard methods of P determination because in highly organic soils there will be a difference between the methods (Pierzynski, 2000).

Another common P analysis applies to soil and solution. Molybdate reactive P is the dissolved filtered (0.45 um-pore-diameter membrane) orthophosphate and the acid extractable particulate P fractions. These portions are considered to represent the immediately aquatic plant available P that possibly contributes to eutrophication. The standard MRP analysis is the Molybdate Blue method by Murphy and Riley (1962). This method uses the molybdate colorimetric test without preliminary hydrolysis or digestion of the sample. Ammonium molybdate and potassium antimony tartrate react with dilute soluble P solutions in an acid medium (pH 2) to form an antimony-phospho-molybdate complex. This complex is reduced by ascorbic acid resulting in a blue color that is proportional to the P fraction that is considered to be the most critical contributor to accelerated eutrophication of surface water bodies (Pierzynski, 2000).

Soil test P is also referred to as Olsen-P or sodium bicarbonate-P. This method (Kuo, 1996) is used in the western U.S. because it is the best method suited for calcareous soils. It uses sodium bicarbonate ($NaHCO_3$) at a pH of 8.5 as a soil extractant. The $NaHCO_3$ solution uses HCO_3^-, CO_3^{2-} and OH^- to decrease the solution soluble Ca^{2+} concentrations by precipitation of $CaCO_3$ and the soluble Al^{3+} and Fe^{3+} by Al and Fe oxyhydroxides thereby increasing P solubility (Pierzynski, 2000).

The soil and runoff sample preparations were as follows. The soil and runoff samples were not frozen as the freezing process would lyse the cells releasing additional P resulting in a falsely high soluble concentration. The soil samples were air-dried and the water samples were stored at 4°C until ICP-AES or spectrophotometric analysis. The MRP samples were analyzed within 24 hours of sampling due to potential P transformations, i.e. cellular turnover. The depth of soil sampling for this research was

set at 15 cm because most soil P remains within this zone because of sorption or plant absorption occurring. The vegetation selected for my research has roots that are predominantly in the 0-15cm. The exception to most P being present in the 0-15 cm depth is under extreme leaching conditions when it is possible for P to move through macropores and go below this depth without being removed along its transport path.

Sampling Protocol

Before each runoff event began, a sample of the input solution to the manifold was taken from the storage container of the water spiked with 10 mg P L^{-1}. The measured MRP concentration of the water sample collected was then divided into the MRP runoff samples' concentrations. This normalization of the runoff samples was done so that the runoff events could be compared and because there were slight variations in the storage solution (ranging from 9.8 to 10.1 mg P L^{-1}). The MRP runoff and storage sample concentrations are listed in Table A1.

Runoff samples were collected at 30-second increments for the first 5 minutes after runoff occurred, at 2-minute intervals for the next 30 minutes, and finally every 5 minutes until steady state was achieved. All runoff water samples were analyzed for MRP (Murphy and Riley, 1962). Soil test P (STP) (Kuo, 1996) was determined for all of the soil samples. After establishment of the vegetation to 15 cm, the runoff events began at intervals of 1 week to allow for the soil to become less saturated. A total of four runoff events took place. Each runoff event occurred until steady state had been achieved. The duration of each runoff event was the only difference between them.

Initial soil moisture samples were collected using a soil-sampling device prior to each run to ensure that the runoff events were occurring on soil with matric potentials between field capacity and wilting point. These samples were taken from outside of the inner box at the upper, middle, and lower sections of the box so that soil within the inner box was minimally disturbed (Figure 2.6). The soil moisture samples were collected randomly in duplicate and were divided into 0-5-, 5-10-, and 10-15-cm depth increments. Initial soil P samples were taken at the top, middle, and lower portions of the box from within the inner area before the first runoff event (Figure 2.6). Final soil P samples were taken after each runoff event, and these values served as the initial soil P value for the following runoff event. The soil was placed into a soil moisture can and dried in a 105°C oven for 24 hours. After soil samples were taken, new soil was placed in the holes and, if WTR was required, then a small amount was placed on the surface. The holes were filled so that soil water flow within the boxes was not impacted.

Chronologically, soil moisture samples were collected from the outside of the inner box. Next, soil P samples were collected before a runoff event. Runoff water samples were collected according to the procedure listed above. Finally, final soil P samples were collected after the soil had dried so that an acceptable soil sample could be obtained. After the first runoff event occurred, the final soil P sample from a previous runoff event represented the soil P sample for the next runoff event.

Plant basal density was counted every 2 cm throughout the 2-m box length. Plant samples from each box were sampled and analyzed (Self and Rodriguez, 1998). The plant basal count and soil bulk density were taken in duplicate per plot before the runoff events commenced and were taken after the runoff events ceased. The plant basal density

counts were taken within the inner box while the bulk density measurements were taken outside of the inner box.

General Soil Characteristics

The unnamed Aridic Argiustoll had a saturated paste pH of 7.5 (Rhoades, 1982a) and electrical conductivity (EC) of 3.6 dS m^{-1}. The soil bulk density was 1.4 g cm^{-3} with a saturated volumetric water content of 0.46. The cation exchange capacity (CEC) was completed using the Rhoades (1982b) method. The WTR had a pH of 7.3, EC of 1.6 dS m^{-1}, bulk density of 1.1 g cm^{-3} and a saturated volumetric water content of 0.6. Additional soil and WTR chemical and physical characteristics are in Table 2.1.and 2.2.

Statistical Methodology

A repeated measures analysis determined whether the runoff events within the VFS boxes were independent of the plot in which they were run. A lack of significance (α=0.01, which means that 1% of the time the null hypothesis could be rejected when it is true) showed that the runoff events were considered independent of each other. As a result of VFS box independence, the data were analyzed using regression.

Determination of Soil Hydraulic Parameters

The soil hydraulic properties needed to predict the direction and flow rate of water and other constituents through unsaturated soils are mainly the soil water content (θ) and hydraulic conductivity (K). The soil water pressure head gradient is important to soil water movement. Parameter relations for $\theta(h)$ and $K(\theta)$ can be

determined simultaneously by using a continuous flow method for rapid measurement of soil hydraulic properties (Butters and Duchateau, 2002). This method uses a combination of direct Darcian analysis and numerical inversion of Richards' equation in order to estimate hydraulic properties suggested by Ahuja and El-Swaify (1976). The K estimate using this analysis is sensitive to the soil sample length and the lower boundary rate of pressure change (Butters and Duchateau, 2002). The analysis allows for wetting and/or draining $K(h)$ and $\theta(h)$ over the entire tensiometer range (0-1500 cm) while keeping the physical significance of the hydraulic parameter estimates. Table 2.2 presents the results of the Butters and Duchateau analysis for the hydraulic properties that were used in Opus2Z.

Flow cell measurements took place with the soil samples from the greenhouse vegetative filter strip boxes and were removed with as minimal of disturbance as possible. Vegetation on the surface was cut to the surface thereby maintaining the integrity of the macropores and micropores that existed while the runoff events occurred. The flow cell data produced hydraulic parameters that were used by Opus2Z.

Results and Discussion

Soil and Water Treatment Residual Physical Properties

The Opus2Z model used the Langmuir isotherm for all P concentrations while the MRP data for the greenhouse experiment used the linear isotherm because the concentrations were less than 100 mg P L^{-1}. Chapter three describes the linear isotherm in detail and illustrates the linear and Langmuir isotherms fit to the batch experiment

sorption data for soluble P concentrations ranging from 0.5 to 200 mg P L^{-1}. Based on this P range, Opus2Z used an Smax of 6300 mL g^{-1} and a k of 0.235 L mg^{-1}. Heil and Barbarick (1989) found that WTR (pH 5.1 and $CaCO_3$ equivalent (CCE) of 170 g kg^{-1}) could sorb 740 to 3500 mg P kg^{-1}. Ippolito et al. (1999) used a WTR (pH 6.9; CCE not reported) that could sorb 12,500 mg P kg^{-1}. Castro and Torrent (1995) found that P retention increases with the ratio of clay to CCE. Since the WTR has more slightly more clay and silt (most likely increased by the presence of the alum polymer) and a little more CCE than the soil, the WTR probably would have a higher P retention capacity in addition to its high Al content (23,000 mg kg^{-1} vs. 1,100 mg kg^{-1} for the soil). Both the unnamed Aridic Argiustoll and the WTR had low initial total P contents (approximately 370 and 60 mg kg^{-1}, respectively), a soil clay content of 33% and WTR clay content of 34%, and CCE's of approximately 0.07% (Table 2.1). A higher clay or CCE would have potentially increased the P sorption capacity of the soil.

Moisture Retention Curves

Research has shown that the application of WTR has beneficial effects. This study found greater porosity with WTR (60%) as compared to the soil (40%). Figures 2.2 and 2.3 show the moisture retention curves obtained for the soil and WTR, respectively, by the flow cell method of Butters and Duchateau (2003). The soil moisture retention curve had a lower saturated volumetric water content and a lower plant available water range than the WTR. Because the WTR had a higher moisture retention capacity than the soil, it could release more water to vegetation.

Vegetative Filter Strip Greenhouse Study

The molybdate reactive P (MRP) concentrations observed from runoff were used in a ratio with the P concentration that was measured from the manifold (input) during its related runoff event. The MRP runoff concentrations per runoff event data are in Table A1. This data is illustrated in figures 2.7 to 2.12 that show the extent of variability between runoff events and within a runoff event for a given WTR rate. Each of the WTR rates had less variability within a runoff event with the replicates for a WTR rate averaged for MRP concentrations than without averaging the replicates for a WTR rate. The averaging of the MRP concentrations was important because it removed replication in the experiment impacting which statistical analyses could be performed with the MRP data. An expanded exponential rise equation fit the data best (Figures 2.13 to 2.18). The expanded exponential rise equation fit was:

$$y = (a + b) - b \exp(-ct) \qquad [2.8]$$

where

y is the normalized (MRP_{out}/MRP_{in}) P concentration, where MRP_{out} is the runoff MRP concentration (mg L^{-1}) and MRP_{in} is the concentration (mg L^{-1}) of the water added to the VFS box,

a+b the maximum normalized P concentration ,

a is the normalized initial concentration,

b is the normalized plateau increment above the initial concentration,

c is a rate constant, and

t is time (represented by x in Figures 2.13 to 2.18).

Figure 2.19 illustrates the exponential rise equation.

There was no replication that could be statistically analyzed for the VFS boxes since the replicate boxes for a WTR rate were averaged for MRP concentrations resulting in one data set for a VFS box. Therefore, the WTR rate that had the most P sorbed per mass applied was determined by comparing the regression equation asymptotes (Table 2.3), r^2 values (Table 2.4), and the average MRP for the runoff events (Table 2.5). The regression equation asymptotes were compared because they represent the maximum P concentration reached. A comparison of the nonlinear regression asymptotes did not clearly indicate what WTR application rate was optimum for P sorption (Table 2.3). Overall, comparing the asymptotes did not provide clarity as to which rate was optimum for P retention.

Figures 2.7 to 2.12 illustrate the MRP data from each runoff event without averaging the replicate data for each VFS box WTR rate. The 0 (all events), 16 (events 1, 3 and 4), 32 (event 1 and 2) and 128 Mg ha^{-1} (event 3) had output:input ratio MRP values above one indicating that there may have been measurement error or runoff water had increased its P concentration most likely due to the amount of P fertilizer applied supplying P to overland flow. The three lowest WTR rates had more values above one indicating that P was being picked up along the surface of the VFS box. The lower rates had less WTR that could retain P and were probably saturated with P. Higher WTR rates had more material that could capture P from the overlying solution.

The r^2 values represent how well eq. [2.8] fits the data. When the r^2 values were compared, the second highest WTR rate (128 Mg ha^{-1}) had the highest correlation values for runoff events one and two (0.71 and 0.70, respectively) after which the r^2 values decreased to 0.41 (Table 2.4). The 16 and 64 Mg ha^{-1} WTR rates had the same r^2 of 0.69

for the fourth run however the lower rate had r^2 values of 0.11 and 0.02 for the second and third runoff events. The 64 Mg ha^{-1} WTR rate consistently had r^2 values that increased with consecutive runoff events. This finding, however, does not identify what WTR rate is optimum for P retention either since it is only a measure of goodness of fit to an equation.

The average normalized runoff MRP concentration, with the VFS box replicates averaged, per runoff event for the six WTR rates were compared (Table 2.5) to determine if a particular WTR rate was able to retain more P resulting in lower MRP runoff concentrations. A decreasing MRP concentration trend was observed as the WTR rate increased. Using regression analysis, the control was significantly different (α=0.10) from the plots that contained WTR with regards to MRP runoff concentrations. The three highest rates were not significantly different from each other (α=0.1) but were significantly different from the two lower WTR rates and the control (α=0.01). This finding is most likely due to the 16 and 32 Mg ha^{-1} WTR rates not having continuous coverage over the soil surface. This comparison was helpful in determining if WTR differed from soil regarding P retention but does not explain why the highest rate did not sorb significantly more P than the next two lower rates.

The amount of P added from the fertilizer and runoff events is calculated by multiplying the inflow volume by P concentration and the application time and then adding the amount of fertilizer-P used to establish the vegetation. The resulting total input is:

$$[0.1 \text{ L sec}^{-1} \times 0.01 \text{ g L}^{-1} \times 3600 \text{ sec}] + 65 \text{ g} = 68.6 \text{ g P} \qquad [2.9]$$

The fertilizer-P addition (65 g) far exceeds the mass input from the runoff events (3.6 g). Although 3600 seconds were used to calculate the amount of fertilizer applied by the runoff events there were exceptions. Initially, samples were collected until steady state flow was achieved per runoff event but for comparison purposes the runoff events were allowed to occur for at least one hour with a few exceptions. A list of the exceptions follows with the runoff event number listed first followed by the amount of time the runoff event occurred: 0 WTR Mg ha^{-1} : 1, 35 min; 16 Mg WTR ha^{-1}: 1, 50 min and 2, 18.5 min; 32 Mg WTR ha^{-1}: 1, 50 min and 4, 50 min; 64 Mg WTR ha^{-1}: 1, 40 min and 4, 45 min; 128 Mg WTR ha^{-1}: 1, 35 min and 4, 55 min; and 256 Mg WTR ha^{-1}: 1, 19 min. The replicate averaged MRP ratios per runoff event are provided in Table A1.

The experimental results indicate that lower water P contents were measured in the VFS box effluent. The loss of P from surface water into a surface that inherently contains P and has had P added via fertilizer occurs because the soil/WTR was able to sorb additional P. The soil/WTR must have been able to sorb more P because if the soil was saturated with P then additional P sorption would not have occurred.

Soil test P concentrations were analyzed to elucidate if an optimum WTR rate for P retention could be identified. If a particular WTR rate was better than another, it would probably have had higher STP concentrations. A comparison of the STP concentrations indicated that no trends or significant (α=0.1) changes occurred from the background STP levels after fertilizer additions to STP levels after the last runoff event. However, the 0-5 cm depth had significantly (α=0.05) more P than the 5-10 and 10-15 cm increments. Figure 2.20 shows four of the six STP background levels for four of the WTR rates. It was expected that the WTR rate with the lowest runoff P concentrations

would have the highest STP concentrations, however the amount of P fertilizer applied greatly impacted this greenhouse experiment resulting in no change in STP levels before and after the runoff events.

The STP level, after the fertilizer had been applied but before runoff events were lower than the soil and WTR TP values measured before fertilizer was applied. This is possible because TP concentrations were measured from soil and WTR material that had been collected from the field and had not had any fertilizer applied. Most of the fertilizer-P remained in the surface layers rather than diffusing through the material to greater depths. Additional factors possibly affecting P concentrations include sampling location, macropore flow, fertilizer remaining on the soil surface, the number of rocks and coagulated colloids in the WTR, vegetation on the surface impacting flow paths, the WTR depth that the runoff came into contact with and for how long, the amount of vegetation on the surface impacting P accumulation and dispersion, and STP analysis methodology in which only 0.5 g material is used to determine STP concentrations. Had more irrigation events occurred before the runoff events began the fertilizer remaining on the surface may have been able to move to greater depths.

Although the manifold water was 10 mg L^{-1}, the soil surface averaged 600 mg kg^{-1} due to the over-fertilization of the VFS. Runoff with lower P concentrations than the soil surface contains was measured throughout the duration of the runoff event. I would not attribute the runoff P to desorption from the soil since the bonding energy between PO_4^{3-} and Al^{3+} is high. The runoff P is most likely due to a minimal depth of interaction between the surface water and soil water and the flow velocity of the input water. A nominal depth of interaction and high flow velocity would result in water being

transported quickly down the box at a P concentration similar to the manifold P concentration. If the contact time between the surface water and soil water were greater and with a decreased flow velocity, the manifold water would have had more of a chance to lose P resulting in even lower runoff P concentrations. Even though the runoff P concentration is near the manifold P concentration it is possible that any pools on the surface of the VFS box could have kept P solubilized and the water being transported across the surface of the box could have picked it up contributing to the runoff P concentration.

The vegetation samples did not differ from before and after the first and fourth runoff events, respectively. The plant basal density counts indicated that each box had approximately the same amount of vegetation (Table A2). Sediment P was not measured because little or no particulate matter greater than 2 um was in the collected runoff.

Opus2Z Model Simulations

Model simulations were completed to determine which factors impacted the model greatest with regards to runoff TP concentrations. The standard model components that each of the altered simulations were compared to was a VFS box at 9% slope, flow rate of 0.1 L sec^{-1}, ω of 0.1 mm min^{-1} [eq. 2.4], WTR $S_{ma,}$ 6300 mg kg^{-1}, 30 mm WTR thickness, 65 g of P fertilizer applied, and a box length of 2 m. There were eight applications (one every three days for four weeks) of dissolved P fertilizer and three irrigations (one per week for three weeks) before the first runoff event. The P fertilizer applications and subsequent irrigations were accounted by the model for the simulations.

The P sorption curve, established by batch studies, is presented in Chapter Three. illustrate a 24-hour snapshot rather than a progression of P movement through time allowing for continual shifts necessitated by kinetics. The kinetics of P sorption and desorption indicate that P may have relocated to the interior of particles leaving surface sorption sites exposed. A timeframe longer than the duration of this research would be required to account for both slow and fast kinetics (Selim, 1998). Therefore, only some of the P may have had enough time to shift from the exterior to the interior of the soil/WTR particles. The SEM-EDS images in chapter three illustrate the identification of P bound to Al at various P concentrations and their location to a particle.

The amount of fertilizer applied was halved in order to determine its impact on the amount of TP observed in the runoff (Figure 2.21). The results from the model simulation showed that with less P input to the system there was slightly less P observed in the runoff. As shown by the WTR thickness results below, the WTR is only as effective in treating surface runoff as the depth of interaction between the runoff and the soil-water. Higher surface runoff TP concentrations were higher than the data from the greenhouse experiment possibly due to a lack of macropore flow in the model simulation creating higher surface P concentrations. High surface P concentrations could contribute to higher P runoff concentrations than were observed with greenhouse data. Figure 2.21 shows that with only enough P applied to establish the vegetation P was deposited onto the soil surface resulting in the lowest TP runoff concentrations. This illustrates that Opus2Z can simulate conditions of P loss as well as its addition to solution. The Opus2Z model does not account for the shifting of the P sorption curves to account for both slow and rapid sorption. The Opus2Z model relies on the fast (24-hour) kinetic portion of a P

sorption curve while interparticle diffusion requires additional time to occur (Selim, 1998).

The slope was changed to 5% and 2% to determine if slope was a determining factor in TP runoff concentrations. The 2, 5, and 9% slopes started runoff at times very close to each other. These results were expected because over a short slope distance (2 m) not much change in TP runoff concentration could occur (Figure 2.22) and the difference for when runoff began is within the error of this model. When the total mass leaving the VFS box were plotted (Figure 2.23), the various slope values were so close that their lines were coincident.

Next, only the flow rate was altered from the standard VFS box components listed above (Figure 2.24). The doubled flow rate had the lowest TP runoff concentrations because it had limited time to gain P from the soil water to the surface water. Its runoff commenced approximately three minutes before the standard flow rate of 0.1 L sec^{-1}. The halved flow rate had the highest TP runoff concentrations because it had the most time to gain P from the soil water into the surface water resulting in higher TP runoff concentrations (Figure 2.24). Runoff began approximately 10 minutes after the standard flow rate's runoff started. Due to the amount of P fertilizer applied, the model simulated the pickup of P rather than its deposition even with half the amount of fertilizer applied. This occurred because there was enough P on the surface present to be taken into the surface flow perhaps due to its loose association to the perimeter of the particles. When the slope was altered in combinations with half the usual flow rate used for the greenhouse experiment, the mass leaving the VFS box were nearly the same. When graphed, the data lines representing three slopes are coincident (Figure 2.25).

The film diffusion coefficient (ω) was halved and doubled (Figure 2.26). The lowered ω allowed for lower TP concentrations because the P could not be picked up from the soil as easily as with the higher ω's. Doubling ω increased the P concentrations by approximately 2 mg L^{-1} per time interval. A ω of 0.1 mm min^{-1} had TP runoff concentrations between the halved and doubled values. Figure 2.27 shows the impact of the film diffusion coefficient on TP runoff throughout the 2 m VFS box. Since the TP runoff concentration increases with distance down the slope, this again suggests that the soil is acting as a source of P to the surface solution. The differences between the coefficient 0.2 and 0.05 mm min^{-1} values become greater toward the end of the VFS box.

The S_{max} was halved to determine its impact on P runoff concentrations (Figure 2.28). The halved S_{max} is closer to the calculated S_{max} (3166 mg kg^{-1}) as determined by the sorption isotherm data. The effect of the higher S_{max}, however, is to retain more P at the soil surface and apparently provide a greater supply of P for desorption into the pore water and the overland flow. The higher S_{max} has higher TP because the Opus2Z model does not account for hysteric P sorption contributing. Therefore, if more P was available at the soil surface for desorption and the desorption process was the same as the adsorption process then the higher TP concentrations by the higher S_{max} would be expected. Figures 2.28 and 2.29 show the two S_{max} 's impact on TP runoff throughout the 2 m VFS box length. The difference with distance between the S_{max} 's is minimal because both S_{max}'s were sufficiently high to result in P being retained by soil particles and not being released within the timeframe of this research.

The model uses the same S_{max} for both the adsorption and desorption processes, therefore, the simulations would show higher TP runoff concentrations than the

greenhouse VFS runoff data. The effect of having desorption that is negligible would result in all of the P that was sorbed remaining with the particle. The transport and fracturing of the particle with the attached P could increase the possibility of P becoming desorbed. However, for this research the P sorbed is considered to be kept by the particles and unavailable for desorption allowing for the removal of P from solution. Chapter three discusses the P sorption-desorption data in detail.

The WTR thickness was originally set to 30 mm, representing the 256 Mg ha^{-1} WTR rate. This thickness was selected because it was assumed that the higher the WTR rate applied, the greater the P retention. The result of the model simulation was that it didn't matter if the WTR thickness of 30 mm was halved because only the top 10 mm was interacting with the runoff as determined from the subsurface data (Figure 2.30). (Most of the TP is found within the top 6 mm but higher TP concentrations exist until 10 mm.) This finding is significant because it was identified that the soil needs to have a continuous WTR layer over the soil. A depth of 10 mm correlates to a WTR application rate between 64 and 128 Mg ha^{-1}. Broadcast WTR applied to the soil surface with a continuous depth of at least 2 mm is necessary for effluent P reduction. Figure 2.309 demonstrates the subsurface TP concentrations from the 256 Mg ha^{-1} WTR rate after one runoff event. This figure shows that most of the TP resides in the uppermost region where the WTR happens to be located.

The TP runoff concentrations observed from the simulations were higher than the MRP experimentally measured from the greenhouse study possibly due to a few circumstances. First, the model is unable to simulate macropore flow resulting in higher surface P concentrations than may have existed in the experiment. It is possible that

residual P on the soil surface could be picked up by the overland flow contributing to higher P concentrations. For this to occur P had to attached to the outer-sphere of a particle and be loosely associated with an ion for it to readily go into solution since a S_{max} of 6300 mg kg^{-1} is sufficiently high to sorb P from surface solution and retain it due to its minimal desorption potential. Occlusion may have occurred but was not identified in this research.

Another possibility is that the simulation of TP runoff concentrations only accounted for the pickup of P from the surface because of the amount of fertilizer P applied however, when the VFS box was not overfertilized the model was able to simulate the sorption of P. This disparity allows for speculation that the surface particles had P transport from the exterior to the interior region creating additional sorption sites on the perimeter of the particle. The experimental data confirms that P adsorption must still be occurring due to MRP concentrations below a value of 1.0. Yet with some of the MRP values above 1, some of the particles may have been saturated on their exteriors and were unable to sorb additional P. The P remaining in solution as well as any P residing on the surface that was not bound or was loosely bound to particles would likely have contributed to effluent P resulting in MRP values greater than 1.0. The Opus2Z model was unable to simulate what occurred in the greenhouse boxes due to its exclusion of slow P kinetics.

A third possibility for a gain of P from the surface is that the model uses the same S_{max} for adsorption-desorption processes, higher P runoff concentrations will exist compared to the greenhouse data. More P is desorbed in the model simulations than experimentally occurred and the experiment does not allow for 100% sorption-desorption

potential due to the inherent physical and chemical properties of the soil of which only a few (i.e. porosity, bulk density, S_{max}) are addressed by the model. Because of the disparity between the model's higher TP runoff concentrations and the MRP runoff data more P was deposited in the greenhouse experiment than the model accounted for. The greenhouse VFS boxes were able to move some of the P that had accumulated on the surface to greater depths because of the presence of these macropores created by the vegetation and by the inherent properties of the soil and WTR. The simulations had higher TP runoff concentrations because all of the fertilizer P resided in the surface layers as if the surface was a bare soil rather than a vegetated surface. As a result, the model simulation showed runoff concentrations higher than the spiked water because P was going into solution rather than being deposited to the soil surface. All of the P that was present at or near the surface was potentially available to be picked up by the runoff therefore contributing to runoff with higher TP concentration. Data from the greenhouse experiment demonstrates that a lower P concentration is present at the surface because loss of P occurs from the runoff event water rather than additional P being picked up as shown by the model.

The aging of the VFS and the saturation of sorptive sites on the WTR particles was indirectly addressed in the model. These components would greatly impact the accuracy of the simulation. Even though a runoff event should ideally be a good test of the model, the model is only as good as the data provided. By no means will the results from a 1 m x 0.5 m x 15 cm plot be able to exactly simulate the processes that would be taking place in a catchment however, they may provide an indication as to the phosphorus pollution potential within an area.

Conclusion

Model simulations of WTR surface addition to soil, based on its inherent physical and chemical characteristics, illustrate that WTR can decrease P runoff concentration compared to soil alone. The MRP experimental data (Table 2.5) demonstrates that if P adsorption is occurring, then P effluent concentrations will decrease. The data also demonstrates that if a particle is saturated with respect to P, it will not sorb additional P until sorption sites are available. In order for sorption sites to become available, P must move into the interior of a particle from its exterior. Phosphorus sorption is both a slow and quick process but the quick sorption occurs on a particle's exterior while its transition to the interior requires time. The P in the VFS boxes had only limited time to be transported, leaving most of the P on the particle's exterior resulting in minimal sorption from the surface water. The loss of P from surface water to soil water demonstrates that equilibrium had not yet occurred. When the MRP ratios were above 1.0 it indicated that additional time would be necessary for P equilibration with a particle to occur which would have allowed more P to be removed from the surface water. Phosphorus could be removed from the surface water to the soil water by P on the exterior of a particle moving to the interior of the particle exposing surface sorption sites. The SEM-EDS images discussed in Chapter three will indicate the effect P concentrations have on the location of P within the particle.

Molybdate reactive P runoff concentrations exhibited a decreasing trend from the control through the highest applied rate of WTR indicating that that a continuous WTR layer above the soil is necessary to significantly reduce runoff P. The 64, 128 and 256 Mg ha^{-1} WTR rates were not significantly different from each other in their MRP runoff

concentrations. A likely explanation for this result is the depth of mixing for surface water and soil-water interaction. The effectiveness of WTR is only as pervasive as the depth at which the surface water and soil-water can interact, therefore, allowing P sorption to occur. Overall, the amount of fertilizer applied before the runoff events impacted this experiment more than the P input during the runoff events, as evidenced by no change in STP concentrations.

The Opus2Z simulations provided an understanding of water treatment residuals and vegetative filter strips impact surface-water and soil-water interactions. This model elucidated that a WTR depth of at least 5-6 mm, that continuously covers the soil, was necessary for greater TP retention per mass of WTR applied. From a model sensitivity analysis of several components, the S_{max} , film diffusion coefficient, P fertilizer rate, slope and flow rate affected TP runoff concentrations. The flow rate variations resulted in significant differences in outflow start times. The Opus2Z model was especially helpful in its ability to simulate TP runoff concentrations per unit discharge. Being able to identify the P mass leaving a system would be helpful in determining P's impact on water quality. Although TP runoff concentrations were similar, the variation of the components would not have had the same impact on a water body.

An Opus2Z model limitation is its inability to differentiate between adsorption and desorption P processes attributing to an overestimation of TP runoff concentrations than was observed from MRP runoff experimental data accounting for most of the difference between the experimental and simulation data. The fact that the experimental P ratio is generally less than 1.0 while the modeled ratio is greater than 1.0 is consistent with the occurrence of P adsorption within the aggregates and the observed sorption

hysteresis (Chapter Three). The model simulations were based on 24 h P sorption, where surface adsorption of P is likely the dominant process. However, over the time scale between addition of P fertilizer and the onset of the runoff experiments, P initially adsorbed at the surface may have migrated to the particle's interior. This would effectively re-open potential sorption sites at the particles surface and allow for additional rapid adsorption to take place once the P influent solution was added. If there is negligible P desorption from WTR, there would be more P sorbed to the plot surfaces than Opus2Z would simulate by using a reversible isotherm. Since the plots with continuous WTR surface coverage demonstrated that adsorption was still occurring, it is evident that equilibrium had not been attained. To accurately predict P transport, more experiments would be necessary to determine the dependence of P sorption on time. It is unknown how much the P sorption curves differ between the 24-hour time period used for batch isotherms and the greenhouse experiment. No clear chemical reaction can be elucidated from the experimental data nor the model because only a 24-hour snapshot of the P kinetics was accounted for.

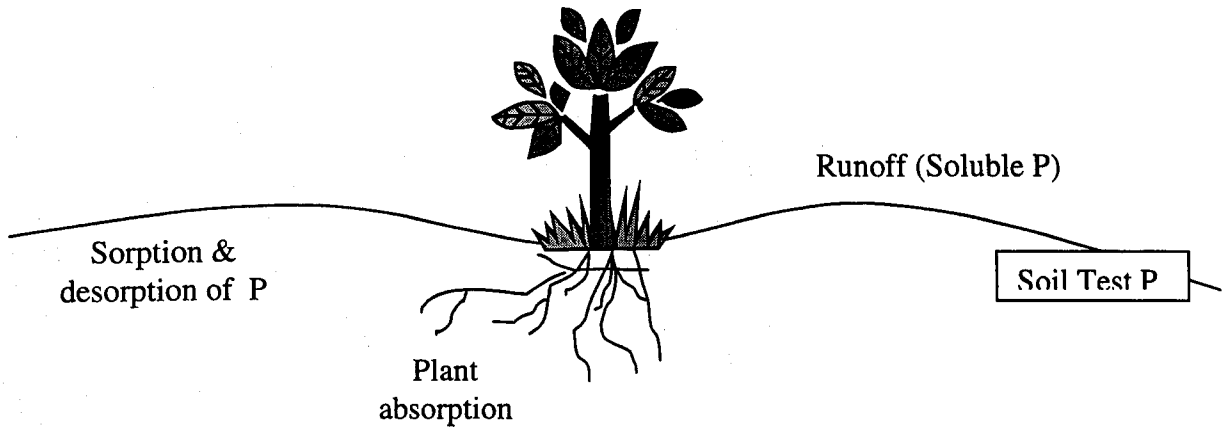

Figure 2.1. Environmental phosphorus components (adapted from Gachon, 1969).

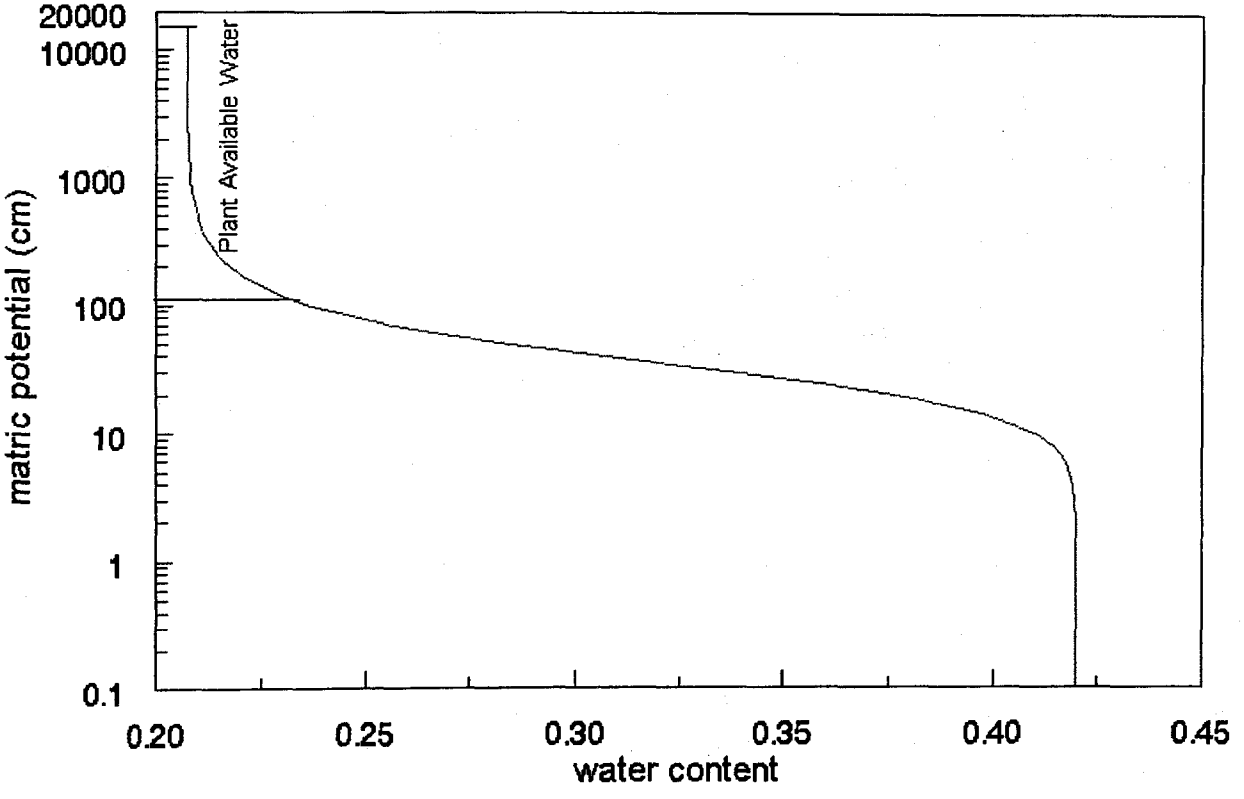

Figure 2.2. Soil moisture retention curve for the sandy clay loam used in the vegetative filter strip greenhouse study. The saturated and residual water contents were determined from the flow cell method of Butters and Duchateau (2002).

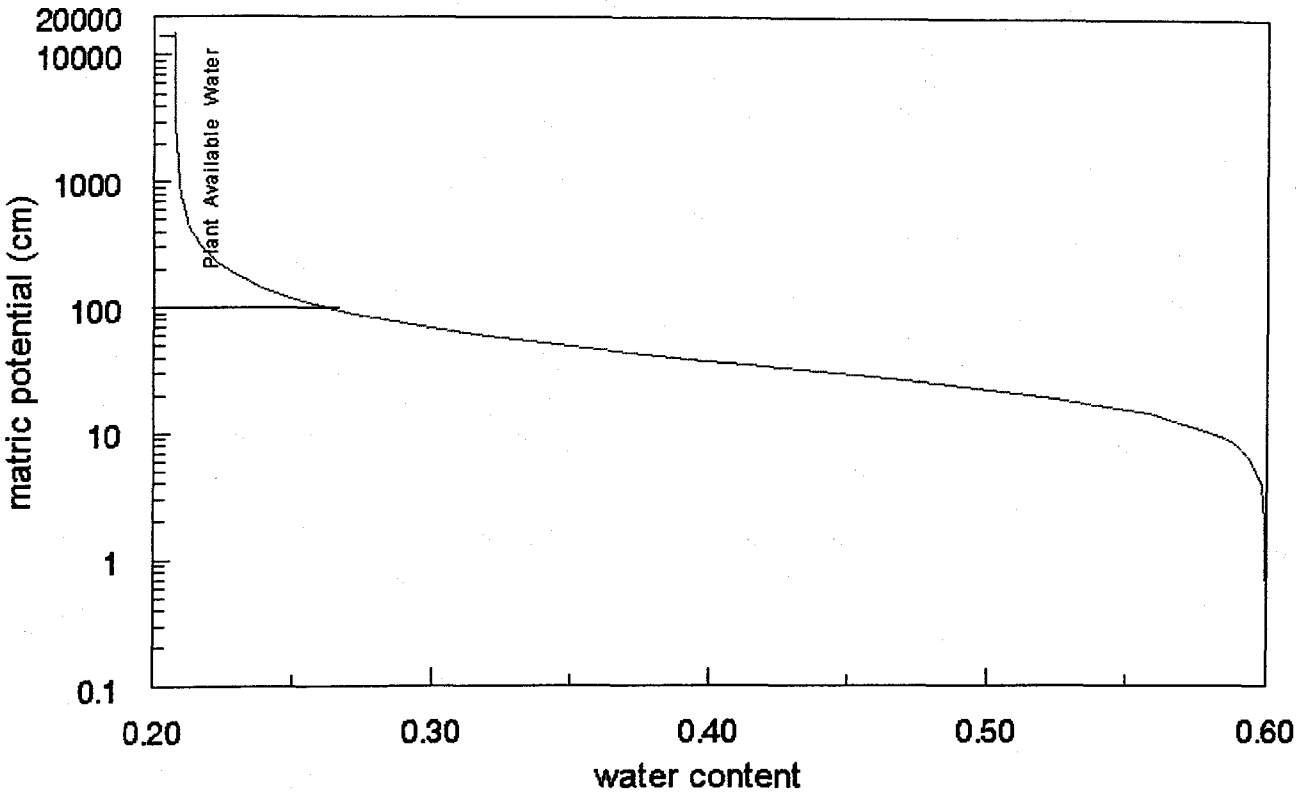

Figure 2.3. Water treatment residual moisture retention curve as determined from saturated and residual water contents from the flow cell method of Butters and Duchateau (2002).

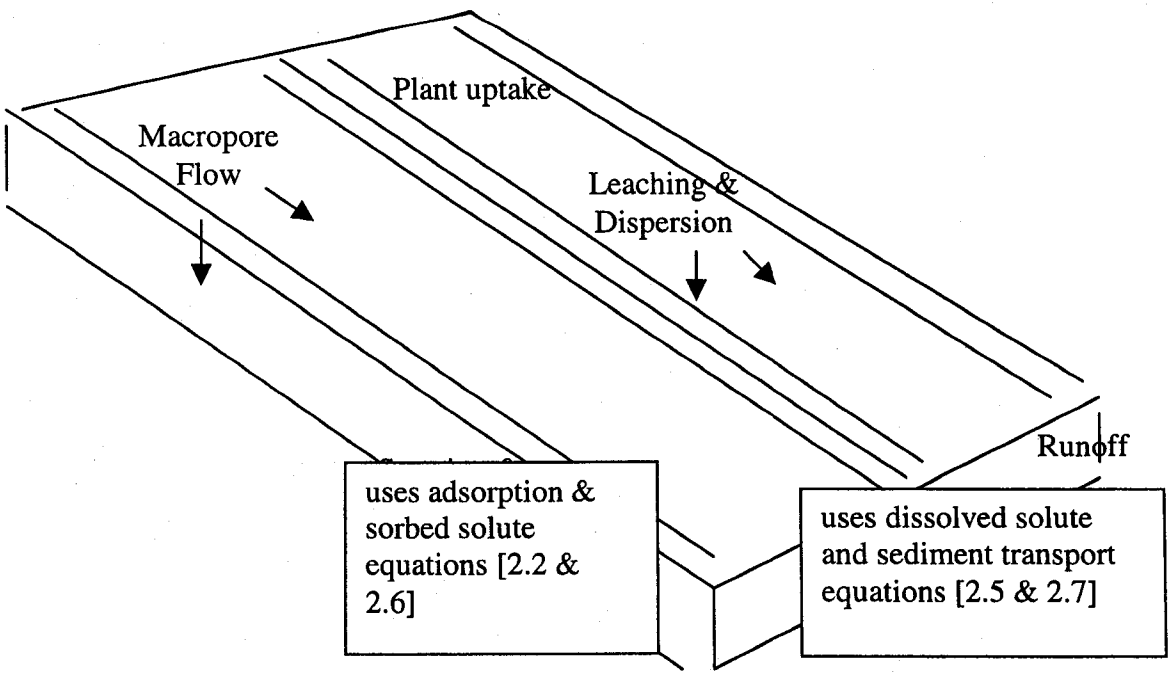

Figure 2.4. Phosphorus processes.

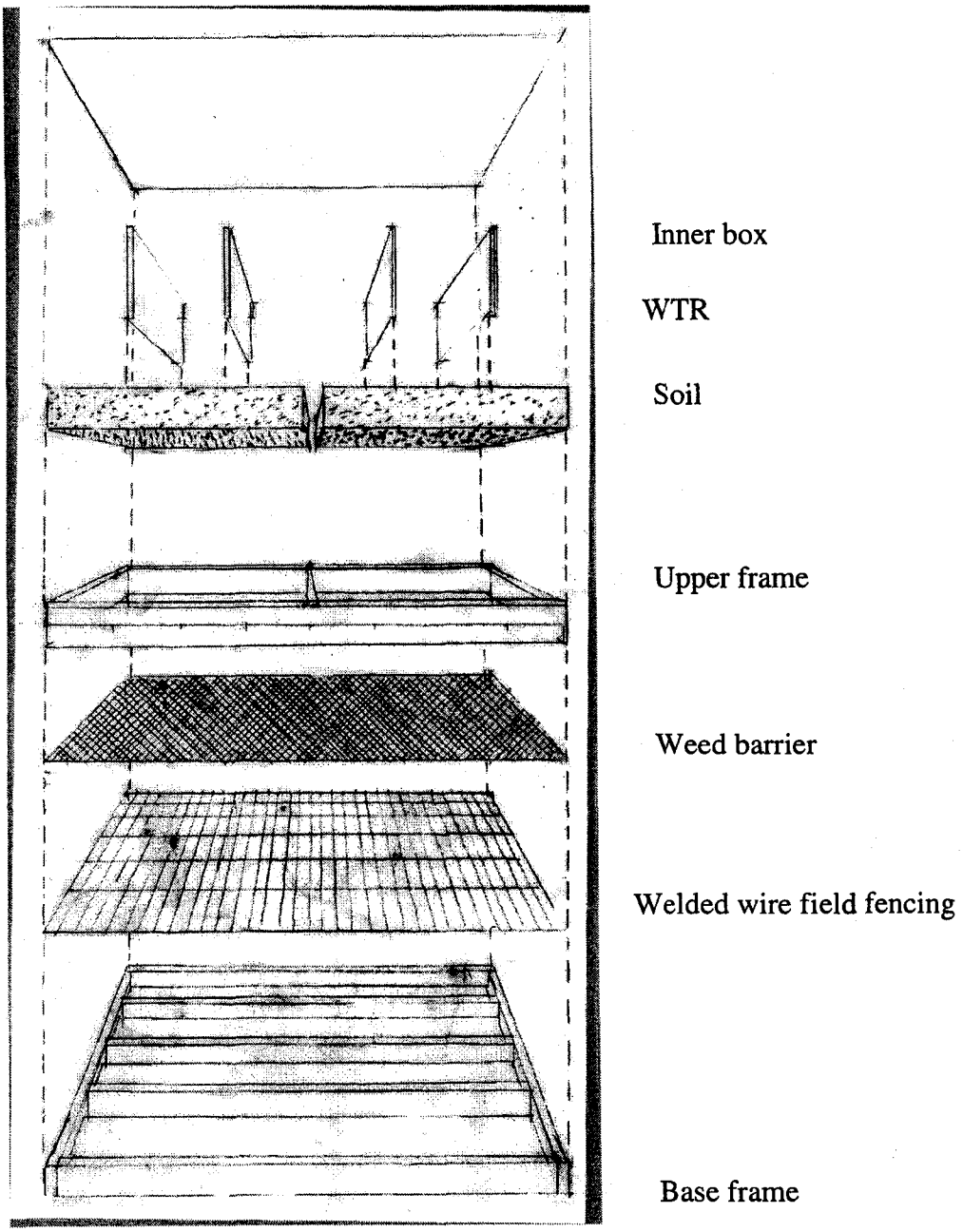

Figure 2.5. Vegetative filter strip box construction.

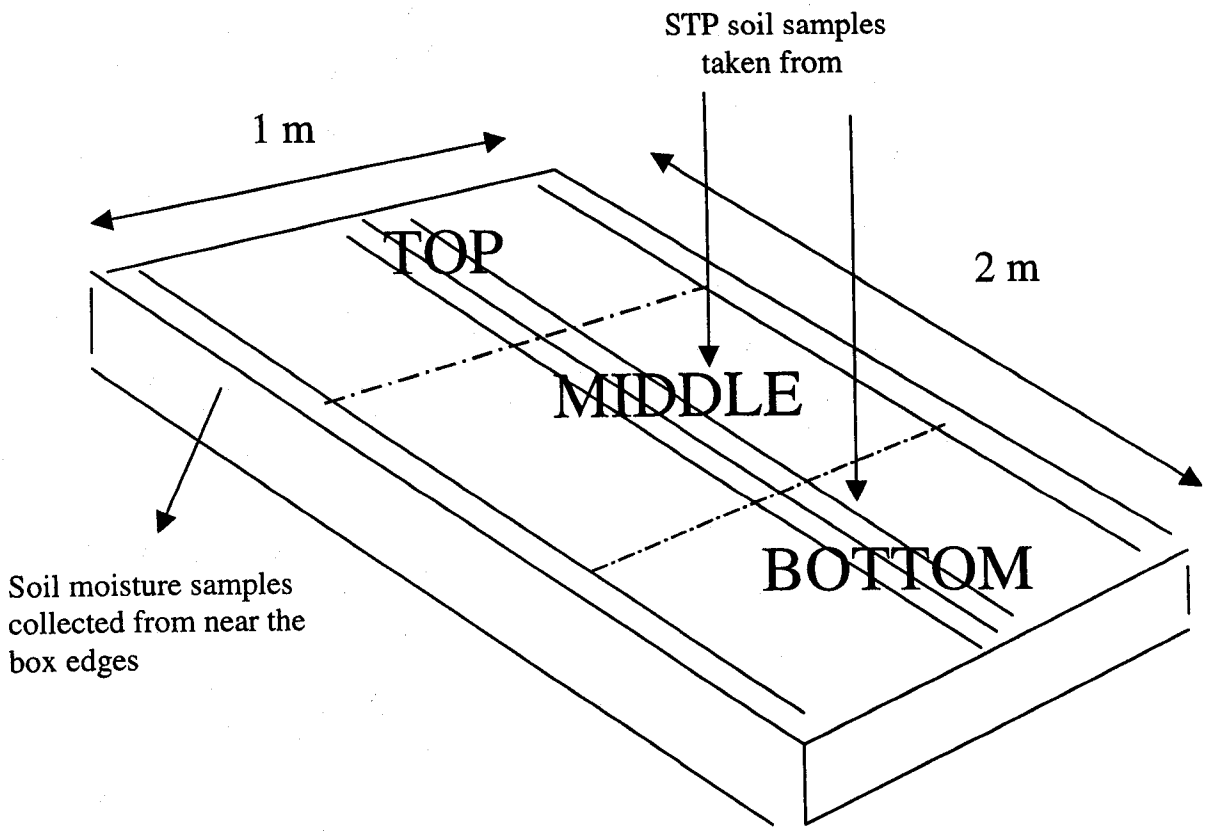

Figure 2.6. Soil sampling locations in vegetative filter strip box.

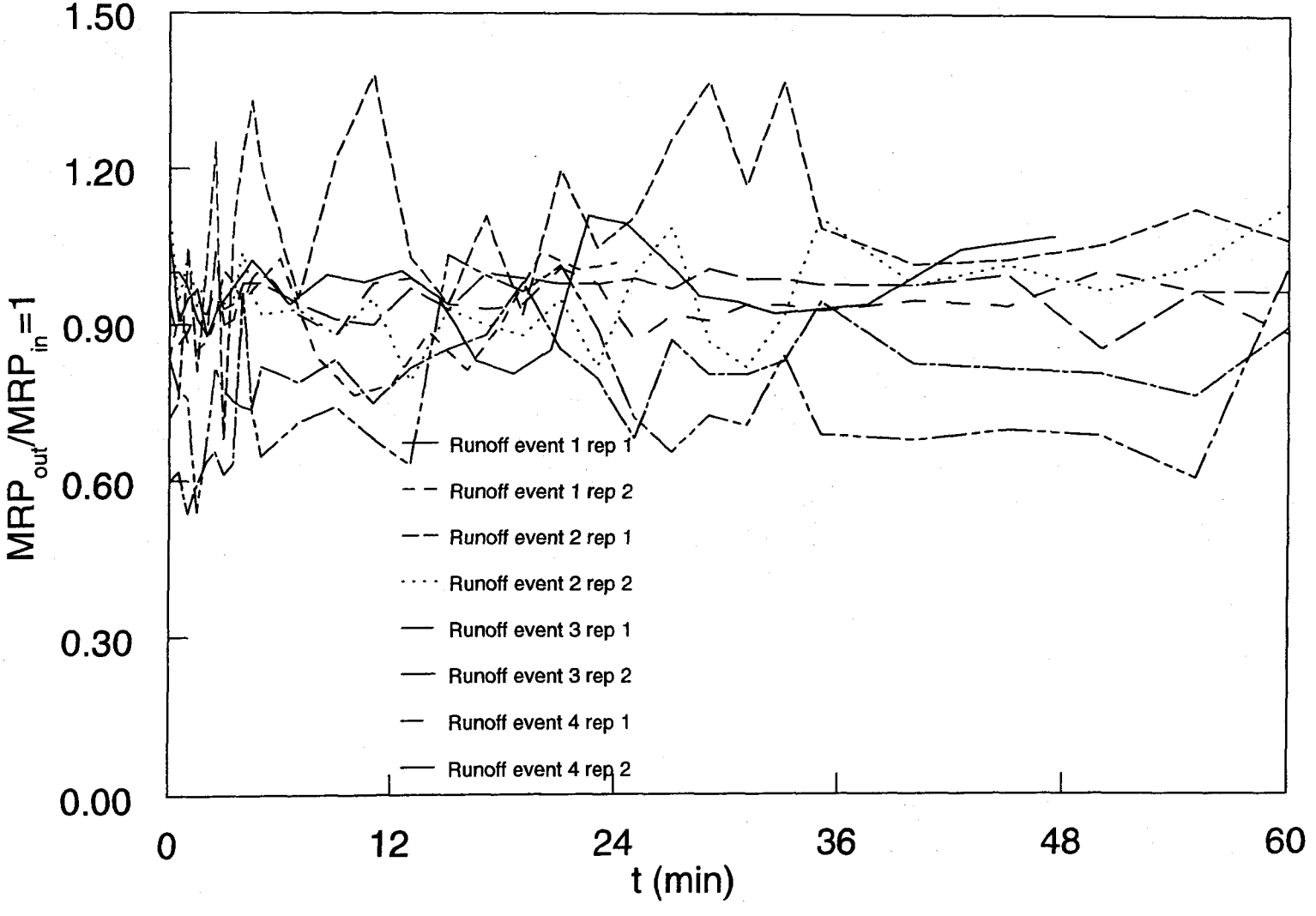

Figure 2.7. Vegetative filter strip runoff events 1-4 for water treatment residual WTR rate 0 Mg ha^{-1} for replicate boxes.

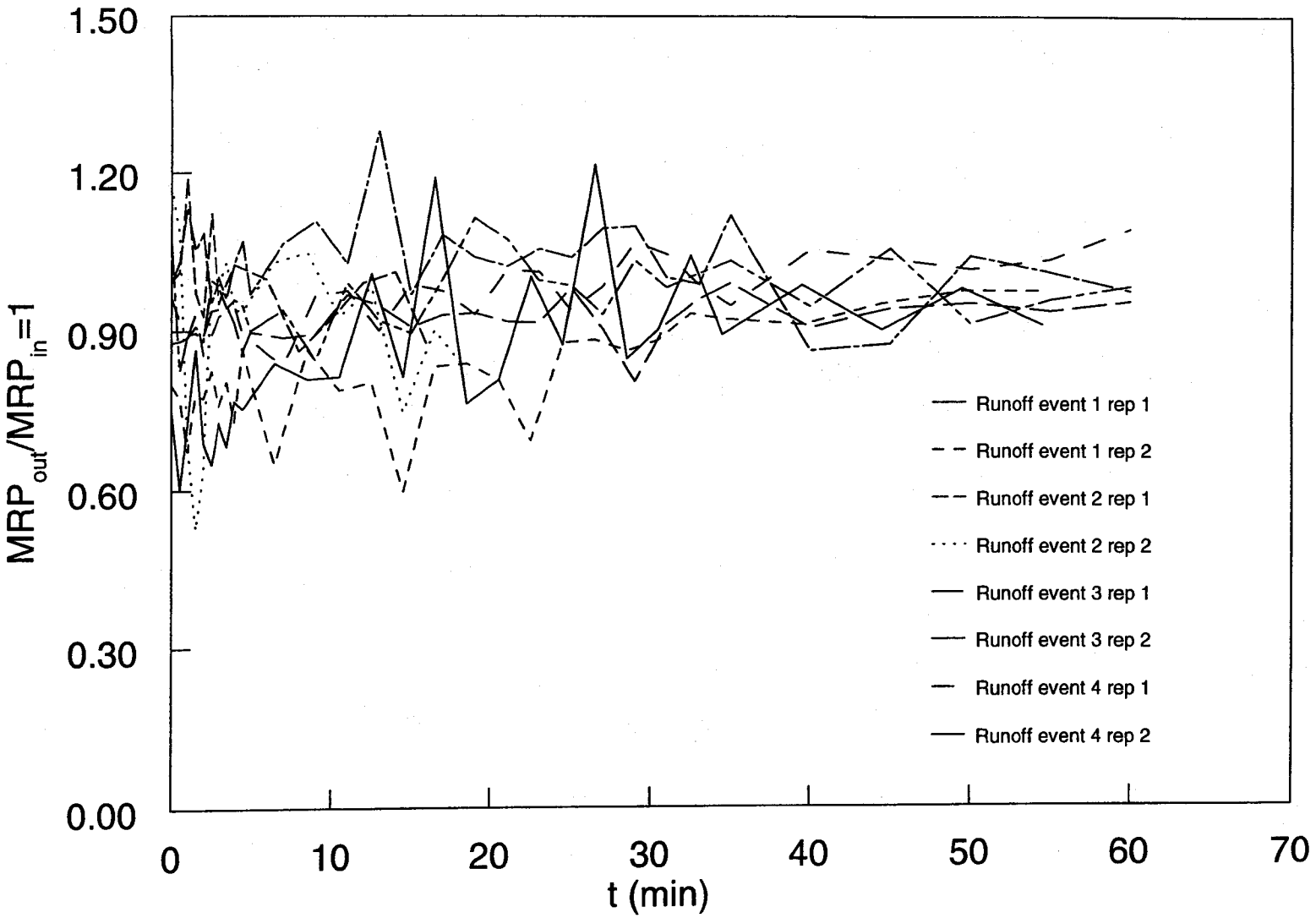

Figure 2.8. Vegetative filter strip runoff events 1-4 for water treatment residual rate 16 Mg ha^{-1} for replicate boxes.

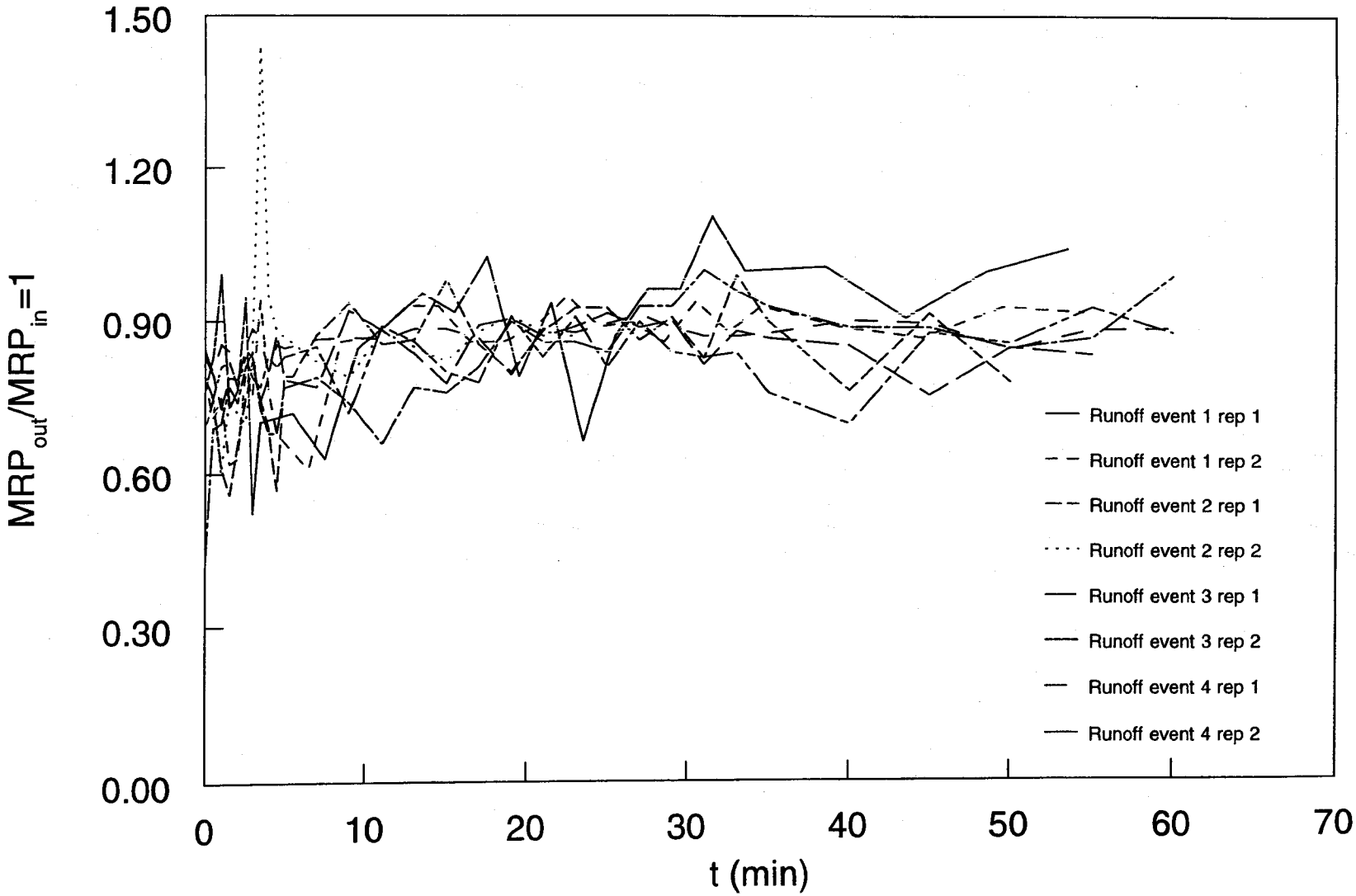

Figure 2.9. Vegetative filter strip runoff events 1-4 for water treatment residual rate 32 Mg ha^{-1} for replicates boxes.

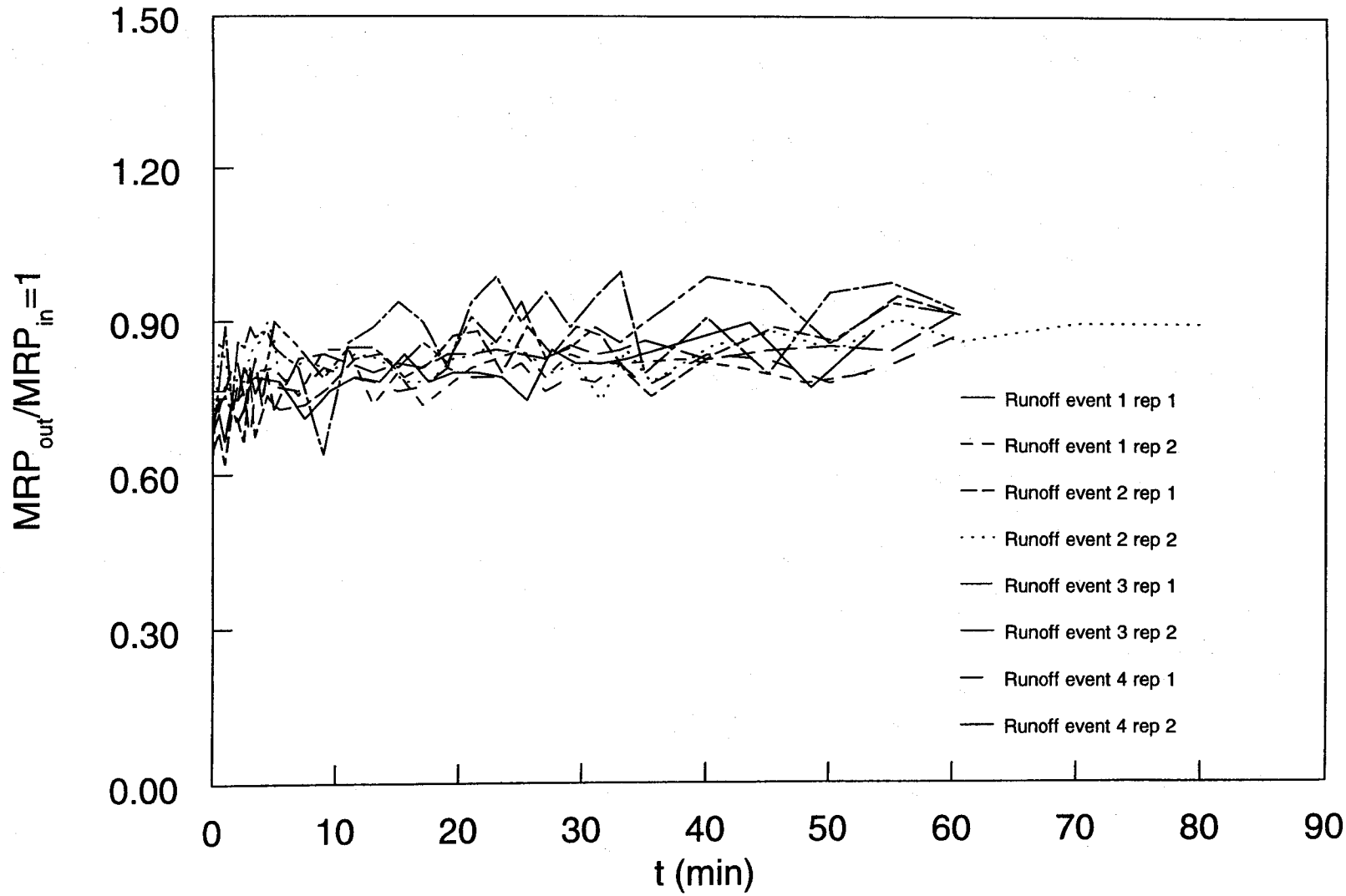

Figure 2.10. Vegetative filter strip runoff events 1-4 for water treatment residual rate 64 Mg ha^{-1} for replicate boxes.

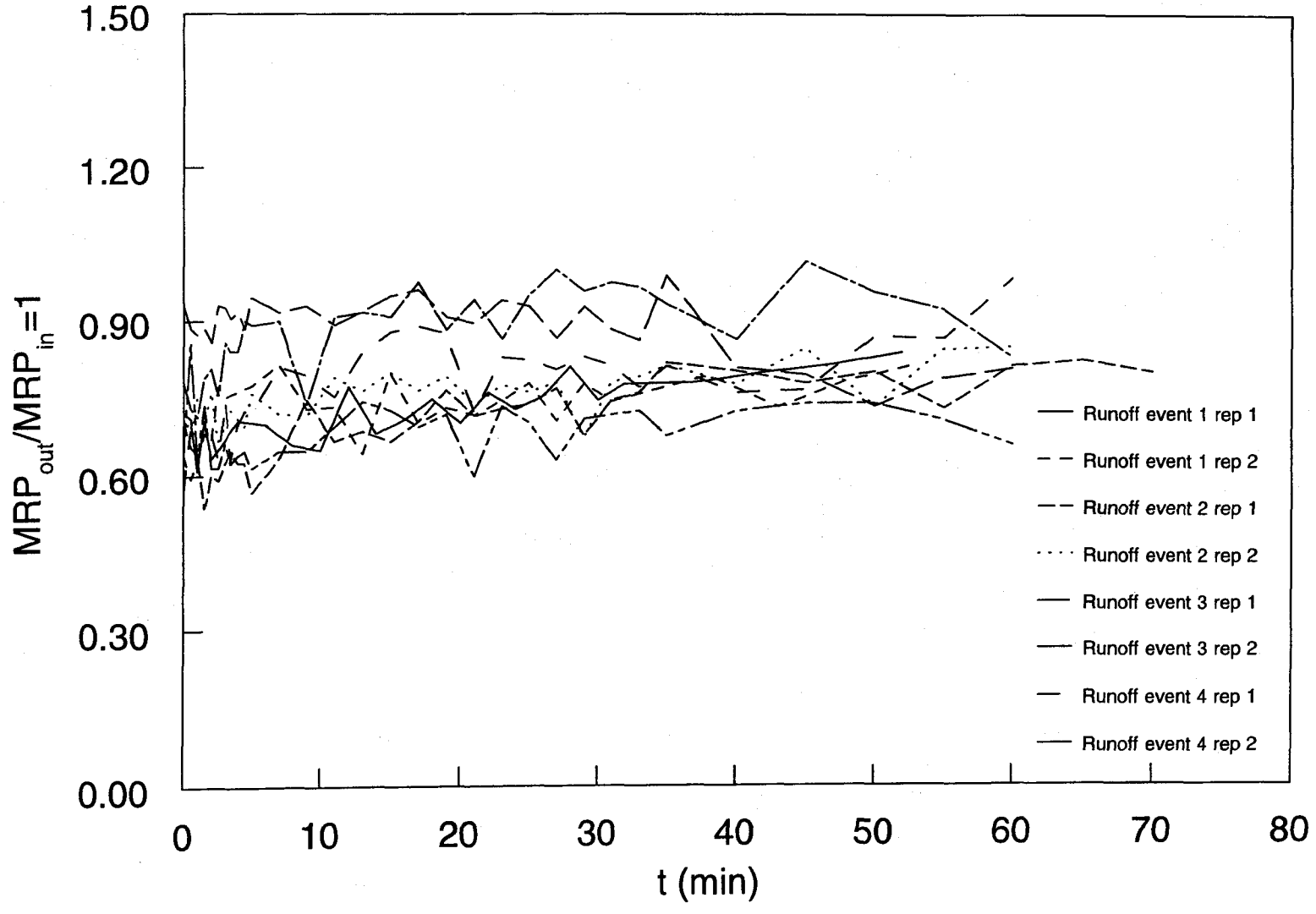

Figure 2.11. Vegetative filter strip runoff events 1-4 for water treatment residual rate 128 Mg ha^{-1} for replicate boxes.

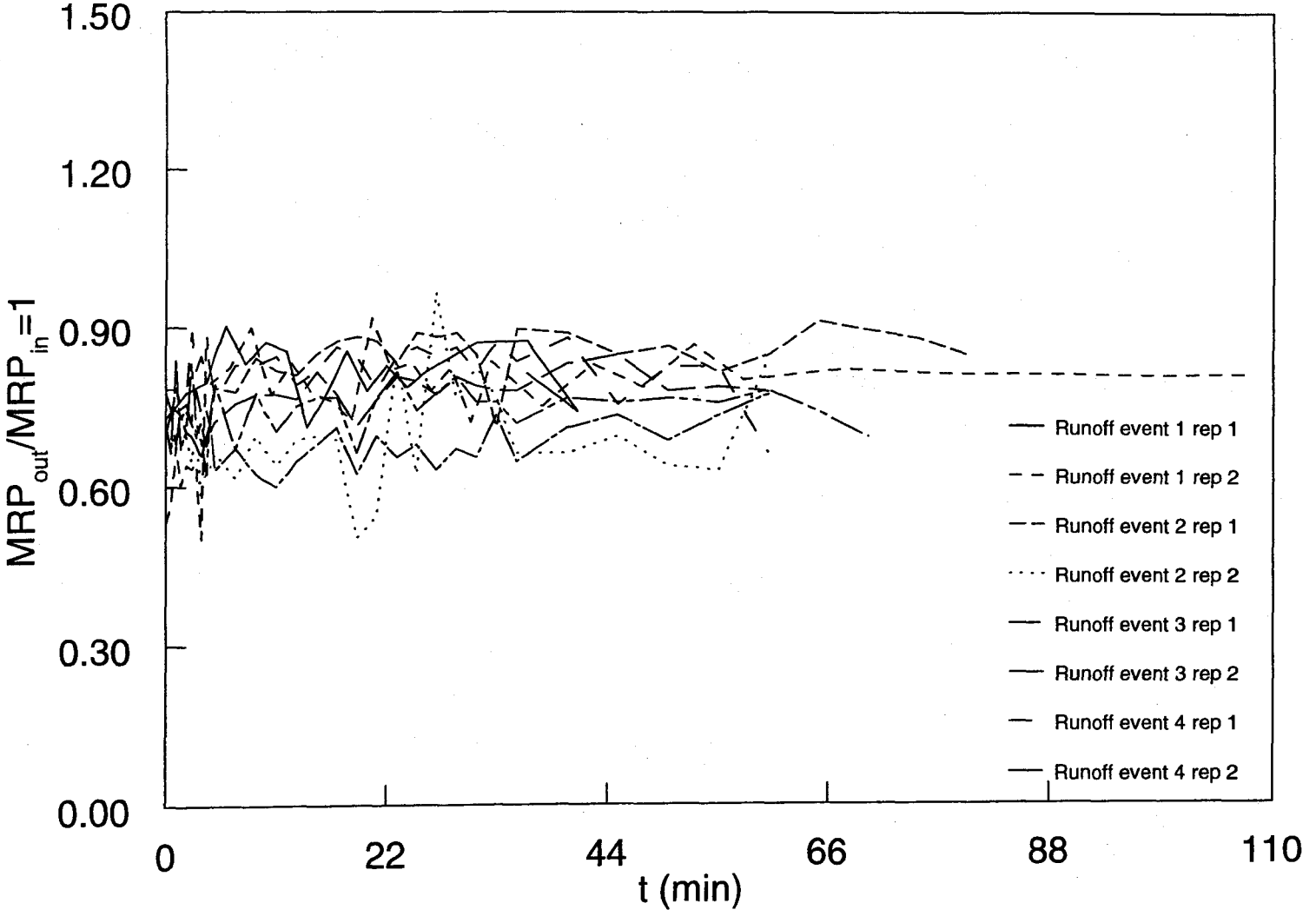

Figure 2.12. Vegetative filter strip runoff events 1-4 for water treatment residual rate 256 Mg ha^{-1} for replicate boxes.

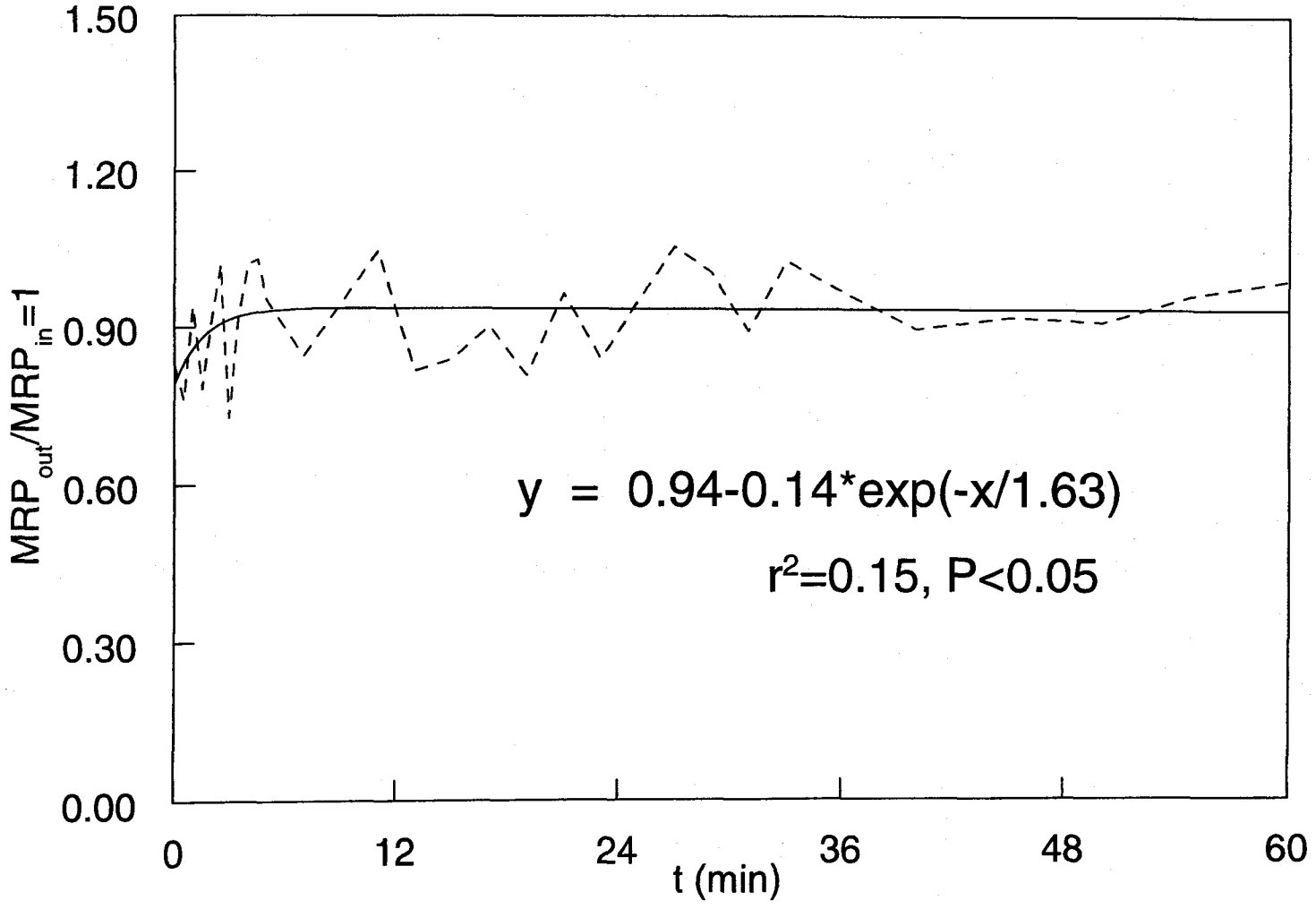

Figure 2.13. Vegetative filter strip runoff event 2 with replicates averaged for water treatment residual rate 0 Mg ha^{-1} for molybdate reactive P ratio concentrations.

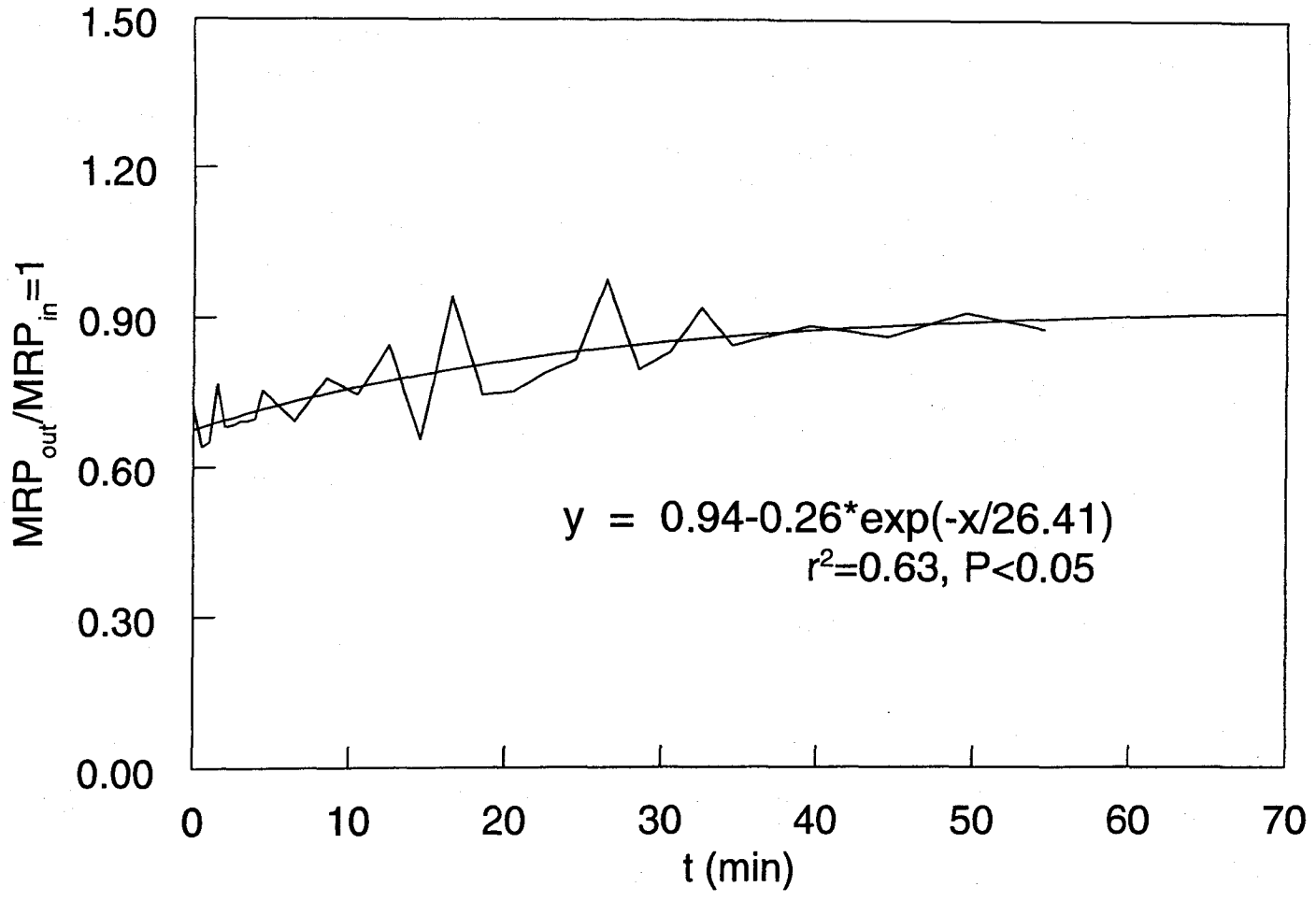

Figure 2.14. Vegetative filter strip runoff event 1 with replicates averaged for water treatment residual rate 16 Mg ha^{-1} for molybdate reactive P ratio concentrations.

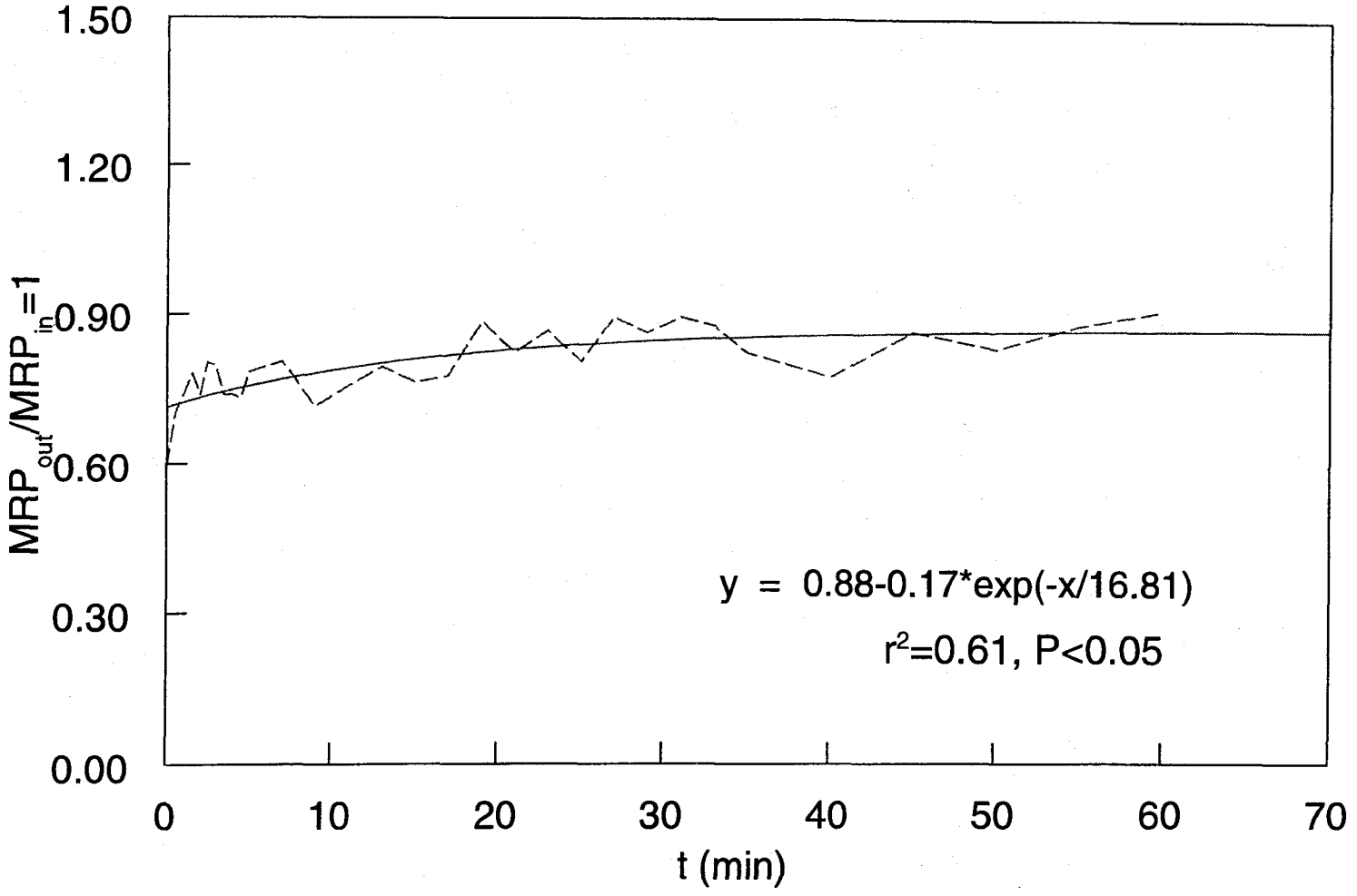

Figure 2.15. Vegetative filter strip runoff event 3 with replicates averaged for water treatment residual rate 32 Mg ha^{-1} for molybdate reactive P ratio concentrations.

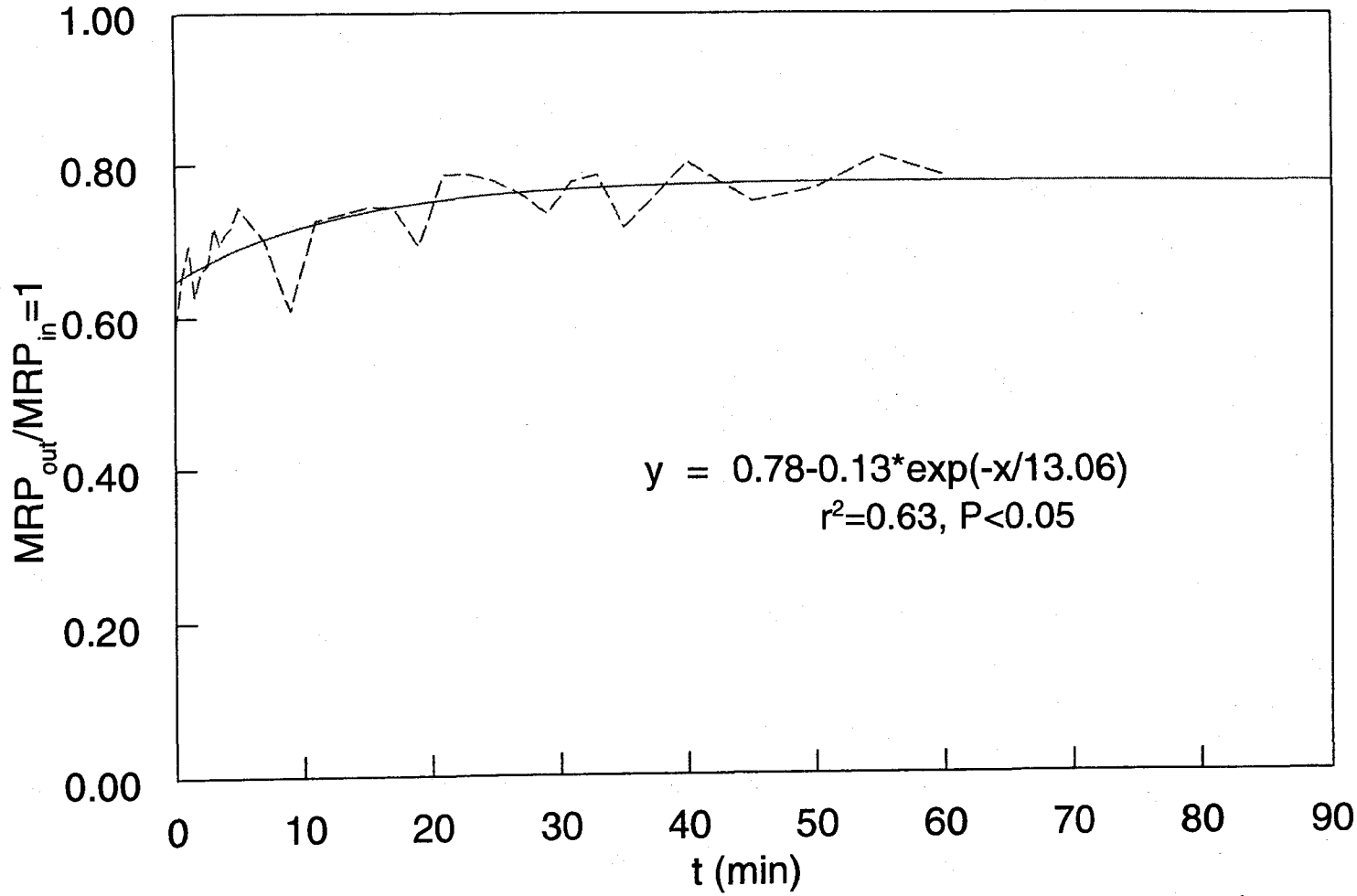

Figure 2.16. Vegetative filter strip runoff event 3 with replicates averaged for water treatment residual rate 64 Mg ha^{-1} for molybdate reactive P concentrations.

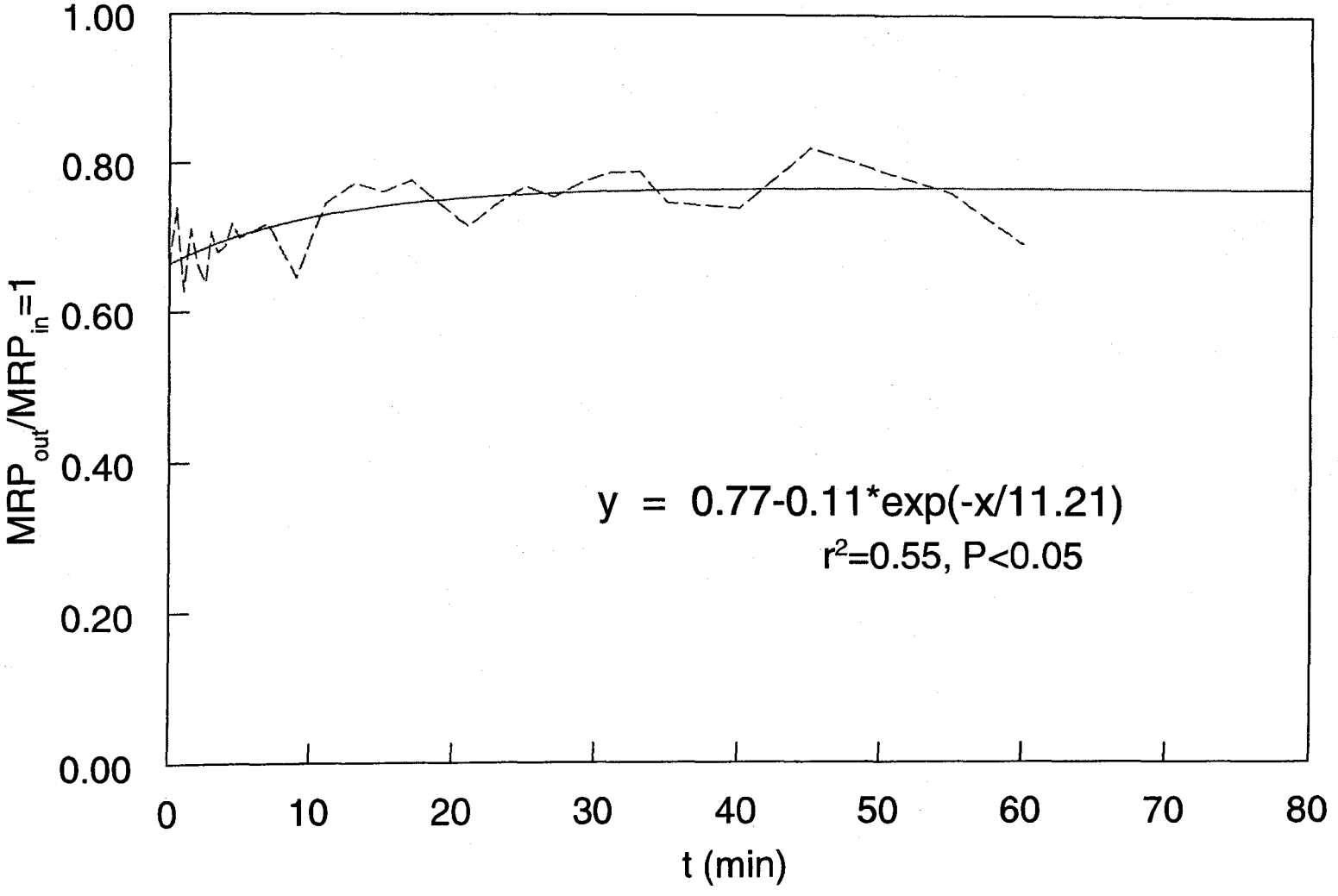

Figure 2.17. Vegetative filter strip runoff event 3 with replicates averaged for water treatment residual rate 128 Mg ha^{-1} for molybdate reactive P ratio concentrations.

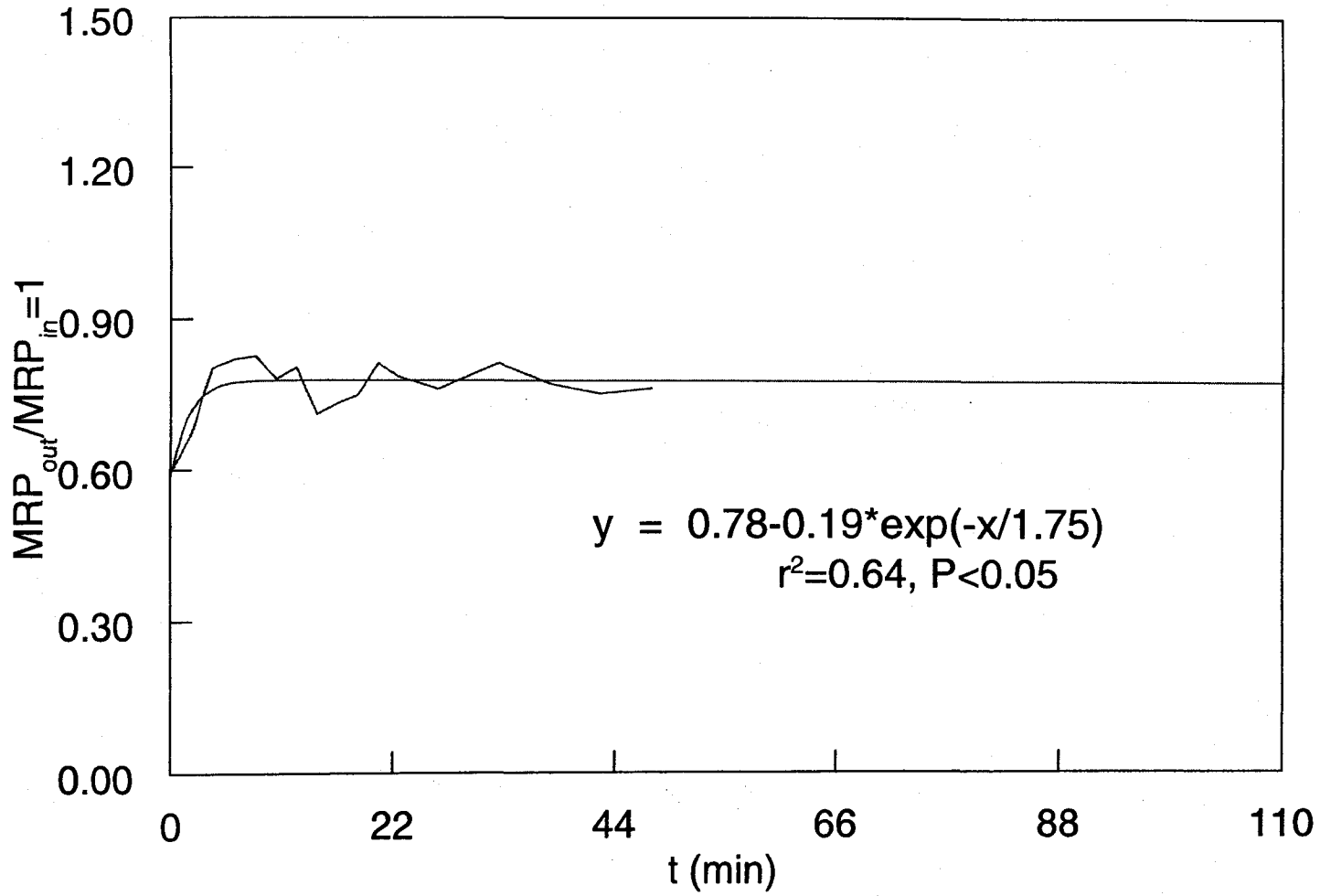

Figure 2.18. Vegetative filter strip runoff event 1 with replicates averaged for water treatment residual rate 256 Mg ha^{-1} for molybdate reactive P ratio concentrations.

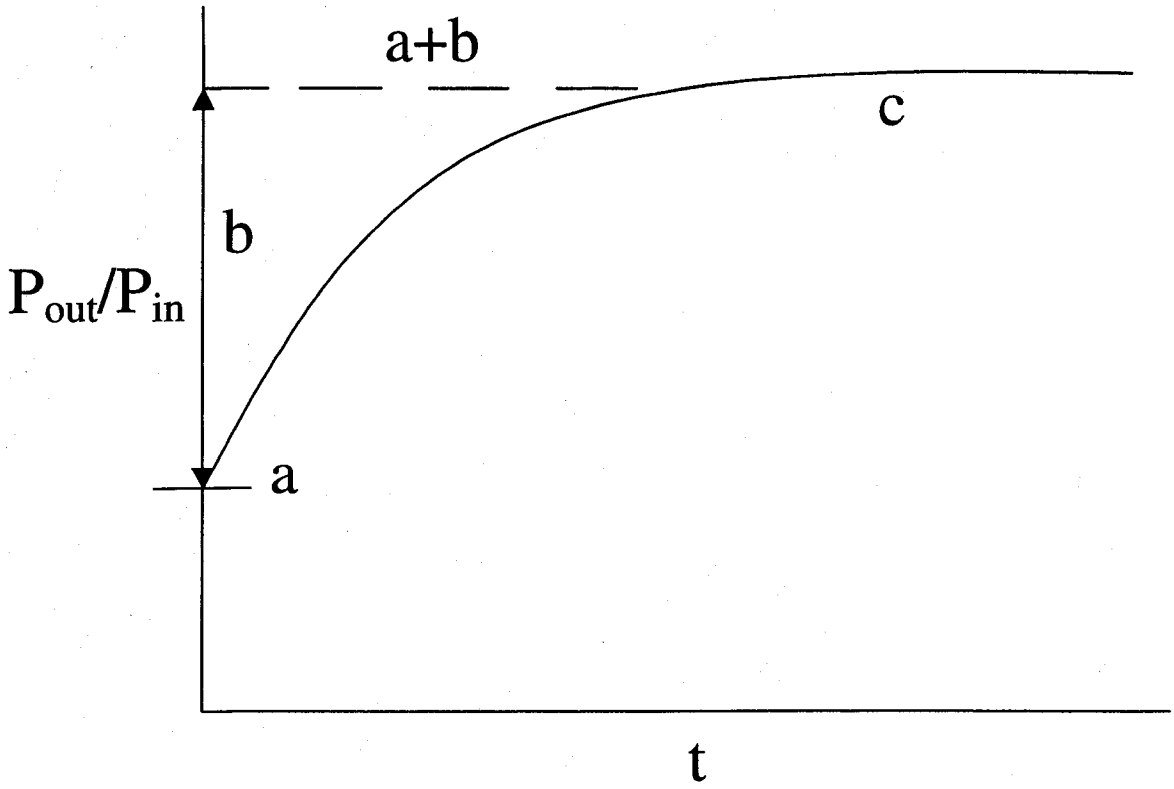

Figure 2.19. Exponential rise equation.

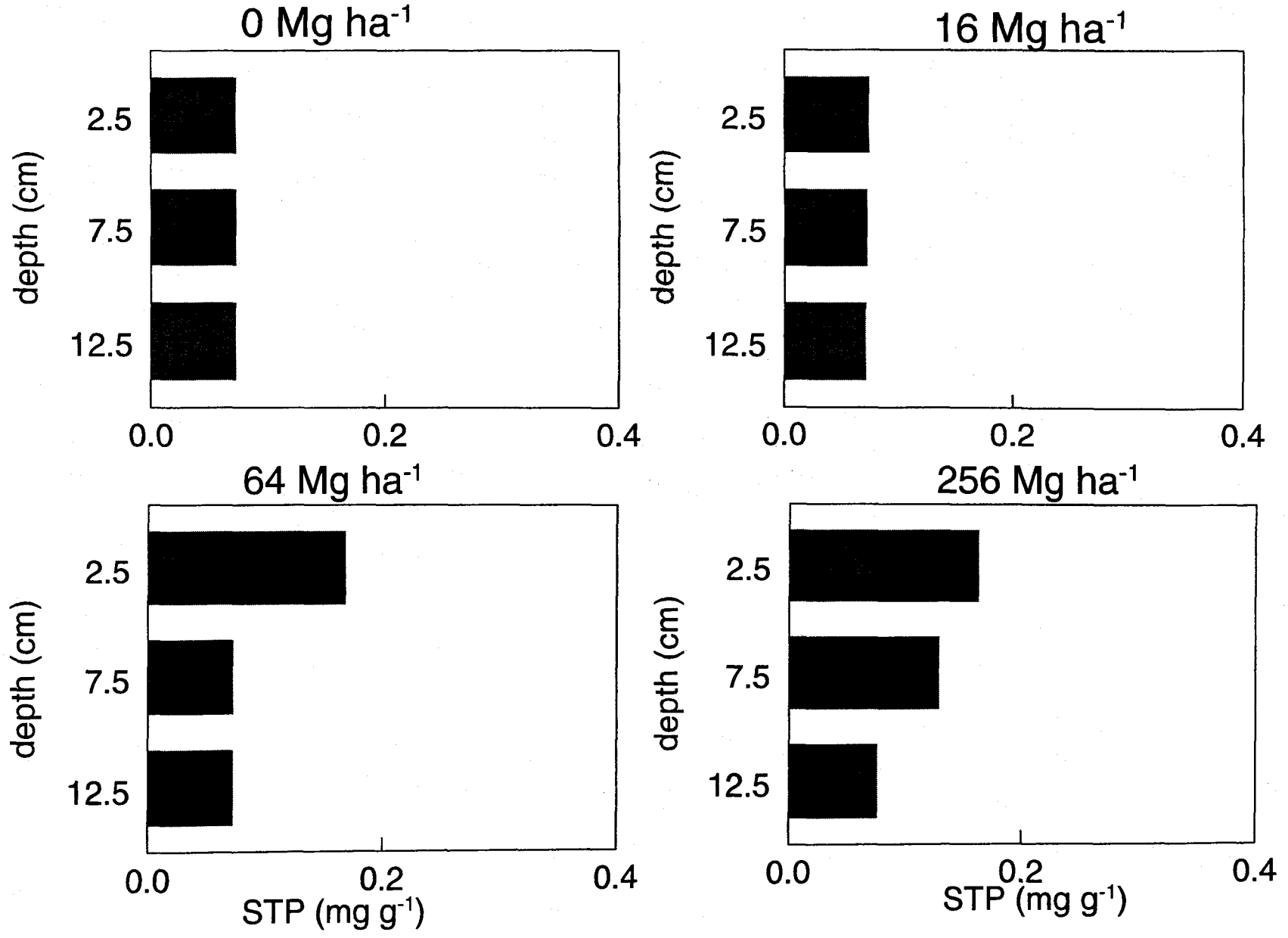

Figure 2.20. Soil test phosphorus background levels after fertilizer had been applied to the vegetative filter strip boxes.

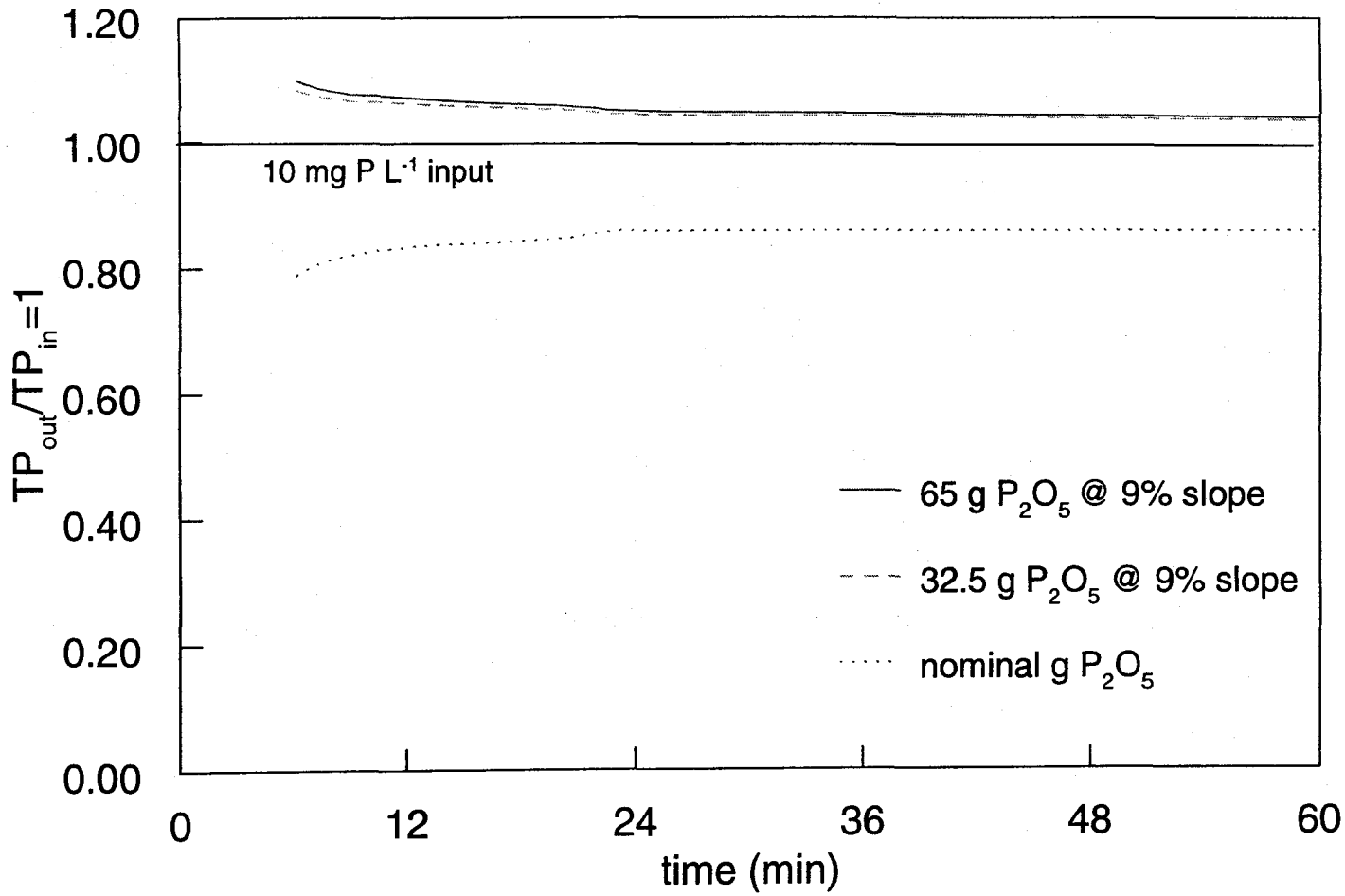

Figure 2.21. Opus2Z simulation of the impact of fertilizer rate on total phosphorus runoff concentrations from the vegetative filter strip box.
*Starting point is where Opus2Z output flow rate stabilizes.

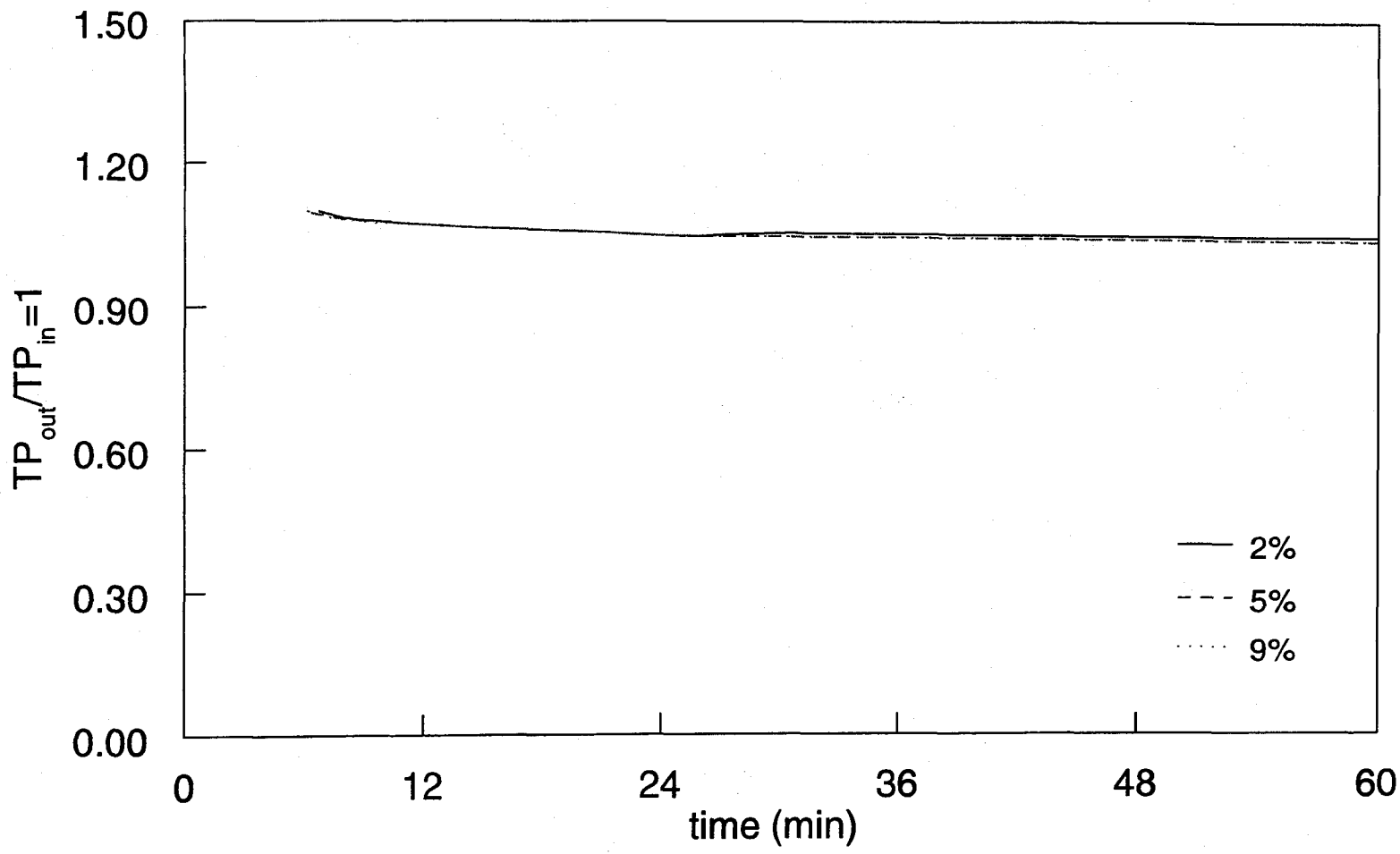

Figure 2.22. Opus2Z simulation of the impact of slope on total P runoff concentrations from the vegetative filter strip box.
*Starting point is where the Opus2Z output flow rate stabilizes.

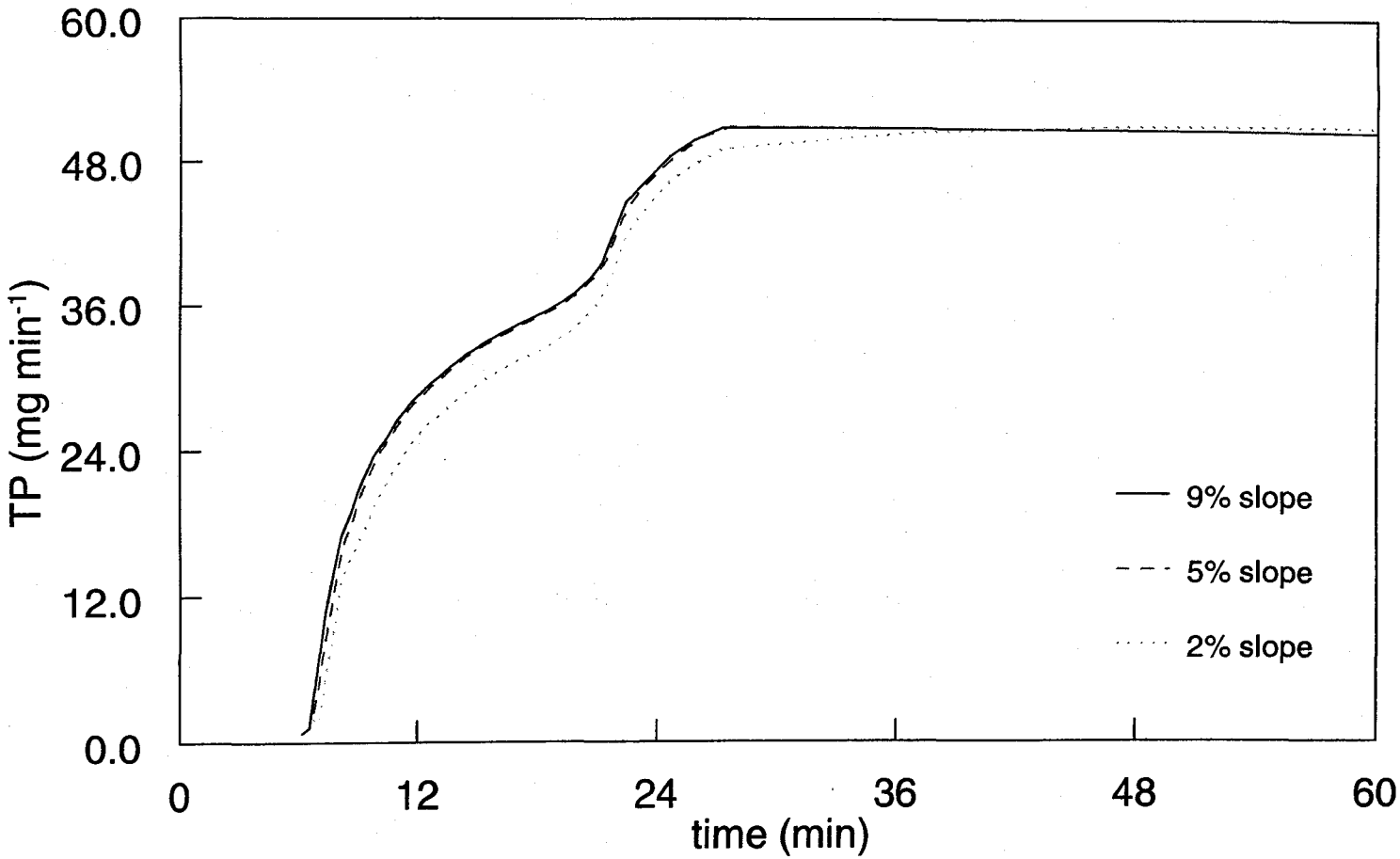

Figure 2.23. Opus2Z simulation of the impact of slope on total phosphorus runoff concentration per unit discharge from the vegetative filter strip box. *Starting point fis where Opus2Z output flow rate is stabilized.

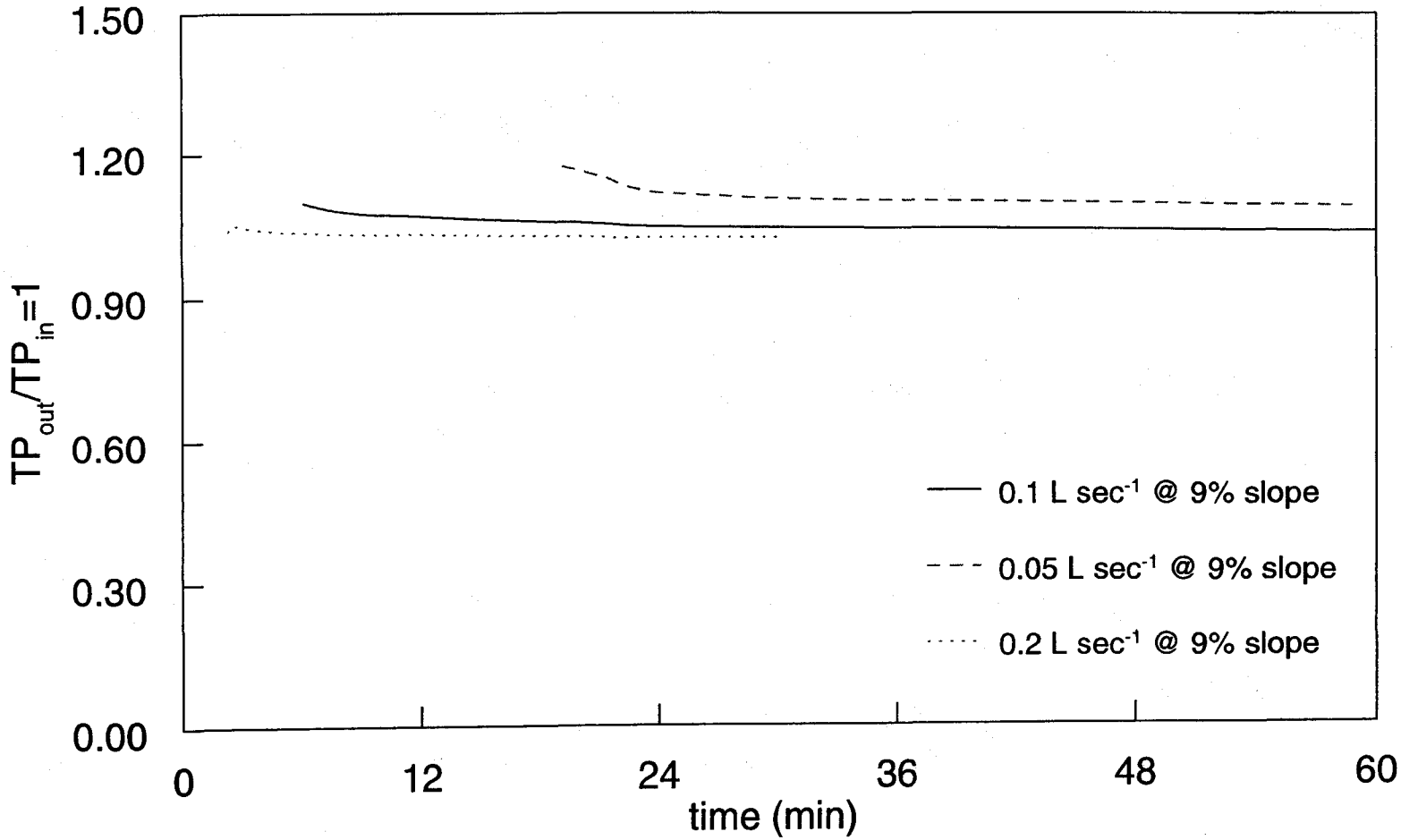

Figure 2.24. Opus2Z simulation of the impact of flow rate on total phosphorus runoff concentrations from the vegetative filter strip box. *The starting point is where the Opus2Z output flow rate stabilizes.

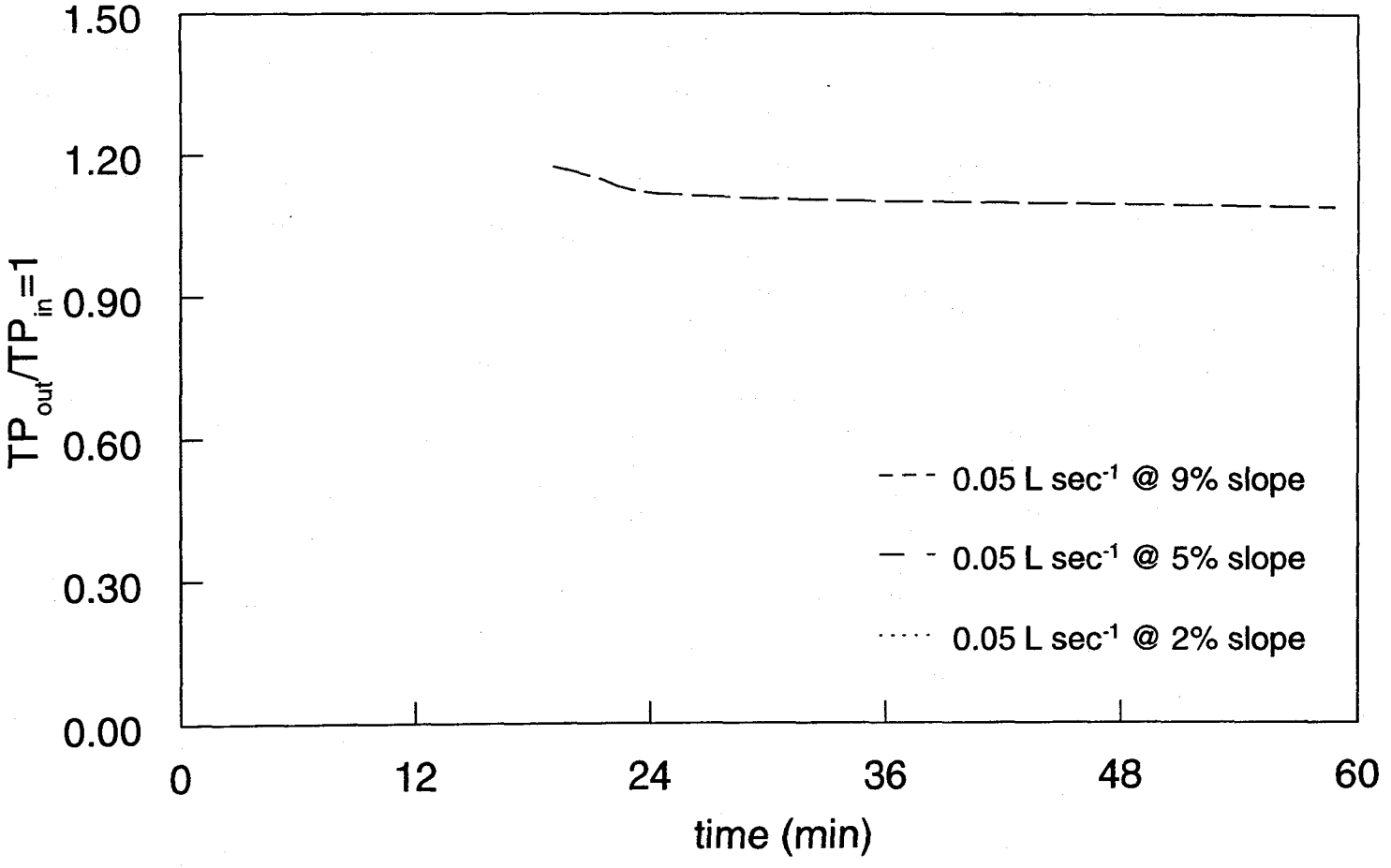

Figure 2.25. Opus2Z simulation of the impact of slope and flow rate on total phosphorus runoff concentrations from the vegetative filter strip box.
*Starting point is where Opus2Z output flow rate stabilizes.
**The three lines are coincident.

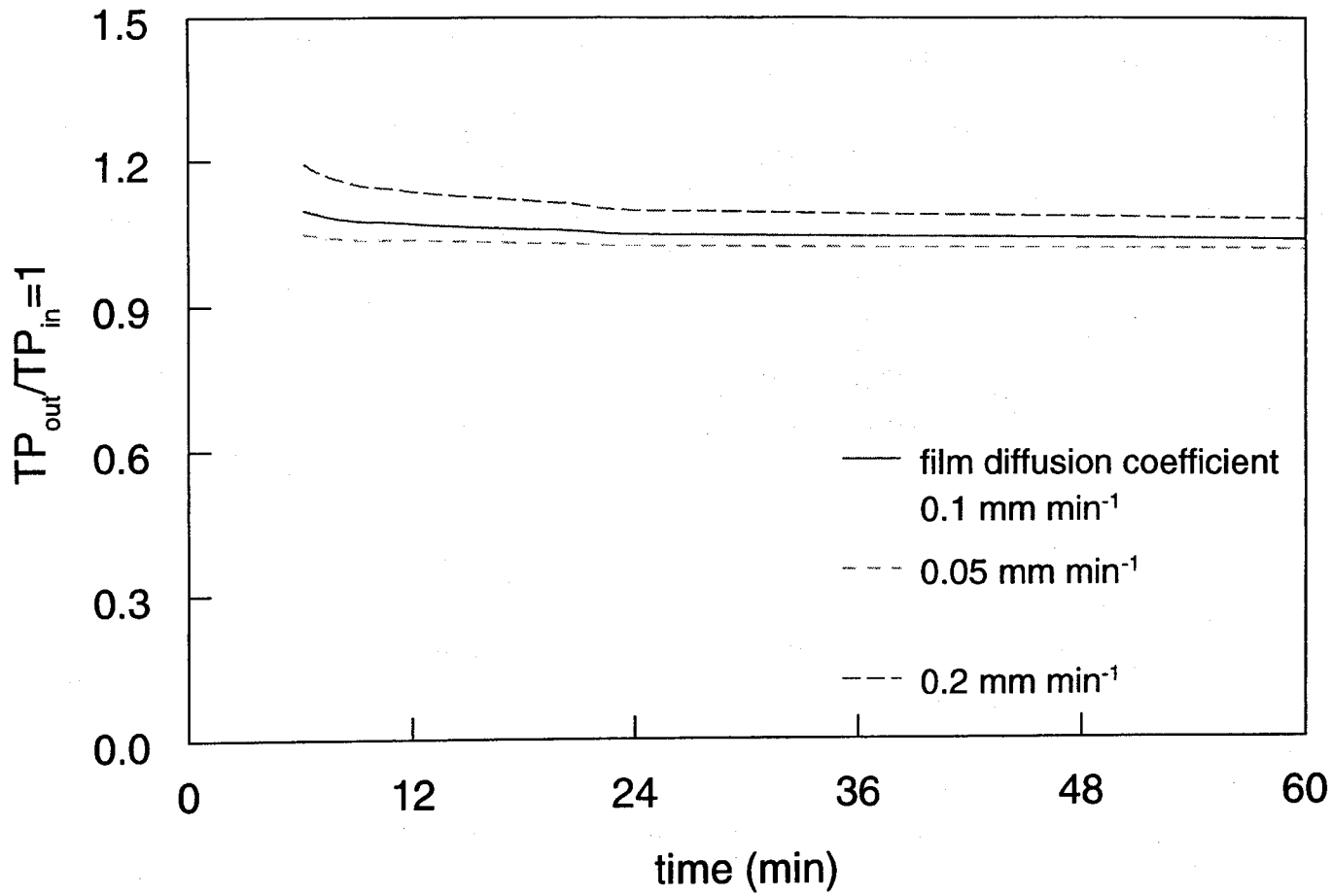

Figure 2.26. Opus2Z simulation of total phosphorus runoff concentrations variation with film diffision coefficients for the vegetative filter strip box distance.

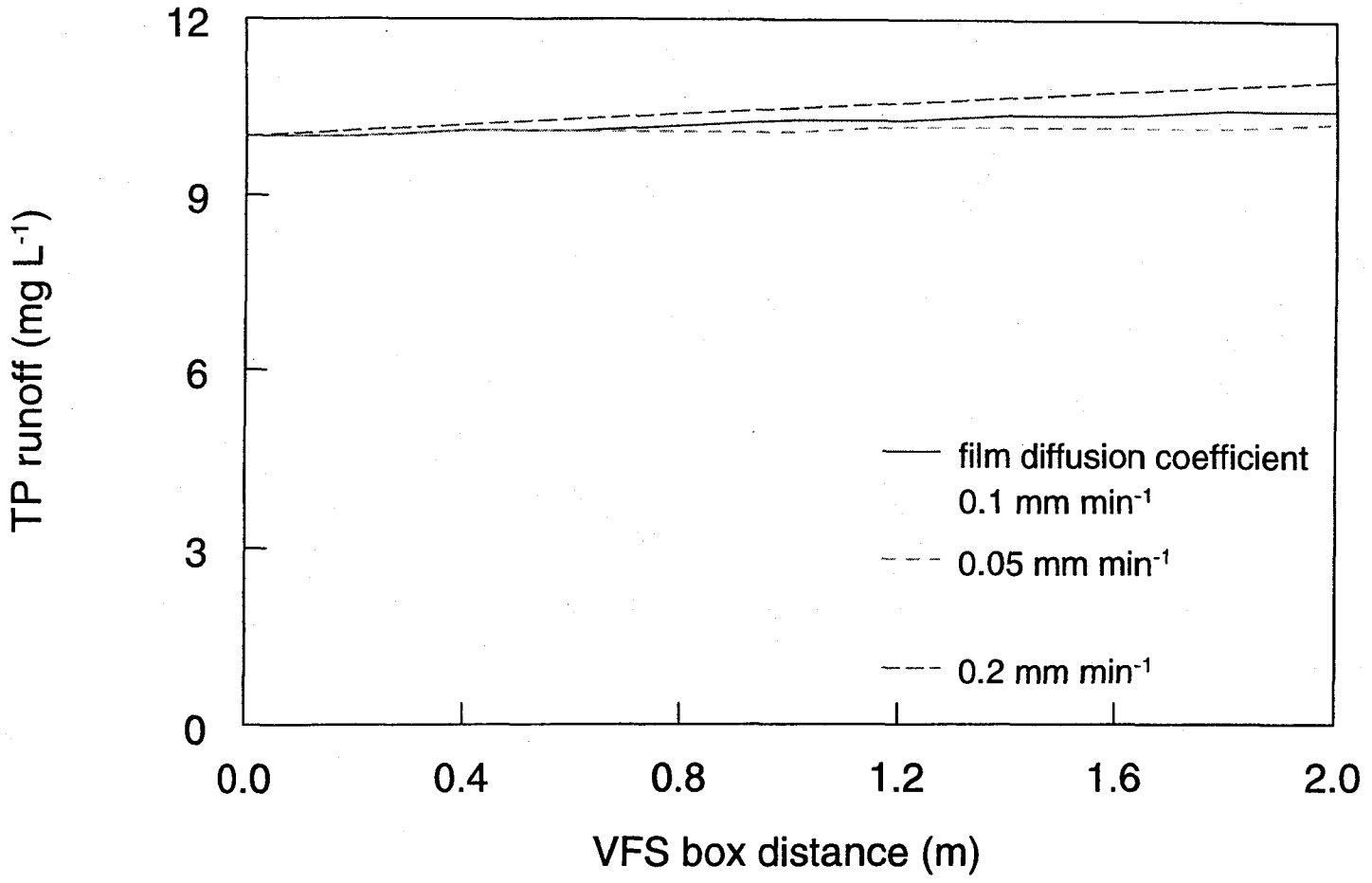

Figure 2.27. Opus2Z simulation of total phosphorus runoff concentrations variation with film diffision coefficients for the vegetative filter strip box distance after 15 minutes.

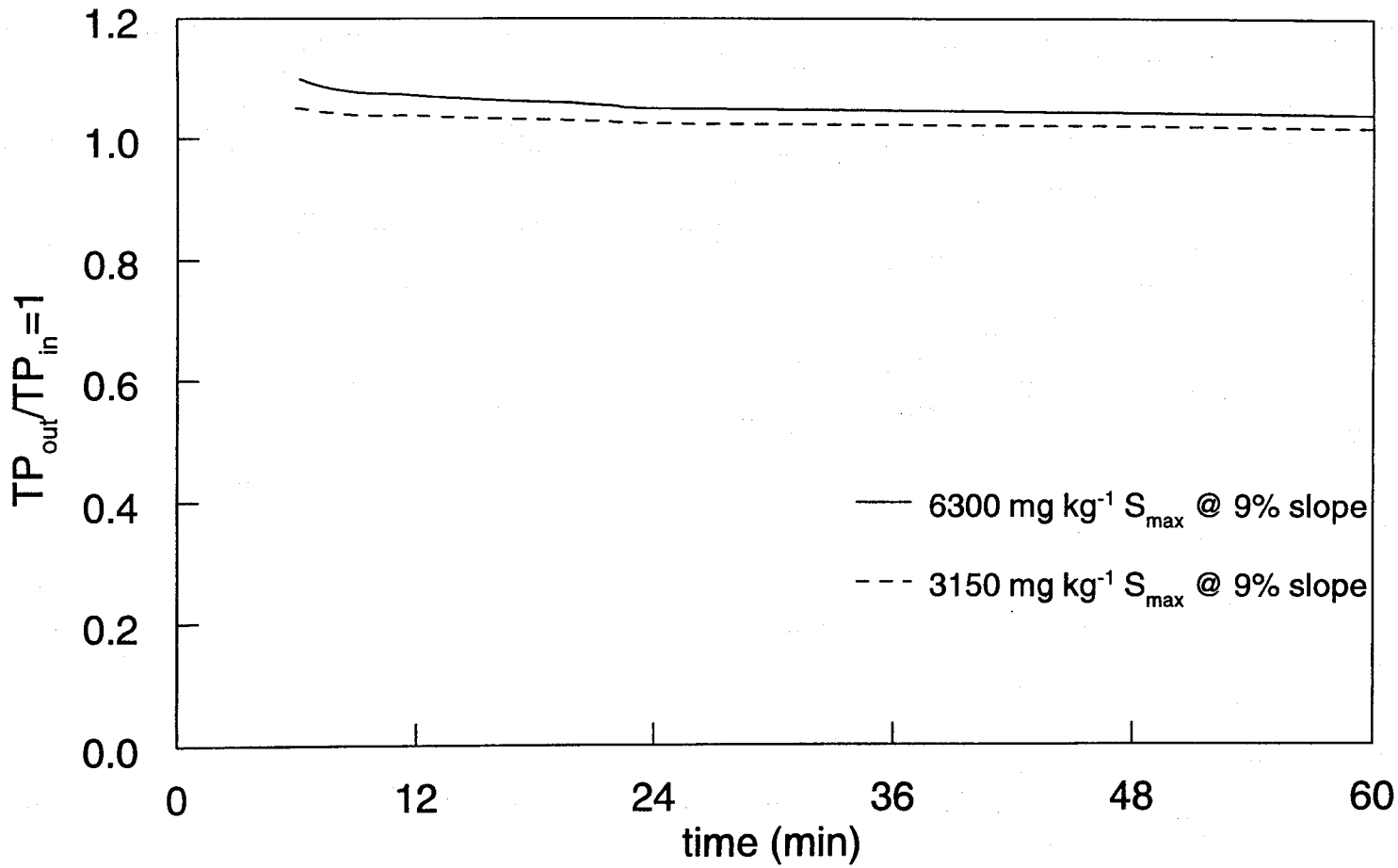

Figure 2.28. Opus2Z simulation of the impact of S_{max} on total phosphorus runoff concentrations from the vegetative filter strip box.
*Starting point is where Opus2Z output flow rate stabilizes.

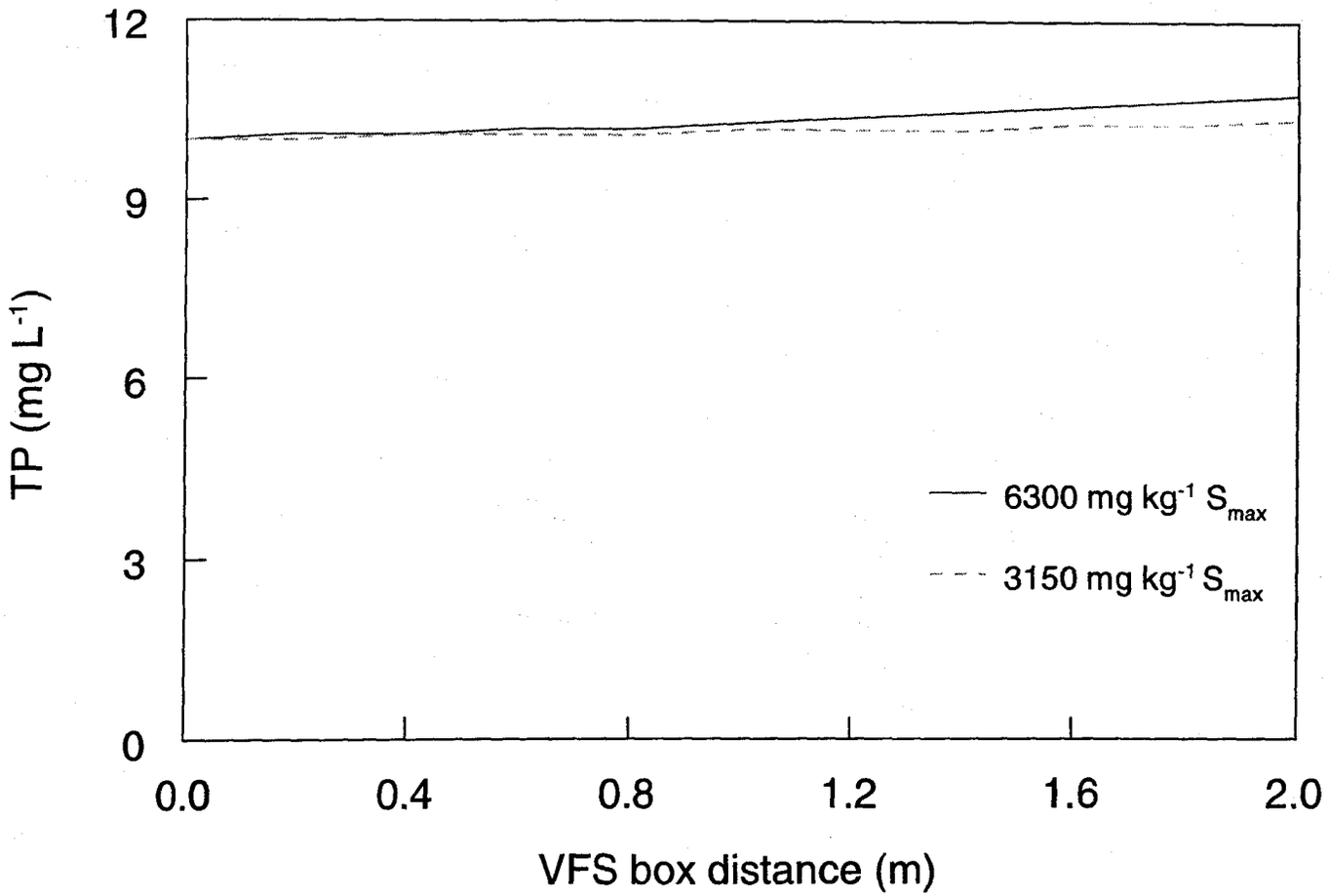

Figure 2.29. Opus2Z simulation of the impact of S_{max} on total phosphorus runoff concentrations for the vegetative filter strip box distance after 15 minutes.

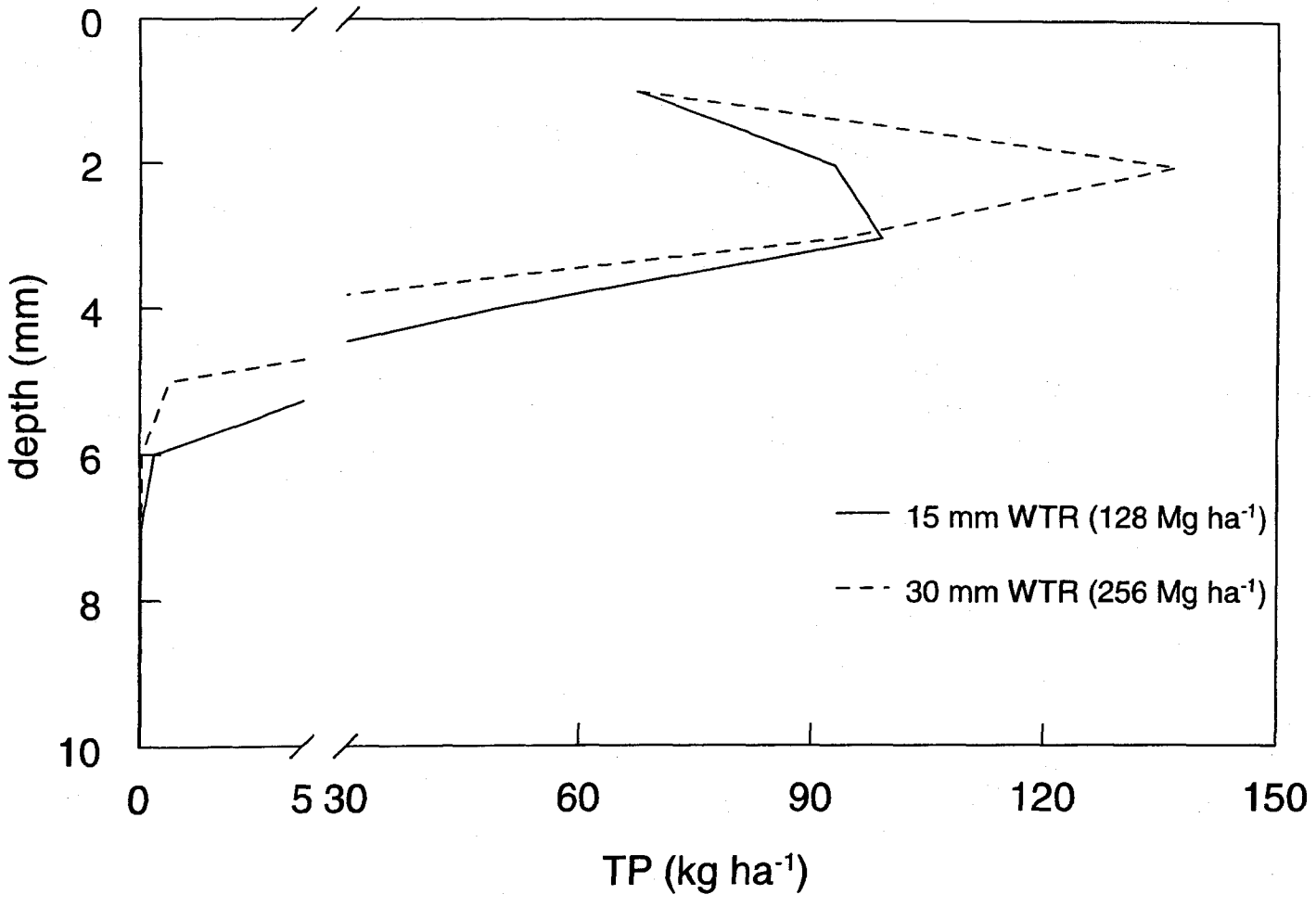

Figure 2.30. Opus2Z simulation of the impact of water treatment residual thickness on total phosphorus subsurface concentrations in a vegetative filter strip box after one runoff event.

Table 2.2. Hydraulic property results of the Butters and Duchateau analysis.

vG-van Genuchten BC-Brooks-Corey, θs-saturated volumetric water content, θr-residual volumetric water content, α-is the angle between the flow direction and the vertical axis, n-is a fitting parameter related to the tortuosity and connectivity of the capillary tubes, l is a fitting parameter, and K_s is the saturated hydraulic conductivity.

Treatment	Depth cm	Model	θ_S	θ_r	α cm^{-1}	n	l	K_S cm min^{-1}
0 Mg ha^{-1} WTR	0-5	vG	0.484	0.2072	0.03568	2.530	0.5136	0.04
		BC	0.484	0.2052	0.12	0.6925	0.2642	0.04
		vG	0.484	0.2069	0.3720	2.173	0.3655	0.04
		BC	0.484	0.1934	0.12	0.4077	0.2288	0.04
	7-11	vG	0.489	0.1950	0.03204	2.620	5.086e-4	0.05
		BC	0.489	0.1850	0.10	0.4739	1.309e-3	0.05
0 Mg ha^{-1} WTR	0-5	vG	0.494	0.154	0.02571	2.292	1.430	0.04
		BC	0.494	0.1412	0.10	0.4539	0.7758	0.04
		vG	0.494	0.1543	0.03152	2.516	0.4418	0.04
		BC	0.494	0.1515	0.10	0.6783	0.07121	0.04
	7-11	vG	0.493	0.1671	0.02891	2.724	0.04546	0.05
		BC	0.493	0.1608	0.10	0.5588	1.772e-3	0.05
64 Mg ha^{-1} WTR	0-5	vG	0.544	0.2344	0.03464	2.072	2.507	0.11
		BC	0.544	.2186	.125	0.3960	2.472	0.11
		vG	0.544	0.232	0.04832	1.697	1.702	0.11
		BC	0.544	0.2192	0.125	0.4006	2.393	0.11
		vG	0.544	0.2343	0.03948	1.935	2.866	0.11
		BC	0.544	0.2113	0.125	0.3498	3.274	0.11
	7-11	vG	0.458	0.2249	0.03526	3.177	0.2721	0.05
		vG	0.458	0.2247	0.04811	2.286	0.1157	0.05
		BC	0.458	0.2237	0.125	0.7506	0.06479	0.05
64 Mg ha^{-1} WTR	7-11	vG	0.458	0.2244	0.04567	1.903	0.8409	0.05

Treatment	Depth cm	Model	θ_S	θ_r	α cm^{-1}	n	l	K_S $cm\ min^{-1}$
		BC	0.458	0.2187	0.14	0.4805	0.8444	0.05
64 Mg ha^{-1} WTR	0-5	vG	0.45	0.166	0.03321	2.325	0.7874	0.10
		BC	0.45	0.160	0.10	0.5295	0.6883	0.10
		vG	0.45	0.166	0.03112	2.315	1.187	0.10
		BC	0.45	0.1603	0.10	0.5383	0.9315	0.10
		vG	0.45	0.1652	0.03591	2.979	1.836e-3	0.10
		BC	0.45	0.1642	0.10	0.8663	1.023e-3	0.10
	7-11	vG	0.494	0.1683	0.02191	2.005	1.698	0.05
		BC	0.494	0.1477	0.10	0.3814	1.225	0.05
		vG	0.494	0.1684	0.02818	2.016	0.3418	0.05
		BC	0.494	0.1479	0.10	0.3547	0.1053	0.05
256 Mg ha^{-1} WTR	0-5	vG	0.497	0.1681	0.3478	2.369	0.1564	0.10
		BC	0.497	0.1667	0.08	0.7928	0.2037	0.10
		vG	0.497	0.1664	0.03125	1.852	1.424	0.10
		BC	0.497	0.1544	0.083	0.4513	1.731	0.10
	7-11	vG	0.435	0.1579	0.02833	2.237	0.3766	0.05
		BC	0.435	0.1457	0.13	0.4349	1.403e-4	0.05
256 Mg ha^{-1} WTR	0-5	vG	0.526	0.2225	0.04749	2.273	1.919e-3	0.14
		BC	0.526	0.2189	0.147	0.6358	8.117e-4	0.14
		vG	0.526	0.2232	0.5001	2.326	0.2827	0.14
		BC	0.526	0.2206	0.147	0.6339	0.1015	0.14
256 Mg ha^{-1} WTR	7-11	vG	0.49	0.1895	0.04599	1.786	0.4286	0.05
		BC	0.49	0.1775	0.143	0.4092	0.5548	0.05

Treatment	Depth cm	Model	θ_S	θ_r	α cm^{-1}	n	l	K_S $cm\ min^{-1}$
		vG	0.49	0.1889	0.02786	1.820	4.789	0.05

Note: In the Brooks-Corey form, $\alpha=|1/h_e|$ where h_e is the air-entry pressure.

Chapter III

Water Treatment Residual Effect on Phosphorus Movement in a Sandy Soil: A Column Study

Soil Characteristic's Effect on Phosphorus Movement

In many soils, P content is greatest in the surface horizons, when compared to subsoil, due to greater biological activity, fertilizer addition, fixation of P, and organic material residing in the surface layers (Chapman and Coombe, 1997). King et al. (1990) found that surface soil P concentration (0-0.5 m depth) was greater after effluent application at a field site versus a concentration found in a laboratory sorption experiment. Mansell et al. (1991), Nair et al. (1998), and He et al. (1999) have demonstrated P sorption with soil depth for several soils.

Soil parent material, texture, and management practices, structure, organic matter, clay type, and type of fertilizer source contribute to soil P content variation. Phosphorus is more susceptible to movement through sandy soils with low P sorption capacities and with preferential flow through macropores and earthworm holes (Bengston et al., 1992; Sharpley and Syers, 1979). Djodjic et al. (1999) found that leached P loads from clay columns were higher than the P loads from sand columns with the dissolved P comprising the predominant form. Most soils contain approximately 50-75% inorganic P, but it can range from 10-90% (Chapman and Coombe, 1997). Castro and Torrent (1998) stated that increasing soil clay and Fe and Al oxides contents increased the amount of phosphate sorbed. A soil's P sorption capacity may be low due to predominately negatively charged surfaces and the complexing of Al and Fe by organic matter (Duxbury and Peverly, 1978; Miller, 1979). Several studies (Vyas, 1964; Gaur, 1969; Nair et al., 1998; Atalay, 2001) have demonstrated P sorption by soils in the company of organic residues.

Phosphorus Sorption

Phosphate is sorbed to materials by replacing a hydroxide compound. This reaction is considered to be a polymerization reaction in which deprotonation and dehydration occur. Eventually a polymeric ring with six Al ions bound by binuclear hydroxide bridges is formed (Sims and Ellis, 1983). As the polymer-ring ages, it expands by the incorporating hydroxyl groups from its edges into structural hydroxyls in the double hydroxide bridge. Anions can replace nonstructural hydroxyl groups because the hydroxyl groups are singly bonded. The anions can then be neutralized by the addition of H ions. This process eventually leads to a decline in P sorption when less single bonded hydroxyl groups are present on the particle's edge as they become structurally double bonded. Two hydroxyl bonds with Al would have to be broken for ligand exchange to occur. The unlikelihood of this happening results in a decrease in P sorption with time (Sims and Ellis, 1983).

In the characterization of P sorption for use in HYDRUS-1D, a linear model was used to approximate the partitioning coefficient of sorption to soil since the concentrations for the column and greenhouse experiments lie in the linear portion of the sorption isotherm. Figure 3.1 illustrates the Langmuir and linear isotherms fit to the batch data. The batch experiment used soluble P concentrations from 0.5 to 200 mg P L^{-1}. The linear model is commonly used to convey chemical transport and is expressed as:

$$C_s = K_d C_l \qquad [3.1]$$

where

C_s is the P sorbed to the solid phase (mg mg^{-1}),

K_d is the partitioning coefficient related to the bonding energy (L mg^{-1}), and

C_l is the equilibrium P concentration in the liquid phase (mg L^{-1}).

A Langmuir isotherm fits the sorption data when soluble P concentrations were greater than 100 mg P L^{-1}. Ippolito (2001) also found that the Langmuir isotherm best fits high concentrations of soluble P.

Phosphorus retention by materials is important in order to understand the environmental fate of P. Although soils have a large capacity to sorb P, P may be limited by the sorption potential of soil colloids (He et al., 1988). Heil and Barbarick (1989) stated that the age, pH, particle size fraction, surface area and P availability would impact the sorptive capacity of WTR. Sorptivity is an all-encompassing indicator of the P sorption capacity of soils (Holford, 1979; He et al., 1988; Atalay, 2001). Phosphorus sorption by soil or other materials is usually determined by batch experiments in which the solid material is equilibrated with solutions of known P concentrations. Ippolitio et al. (2003) demonstrated through SEM-EDS images that P-Al complexes formed during batch experiments with a biosolids-WTR combination. Scanning electron microscopy-electron dispersive spectrocopy images were used in this research to identify whether P-Al complex images differed for varying soluble P concentrations.

Electron Microprobe Analysis

Kumar (1994) used electron microprobe analysis on apatite and fertilized soil grains to identify residual P compounds and found no difference between them. Ippolito et al. (2003) was able to use electron-microprobe analysis using wavelength dispersive spectroscopy (EMPA-WDS) to show that P was associated with the WTR Al-fraction and not the Ca-fraction. These authors suggest that the P is probably chemisorbed to the Al in

the WTR. Galarneau and Gehr (1997) found that a minimum of 2200 mg P L^{-1} orthophosphate concentration at pH 7 is needed to be in equilibrium with $Al(PO_4)$. Sawhney (1973) used electron microprobe analysis to identify P precipitates in soils. This author found that soil phosphates were complexing with Al, Fe and Si. Samadi and Gilkes (1999) used scanning electron microscopy-electron dispersive spectroscopy (SEM-EDS) for soils that contained mostly Al, Si, Fe and Ca. They found that P was not associated with these elements but surface area and extractable Al-fraction accounted for 43% of the variation in 0.5 M NH_4F-soluble P. Pierzynski et al. (1990a) used a transmission electron microscopy with EDS to identify that P was associated with Al, Si, Ca, and Fe. These authors (1990b) also found that Al and Si were the dominant elements associating with P due to their higher concentrations in soils than Ca, Fe, or Mn.

Objectives

The objectives to be addressed in this chapter are:

1. Identify whether columns with WTR broadcast on the soil surface will retard P transport compared to the soil alone.
2. Determine whether the columns with WTR on the surface have lower effluent soluble P concentrations than the columns with only soil.
3. Observe if EMPA-WDS images indicate the presence of P-Al complexes differently for various soluble P concentrations.

Materials and Methods

Water Transport Theory

The HYDRUS-1D (Simunek et al., 1998) model can simulate water and solute movement in one-dimensional media. The linear sorption model was used in HYDRUS-1D. HYDRUS-1D numerically solves Richard's (1931) equation for variably-saturated water flow and convection-dispersion type equations for solute flow. Richards' equation is based on dynamic, one-dimensional form of soil-water conservation with Darcian flux [eq.2.2]. The value q is described by Darcy's law, which relates flux to the gradient of the total potential (H) as follows (Smith, 1992):

$$q = -K(\theta)\frac{\partial H}{\partial z} \qquad [3.2]$$

where

K is the hydraulic conductivity (L T^{-1}),

z is the depth from surface (L),

H is the total soil (gravitational and matric) potential ($\psi + z$), and

ψ is the capillary potential of soil water (L) so that

$$\frac{\partial H}{\partial z} = \frac{\partial \psi}{\partial z} + 1 \qquad [3.3]$$

The water flow portion of the model allows for set head and flux boundaries. The theory of transport that will be used to study the movement of labile P allows for nonlinear equilibrium reactions between the solid and liquid phases. Solute transport is treated as an advection-dispersion process described by eq. [3.4].

$$\frac{\partial}{\partial t}(\rho_b C_s + \theta C_l) = \frac{\partial}{\partial x}\left[\theta D \frac{\partial C_l}{\partial x}\right] - \frac{\partial}{\partial x}[qC_l] \qquad [3.4]$$

where

D is the effective diffusion-dispersion coefficient ($L^2 T^{-1}$) and is expressed by eq. [3.5].

$$\theta D = D_L|q| + \theta D_w \tau_w \quad [3.5]$$

where

D_w is the molecular diffusion coefficient in free water (L2 T-1),

D_L is the longitudinal dispersivity (L) and

τ_w is a tortuosity factor in the liquid phase (-).

The tortuosity factor for the liquid phase is evaluated in HYDRUS-1D as a function of the air and water contents.

Column Components

Prior to the leaching studies, soil and WTR practice columns were independently leached with water to obtain a flow rate that would not allow for ponding. Solution dispersivity was determined using yellow #5 dye in the practice columns that had WTR broadcast on the surface of the soil and the soil alone (Figures 3.2 and 3.3). Figures 3.2 and 3.3 illustrate the convection-dispersion model fit to the yellow dye solution breakthrough curve. The best-fit dispersion (D) and velocity (V) parameters yield the estimated dispersivity (D/V = 0.48 cm) for use in the P modeling. The pore water velocity and pore volume determinations were calculated by the following equations, respectively. The average PWV is expressed as:

$$PWV = \frac{q}{\theta} \quad [3.6]$$

where

q is the flux of the solution (cm d^{-1}) and,

θ is the volumetric soil water content..

The pore volume (PV) was established by:

$$PV = \theta \pi r^2 h \qquad [3.7]$$

where

r is the radius of the column, and

h is the height of the material in the column (cm).

From the average pore water velocity (PWV) [eq. 3.6] and dye dispersivity, it was determined that 12 pore volumes eq. [3.7] were needed to disperse the 20 mL of 100 mg P L^{-1} solution. A column pore volume was approximately 1040 mL. An initial pore volume was leached in order to obtain background P concentrations. The soil-WTR combination has a smaller velocity and dispersivity due to the inherent physical characteristics of the WTR, i.e. the WTR has a saturated volumetric water holding capacity of 60% (versus 40% for soil). Since the column leaching study uses 100 mg P L^{-1} it is reasonable that HYDRUS-1D can use either of the linear or Langmuir isotherms as evidenced by Figure 3.1 where their approximations are compared.

The columns consisted of vertically oriented schedule 40 PVC pipes (25.4-cm length by 15.2-cm diameter) filled to a height of 15 cm. The soil used is an unnamed Aridic Argiustoll collected from the top 15 cm of a site adjacent to a feedlot in northern Colorado. The collection site did not have prior manure applications and had not received runoff from cattle areas. The WTR was collected in fall, 2001 from the Fort Collins Municipal Water Facility. Both the WTR and the soil are considered to be random samples since they are each composites of larger samples.

As determined from Chapter Two, the middle WTR rate (64 Mg ha^{-1}) that lies within the most effective range (32-128 Mg ha^{-1}) for P sorption per mass was used as the ideal WTR rate for the column study. Each column contained 3600 g of soil or soil with WTR. The WTR was broadcast on the surface of three columns and comprises the top 3.0 cm of each treated column. The WTR treatment then consisted of 150 g WTR broadcast on 3450 g soil. The experiment was run in triplicate for a total of six columns, three columns with soil and WTR and three columns with soil only. The bottom portion of the column was screened with six layers of fiberglass window screen for ready removal of water.

A mariotte bottle was used to deliver 0.005 M KCl solution that was leached through the column until 12 pore volumes had been collected. The dripper head (Figure 3.4) had a connection so that the tubing will fit one end while the other end allowed the solution to flow freely into the needles. The connection had a stopcock so that a second dripper head could release 20 mL of 100 mg L^{-1} P (totaling 8.1 ug g^{-1}). Needles were not placed near the edges of the column to avoid an edge-effect. The solution-dispersing device's outer-holes were approximately 2 cm from the edge while the inner-holes were 1 cm apart. In total, there were 12 needles distributing solution. Due to the size of the hypodermic needles, the solution droplet impact on the soil was considered to be minimal. The water tension in the column was held at approximately -10 cm (between gravitational conditions (-10 cm) and field capacity (-33 cm)) to ensure that saturated conditions did not occur.

Column leachate was continuously collected from the bottom of each column for each 24 hour period and a composite sample was immediately analyzed for molybdate

reactive P (MRP) using the Molybdate Blue method (Murphy and Riley, 1962) (Table 3.1) and total dissolved P (TDP) by inductively coupled plasma-atomic emission spectroscopy (ICP-AES). After 12 pore volumes had been collected from the bottom of the columns, the column contents were carefully pushed out with a plunger and then sliced horizontally in one cm increments and air-dried for additional P analysis. To determine soil MRP within each depth increment, 50 g of soil were taken from a soil column layer composite. The air-dried soil was shaken with 250 mL 0.005 M KCl (made with deionized (DI) water) for 16 hours. The sample was centrifuged in 250-mL polypropylene bottles at 25°C at 10,000 rpm for 20 minutes. The filtrate was then analyzed for MRP. Total P (TP) analysis for the soil followed the digestion method by Kuo (1996).

Batch Studies

Batch studies were performed to determine P sorption isotherms for the unnamed Aridic Argiustoll and the WTR. For the soil P desorption isotherm, 1.0 g of soil per 25 mL of soluble P (Sims, 1997) was used and 1.0 g of WTR per 25 mL of soluble P was used for the desorption isotherm. These combinations were shaken for 24 hours in 50-mL polypropylene centrifuge tubes. The samples were centrifuged for 20 minutes at 10,000 rpm at 23°C. Each subsequent day after centrifugation, 5.0 mL of the filtrate was withdrawn and was replaced by 5.0 mL of DI water. The samples would be re-shaken; the procedure continued until no P was detectable as determined by the Molybdate Blue method. The soil desorption isotherm consisted of soil in 10 and 20 mg L^{-1} P solution that were shaken for 24 hours, 5 mL of solution was withdrawn, then 5 mL of 0.01 M KCl

was put into the sample vials and then the cycle started again until no P in solution could be detected by the molybdate blue method. The WTR desorption samples went through the same process as the soil but were placed in 250 and 500 mg P L^{-1} solution.

The sorption isotherms helped determine the retention of P by the soil and the WTR (Figures 3.1 and 3.5). For the soil and WTR sorption isotherms (Figures 3.1 and 3.5, respectively), six samples at five solution concentrations were selected. One g of material was placed in 25 mL of the appropriate solution, which contained 0.1 M KCl (made with DI water), into a 50-mL polypropylene centrifuge tube and was shaken for 16 hours. The samples were then centrifuged at 10,000 rpm for 20 minutes at room temperature. Five mL of the filtrate was withdrawn until the MRP was completed. Sorption isotherms were created by plotting the final P concentration in the liquid phase (C_l; mg L^{-1}) versus the concentration in the solid phase (C_s; mg kg^{-1}; determined from eq. [3.8]).

$$C_s = \frac{V_a(C_a - C_l)}{M} \qquad [3.8]$$

where

V_a is the volume added (L),

C_a is the concentration added (mg L^{-1}), and

M is the mass of soil material (kg).

The desorption isotherms (Figures 3.6 and 3.7) use an extension of eq. [3.8] to account for the volume withdrawn to measure P in solution (eq. [3.9]).

$$C_s = \frac{1}{M}[V_a(C_a - C_j) - \sum_{j=1}^{n} C_{j-1} V_j^w] \qquad [3.9]$$

where

C_j is the final liquid concentration (mg L^{-1}),

C_{j-1} is the final liquid concentration from the previous sample (mg L^{-1}), and

V_j^w is the volume withdrawn for the sample's liquid concentration (L).

Scanning Electron Microscopy-Electron Dispersive Spectroscopy

To identify elemental associations with P, the SEM-EDS, electron microprobe analysis using wavelength dispersive spectroscopy (EMPA-WDS) was used. Samples were placed in a monolayer in individual plastic boats that were 0.7 cm by 1.6 cm by 1 cm deep. The Acrylimet epoxy (South Bay Technology, Inc., San Clemente, CA) was carefully poured over the samples and cured for 24 hours at 25°C at 138 cm tension (Ippolito, 2001). The expoxy-coated samples were wet wheel-polished after being removed from the plastic boats. The samples were wet wheel-polished with an Exakt automated microgrinder using 800- and 1200-grit polishing paper, respectively, to remove approximately 0.15 mm of material. As per Ippolito (2001), the amount removed was about equal to half the diameter of the sample particles. The samples were then carbon coated in a vacuum evaporator (Kinney vacuum evaporator Model KDTG-3P). Samples were analyzed using a JEOL JXA-8900 Electron Microprobe analyzer (JEOL USA, Inc., Peabody, MA) at an accelerating voltage of 15 keV. These samples were magnified between 300x and 550x the original sample size. Backscattered electrons were used for collecting images of the sample surface.

Soil and Water Treatment Residual Characteristics

The same soil and WTR that were used for the greenhouse experiment were used for laboratory experiments. Their physical and chemical characteristics are listed in Table 2.1.

Results and Discussion

Isotherms

The concentrations of interest for this study lie in the lower portion of the linear model (Figures 3.1 and 3.5). The P partitioning coefficients (K_d's) for the soil and WTR were 27 and 161 L kg^{-1}, respectively when calculated using the linear model. The WTR linearized isotherm K_d (161 L kg^{-1}) is similar to the Opus2Z Langmuir isotherm S_{max} (6300 mg kg^{-1}) in that both account for P to highly sorb to the soil and WTR material. The sorption isotherms were not reversible (Figures 3.1 and 3.5 to 3.7). The results of Mansell et al. (1977) were similar to my experimental isotherm data. They stated that through unsaturated soil cores, the adsorption-desorption relationships were not reversible at equilibrium and were insufficient to describe the transport of orthophosphate (MRP). From the six days in which the desorption experiment took place, it was found that a total of 0.2% and 0.12% of P desorbed from the soil and WTR.

Scanning Electron Microscopy-Electron Dispersive Spectroscopy Image Analysis

The scanning electron microscopy-electron dispersive spectroscopy (SEM-EDS) images show that P complexes to the perimeter of a particle at lower concentrations and to the interior and exterior of a particle at higher P concentrations (Figures 3.8 to 3.13).

The results can be identified by the image color; the more intense the color, the more the element is present at that particular location or for black and white prints, the lighter colored locations indicate the presence of the respective element. Using EMPA-WDS, Ippolito et al. (2003) identified that P was complexing with the Al-fraction of the WTR. These authors also inferred that the P was most likely chemisorbed to Al because the samples were polished to remove half of the particle, thereby showing the interior of a particle.

With the SEM-EDS images showing that P resides in the interior of a particle at higher soluble P concentrations, it is likely that this P does not become resolubilized as readily as precipitated or sorbed P at the particle surface. The minimal P desorption results from the batch experiment discussed above indicate that since phosphate is tightly bound by Al^{3+} (Bohn et al., 1985; Lindsay, 1979), the P in the interior of a particle most likely will become susceptible to dissolution if the particle's interior becomes exposed. The P adsorption-desorption isotherms from the batch experiments demonstrated that the P sorption processs is hysteretic. From the P isotherms and SEM-EDS images, I would speculate that P dissolution kinetics is an extremely slow progression; only minimal P desorption was observed within the time frame of the batch experiment.

The SEM-EDS overlays (Figures 3.12 and 3.13) demonstrate that P is sorbed by Al more so than by Fe or Ca. In fact, by comparing the color intensities it does not appear that P sorption is related at all to Fe or Ca as indicated by being able to separate the corresponding elemental colors. For example, initially Al is red and P is blue but at high P concentrations (500 and 1000 mg P L^{-1}) when I overlay the two elements the color is pink. Because the red and blue cannot be separately distinguished in the overlay, it

indicates that P is associated with Al. By contrast, when Fe or Ca is overlain with P their individual colors can be distinctly identified. This could be a result of Al being present in excessively high concentrations and having a stronger bonding intensity than Fe or Ca to P. The most spectacular of these images is with the WTR at P concentrations of 500 and 1000 mg L^{-1} (Figures 3.13c1 to 3.13d2). In these images the P and Al colors merge together indicating that Al is the predominant element binding P. Castro and Torrent (1998) and Atalay (2001) found that increasing soil clay and iron and aluminum oxide contents sorbed more phosphate. Aluminum and Fe-enriched clays account for a significant portion of P sorption to colloids (Reddy et al., 1980; Durrera and Robarge, 1999; Bache and Williams, 1971). The WTR used for this study contained approximately 24,000 mg kg^{-1} Al and Fe as determined by ICP-AES analysis and is probably composed of amorphous aluminum oxides. The lower soil and WTR P concentrations may not have been able to show the Al-P association well or may have been non-existent due to the detection limit (1%) of the instrumentation.

Column Effluent Analysis

Due to the WTR linear K_d of 161 mL g^{-1}, it was likely that the columns treated with WTR would retard P movement. Neither the column with WTR or without WTR had P in the effluent throughout the leaching of 12 pore volumes (Table 3.1), as measured by the molybdate blue method.

Soil and Water Treatment Residual Phosphorus Analysis

Having divided the columns into 15 1-cm increments I was concerned that any differences in MRP concentrations with depth would be lost by comparing so many depths. As a result, I divided each of the columns into three zones; the first zone was from the first to the third cm, the second zone was from the fifth to the eighth cm and the third zone was from the 10^{th} to the 15^{th} cm. The fourth and ninth cm's were considered buffer zones and were not included in the statistical analysis. When the soil from the columns was analyzed for MRP, no significant difference (α=0.10) was found between the replicates within a treatment indicating that the columns were true replicates within a treatment (Figures 3.14 and 3.15). The first zone was significantly different (α=0.01) between the two treatments. The second zone was not significantly different between treatments (α=0.10). The third zone was significantly different (α=0.01) between treatments. Statistics were completed using SAS version 8e (2003).

The MRP results from the columns divided by depth increment were different for the treatments. The soil with WTR applied on the surface had low MRP in the top 3 cm's and had higher concentrations from 4 to 15 cm. The top three cm's most likely had low MRP concentrations because the WTR resided in the top three cm of each treated column. Due to the high K_d of the WTR and minimal propensity for desorption, the P was held tightly in the uppermost layers. Additional pore volumes dispersed P to greater depths resulting in higher MRP concentrations below the 3 cm depth. The untreated column's MRP concentrations increased to a depth of approximately 6 cm's and then decreased with increasing depth. Greater soil depth was necessary before the MRP concentration began to decrease due to K_d disparity between the soil and the WTR.

The same three-zone approach taken for MRP was used for TP statistical analysis. The top 3 cm of the treated columns retained more TP when compared to the untreated soil columns (Figures 3.16 and 3.17). The experimental data was not significantly different (α=0.01) for each zone within a treatment. There was a significant difference (α=0.05) between treatments for zone one. No significant difference (α=0.10) was found for zones two or three between treatments. Significance between treatments for zone one is reasonable considering that the WTR was surface applied and only resides in zone one. I would expect more TP to be retained in zone one by the WTR based on its P sorption capacity and minimal P desorption. The soil from the columns with the WTR had higher soil TP than the columns without the WTR. A higher TP concentration in the first zone would be expected because the WTR has a high P retention capacity (K_d=161 mL g^{-1}) compared to the soil (K_d=27 mL g^{-1}).

HYDRUS-1D Model Predictions

Figures 3.16 and 3.17 illustrate soil and WTR TP concentrations compared to the HYDRUS-1D model predictions. The experimental data were averaged for the three column replicates. The untreated soil column's experimental data show a center of tendency (maximum concentration) at 3.5 cm from the surface while the model predicted it to be at approximately 4.2 cm (Figure 3.16). HYDRUS-1D predicted 91% of the maximum TP concentration. The variance of distribution between the experimental data and the model demonstrates that the TP mass distribution was unable to be precisely predicted (Figure 3.16). The HYDRUS-1D model simulation predicted greater TP spread from 5.5 to 9.5 cm than was experimentally measured. While HYDRUS-1D accounted

for the total P mass put into the system (8.1 ug g^{-1}), 75% was accounted for by the experiment (6.11 ug g^{-1}). This may be due to the sampling of less than 100% of the cross sectional area of the column and having only applied the P at multiple discrete points resulting in less than 100% dispersion over the column's area.

The center of tendency for the soil columns with WTR was 3.54 ug P g^{-1} of material at 0.5 cm (the average of the 0-1 cm depth increment) while the model predicted it to be 2.9 ug g^{-1} of material at 1.8 cm's depth (Figure 3.17). Both the predicted and experimental data for the WTR treatment show that the first zone retains more P than the underlying zones (Figure 3.17). The model simulation's TP mass distribution accounted for all of the P put into the system (8.1 ug g^{-1}) while 84% was accounted for by the experiment (6.81 ug g^{-1}). The areas of high TP concentrations reside in the top 2.5 cm of the column (the WTR was in the top 3 cm) (Figure 3.17). The HYDRUS-1D model simulation predicted greater TP spread from 3.5 to 8 cm than was experimentally measured. As stated above, the method of P application and the sampling of less than 100% of the cross sectional column area could have affected the model's accuracy. Both treatments had experimental data TP concentrations slightly higher than the model had predicted. The difference in the center of tendencies and total mass distributions were insignificant (α=0.1) between the model predictions and the experimental data for both the treated and untreated columns. While HYDRUS-1D does not exactly predict P transport throughout the WTR, the batch desorption study reaffirms the negligible P movement in the WTR.

Conclusions

The columns with WTR broadcast on the surface retard P transport when compared to the soil alone as evidenced by soil and WTR TP and MRP data. The effluent MRP and TDP concentrations were higher in the columns with the WTR than from the soil columns without the WTR surface applied. This may have occurred due to desorption of P from the WTR or from the soil. The soil and WTR desorbs approximately 0.2% and 0.12%, respectively, within the six days of the batch experiment. The results of the column indicate that there must be adsorption capacity at the soil surface or a loss of P from solution will not be observed.

The soil and WTR sorption isotherms determined the P partitioning coefficients. The soil's K_d of 27 L mg^{-1} resulted in more P being distributed throughout the column than the column that contained WTR at the surface. The WTR had a K_d of 161 L kg^{-1} resulting in most of the P residing in the top 3 cm's of the column. Desorption isotherms demonstrated that the sorption process is not reversible and that the WTR used for this research does not readily release P within the time frame of the experiment.

The EMPA-WDS indicated the presence of phosphate complexes at varying soluble P concentrations and especially at the higher P concentrations. Through SEM-EDS images, P was identified as being associated with the Al-fraction of the WTR and not with Ca or Fe. At lower P concentrations, P is primarily sorbed to the perimeter of a particle and at higher concentrations is found at the perimeter and the interior of a particle. Together, the SEM-EDS images and desorption isotherms indicate that P held in the interior of a particle may be a reason why P desorbs at a different rate than it adsorbs to particles, reducing its availability for dissolution processes.

The HYDRUS-1D simulations modeled the soil and WTR P concentrations with greater than 80% accuracy. The model predicted that more P would be retained in the first 3.0 cm of the profile with the WTR surface applied. The TP experimental data agreed with the model predictions. The model prediction for the soil and WTR mass distribution accounted for 75% and 84% of the experimental data, respectively. The goodness of fit from the predicted data may have been limited by the sampling methodology using less than 100% of the column cross sectional area and the P having been applied discretely through hypodermic needles to less than 100% of the column cross sectional area. Twenty-four hour batch studies indicate negligible transport of P through the WTR at the column surfaces however, the results from the greenhouse study and the column study differ.

Since the columns and the greenhouse VFS boxes had more time for P equilibration, the conclusion that P must leach somewhat from soil/WTR with additional time is appropriate. The leaching study data demonstrates that there must be some P leaching otherwise all of the P should have remained in the top one cm approximately. Phosphorus would not have been able to sorb into the soil solution from the surface water (values less than 1.0 with the MRP data).

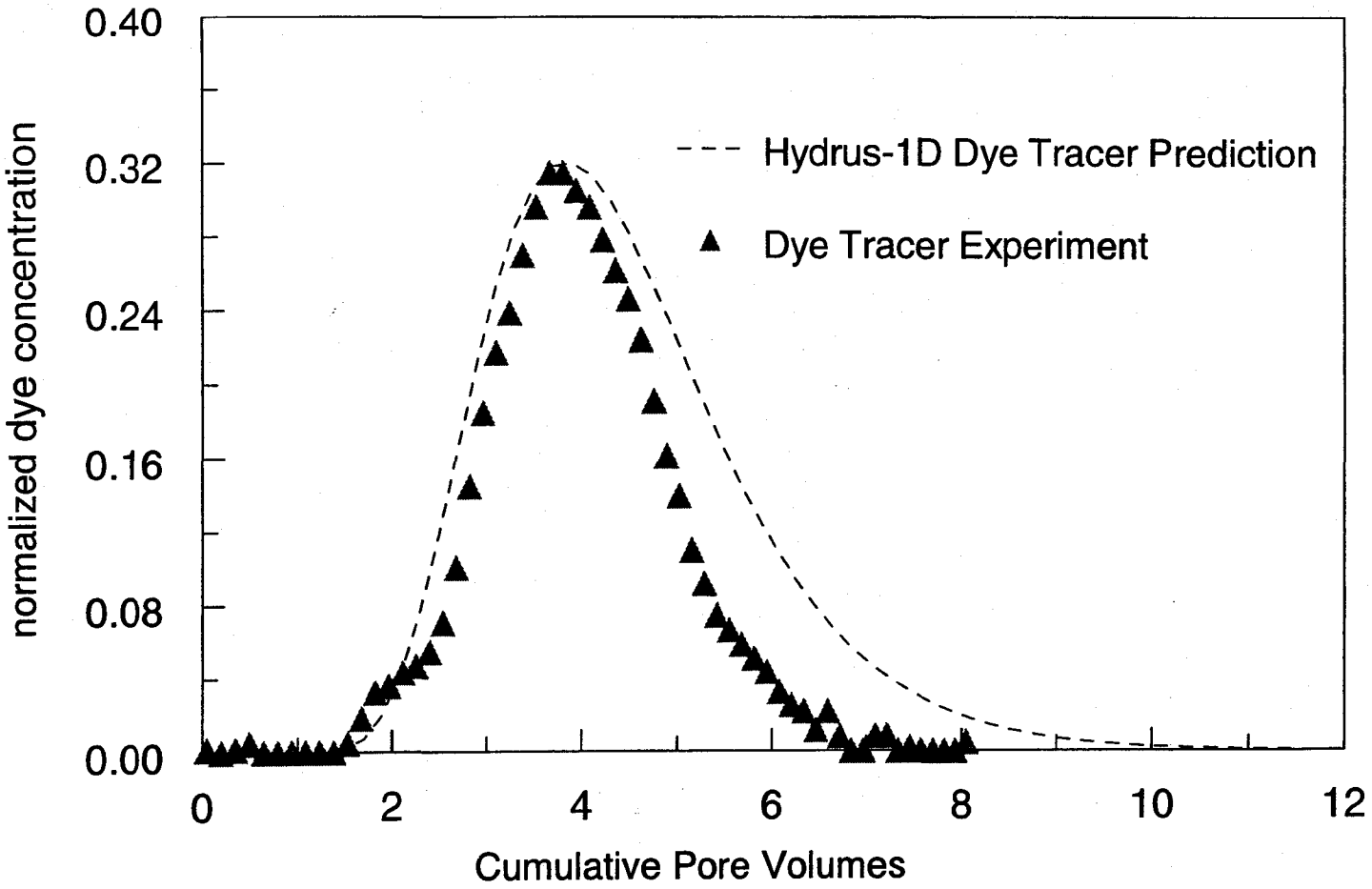

Figure 3.2. Soil dye tracer breakthrough curve (1 pore volume=1040 mL).

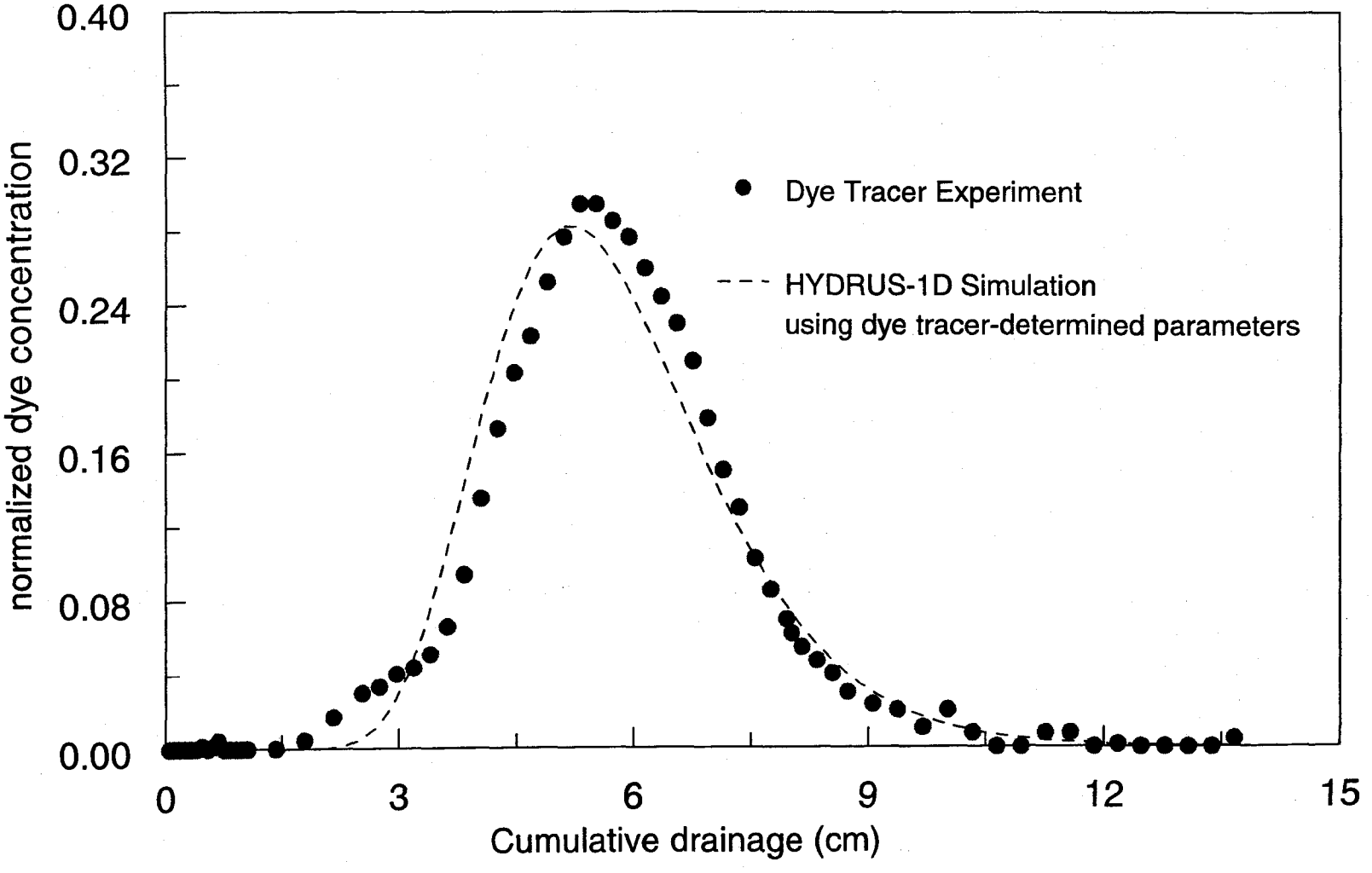

Figure 3.3. Soil and water treatment residual dye tracer breakthrough curve.

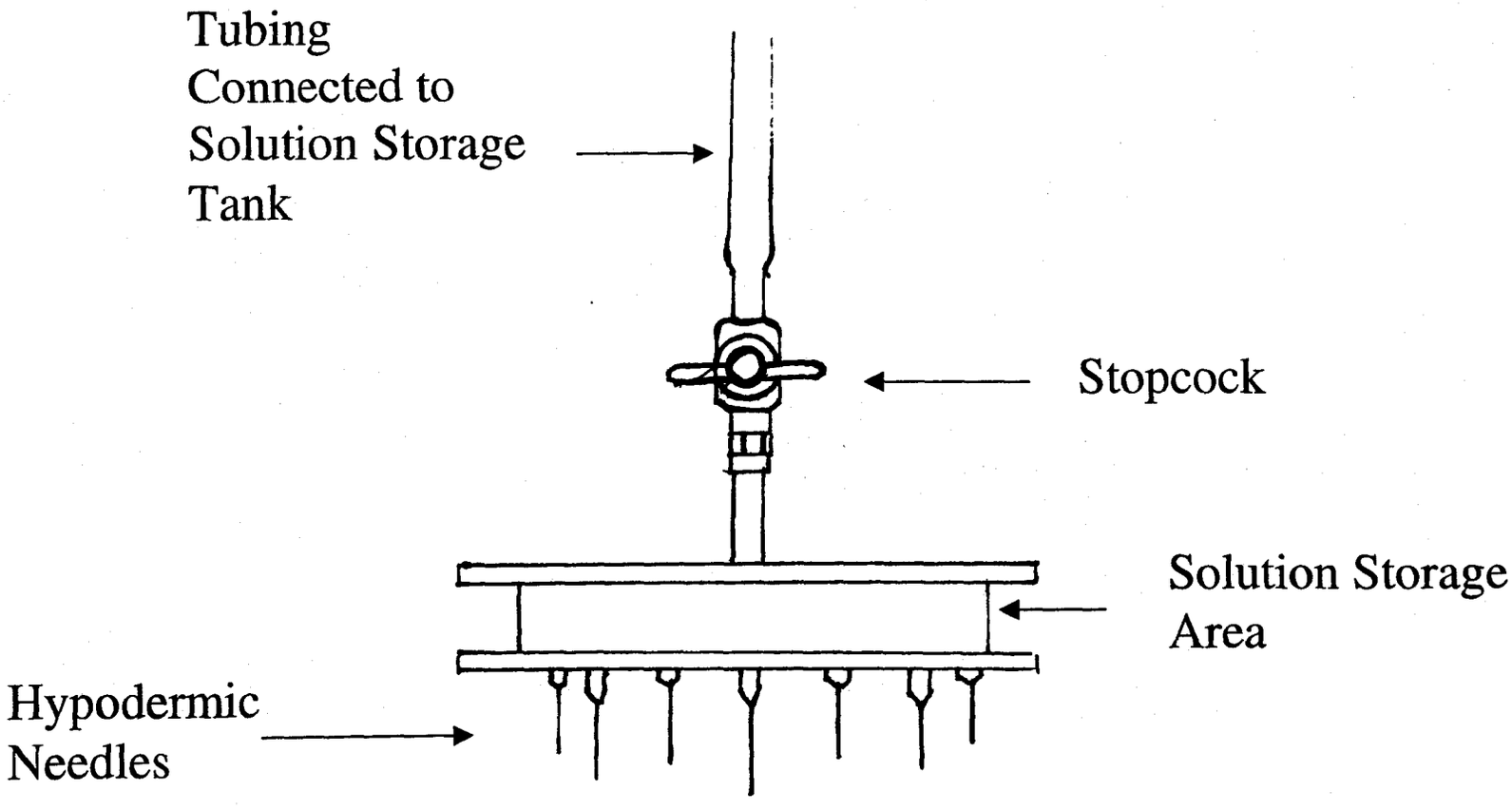

Figure 3.4. Column Dripper

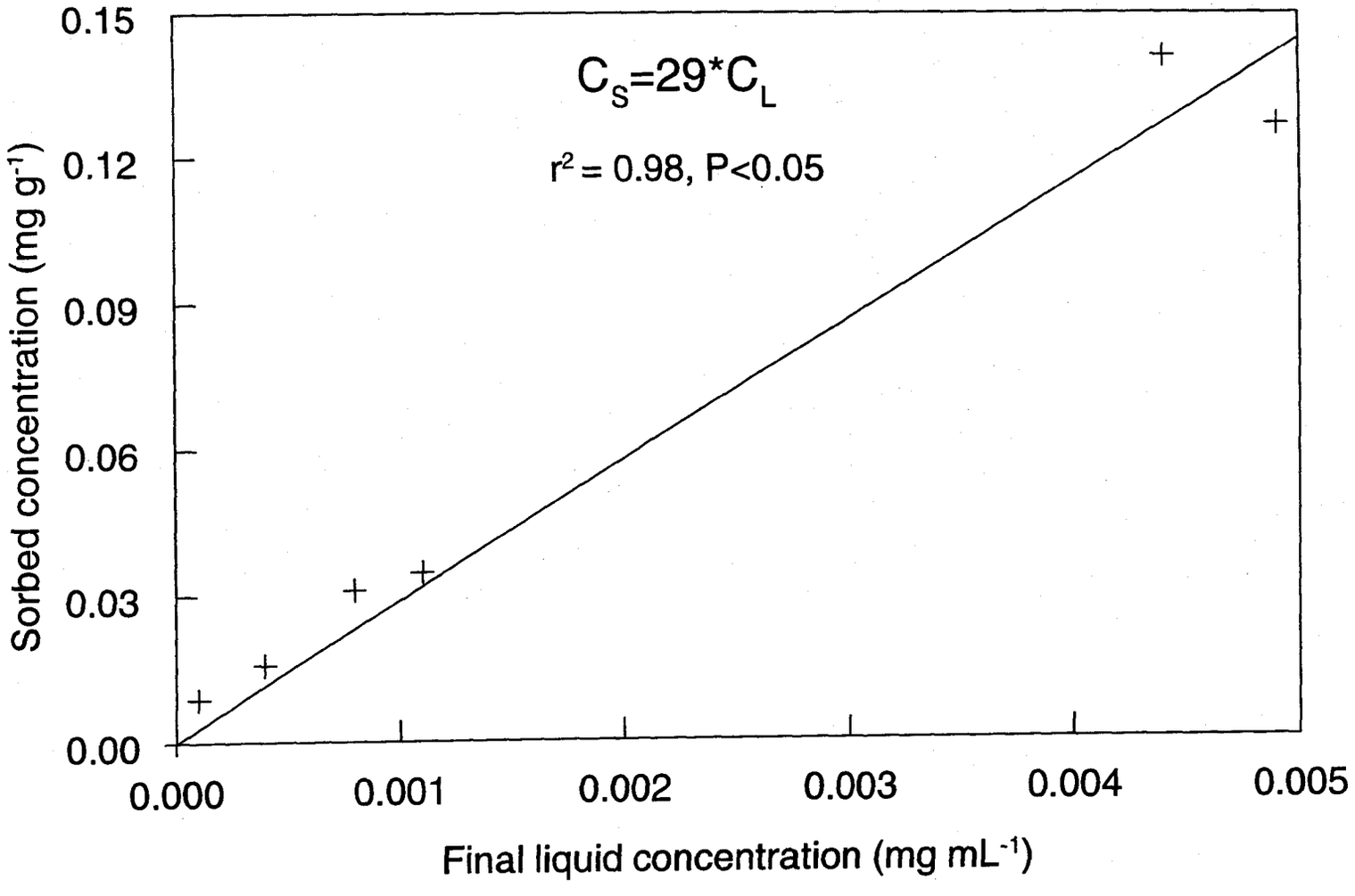

Figure 3.5. Soil phosphorus sorption linear isotherm.

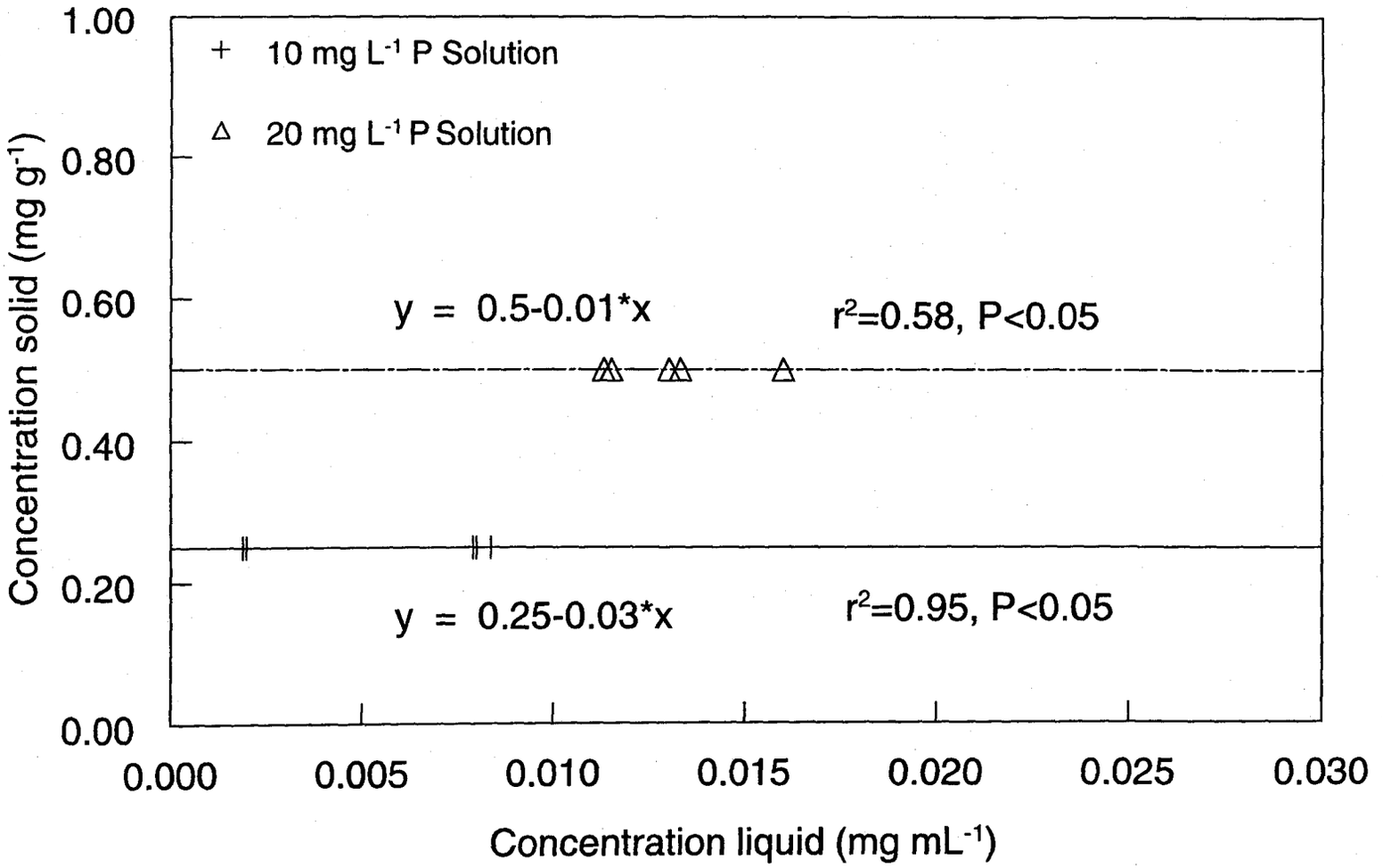

Figure 3.6. Soil phosphorus desorption isotherm.

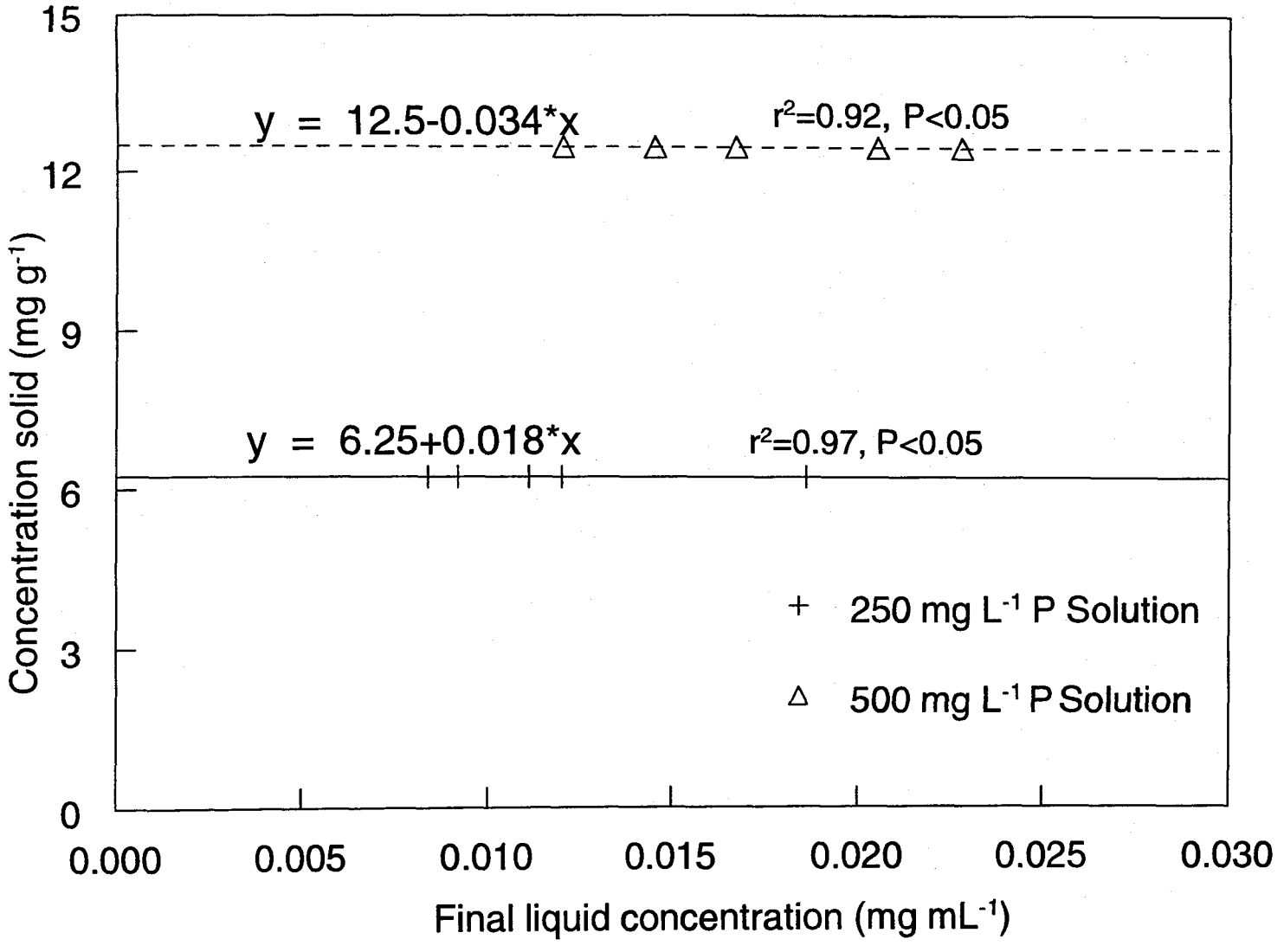

Figure 3.7. Water treatment residual phosphorus desorption isotherm.

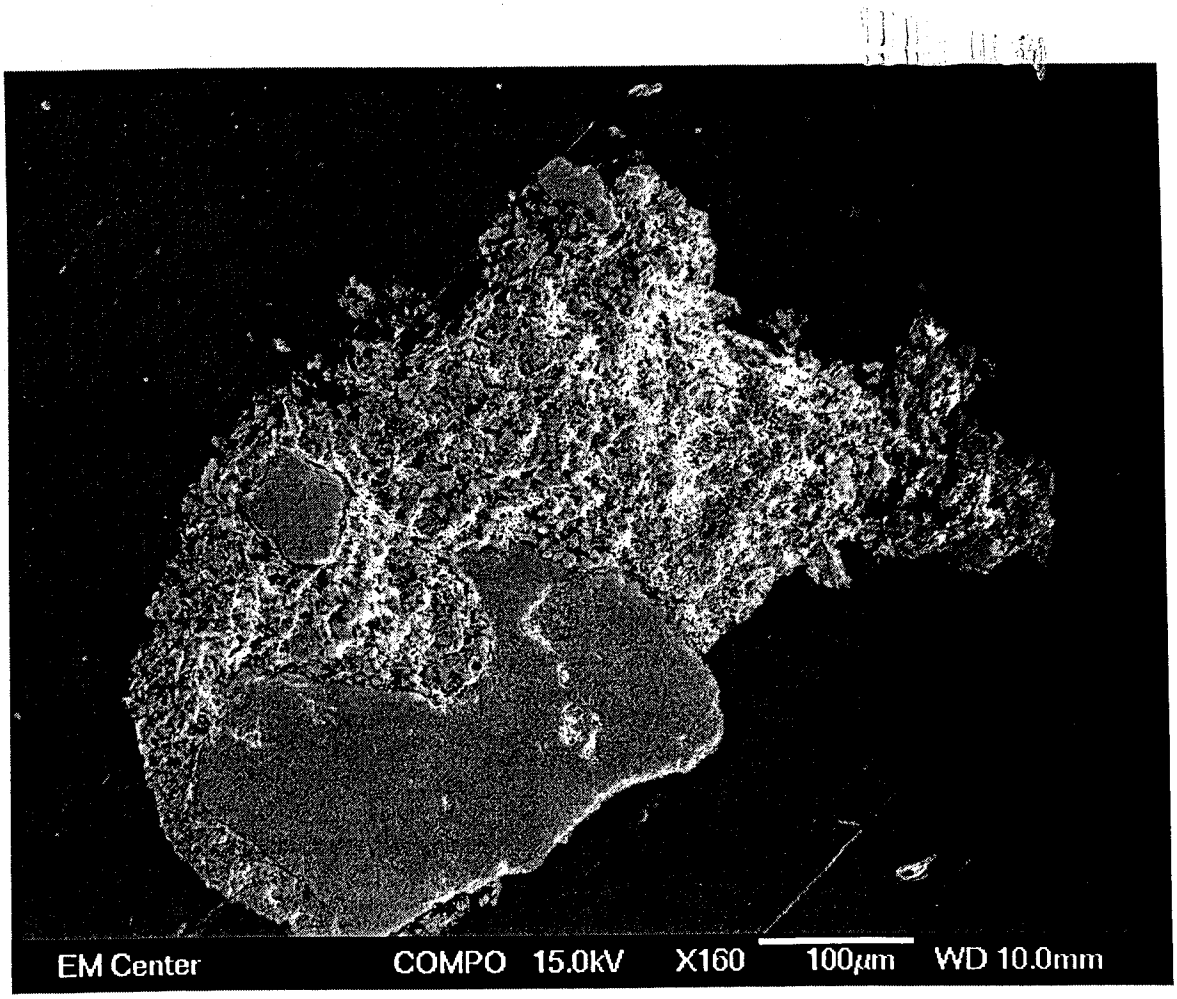

Figure 3.8a. Soil particle (0 mg L^{-1} P). The light-colored portions on the map indicate the presence of P associated with the particle.

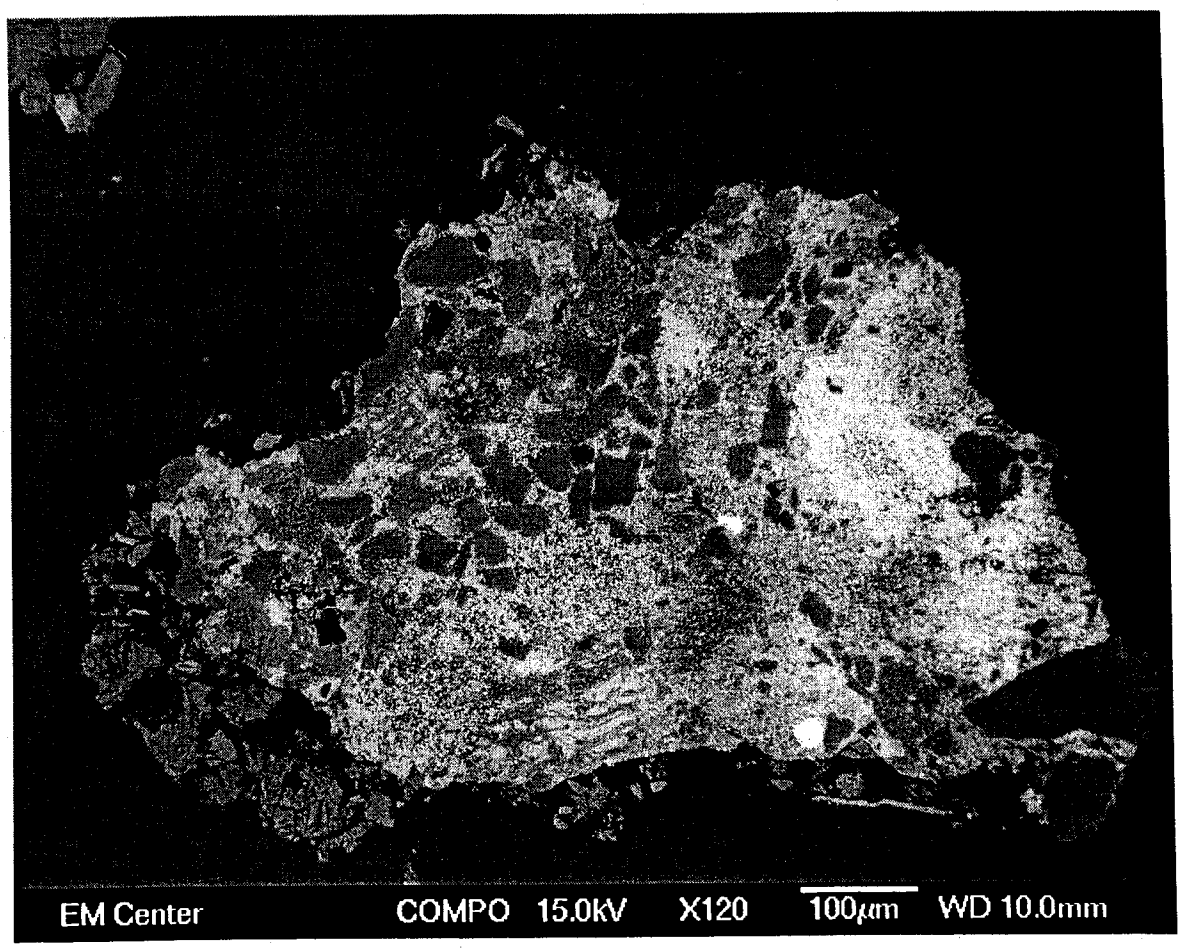

Figure 3.8b. Soil particle (10 mg L^{-1} P). The light-colored portions on the map indicate the presence of P associated with the particle.

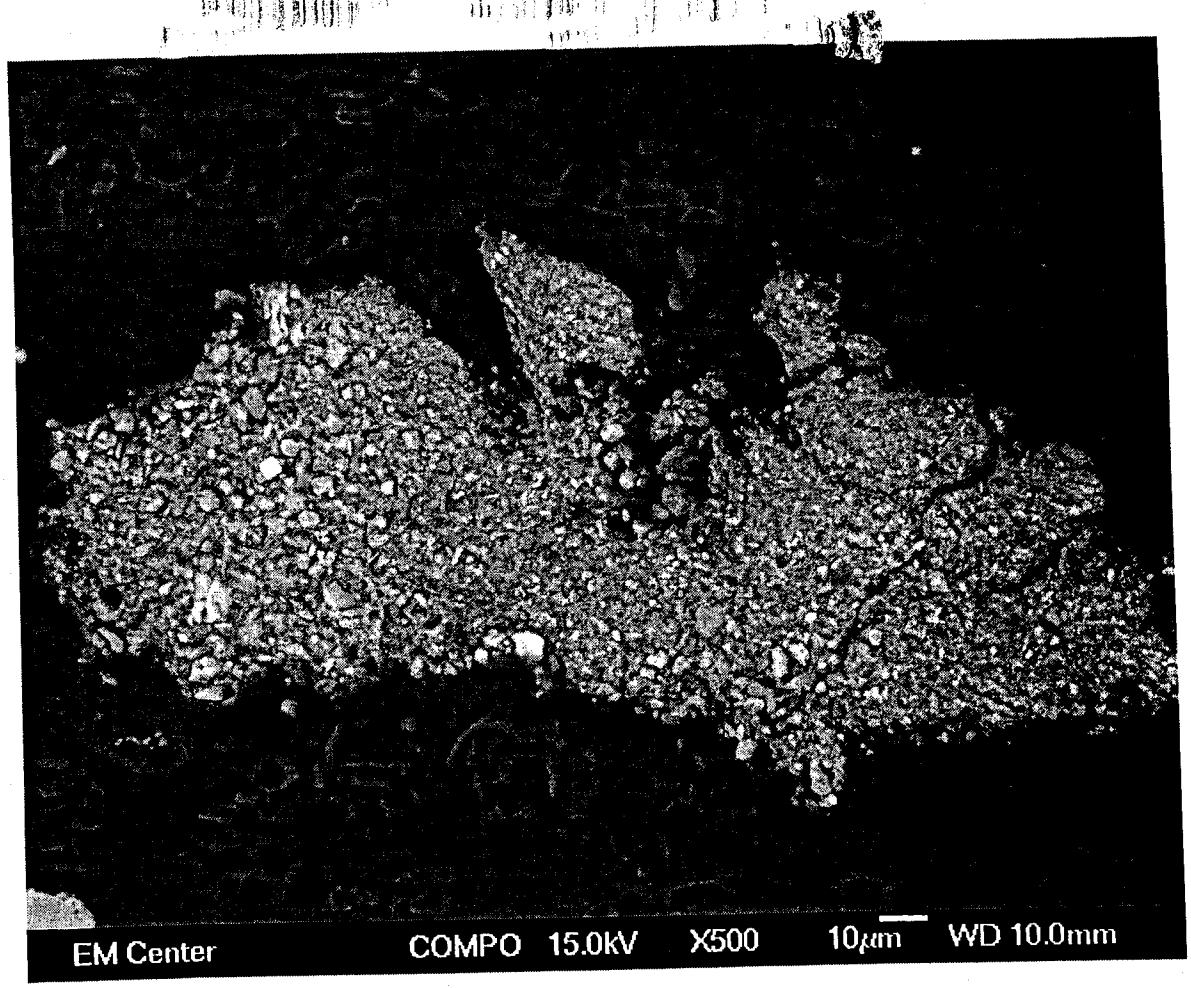

Figure 3.8c. Soil particle (20 mg L^{-1} P). The light-colored portions on the map indicate the presence of P associated with the particle.

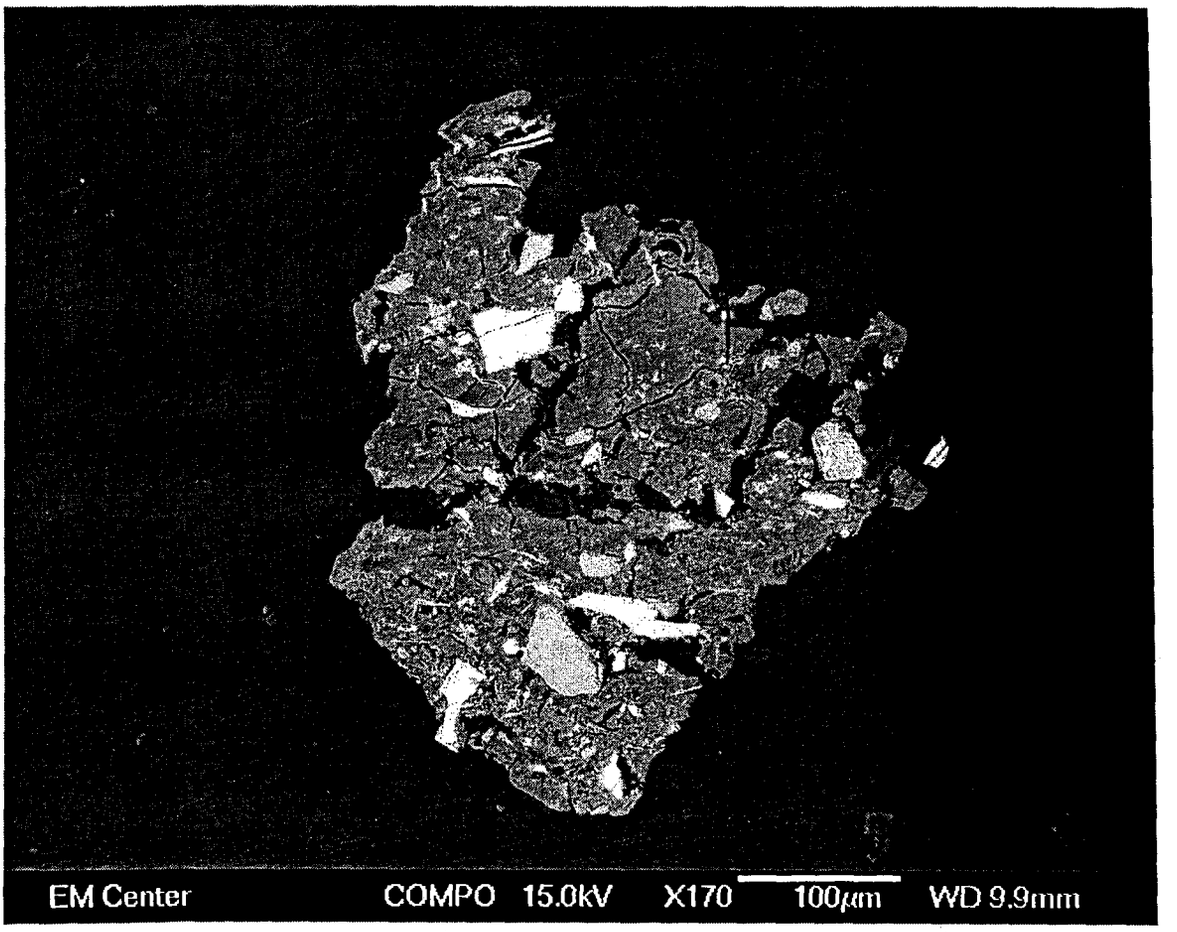

Figure 3.9a. Water treatment residual particle (0 mg L^{-1} P). The light-colored portions on the map indicate the presence of P associated with the particle.

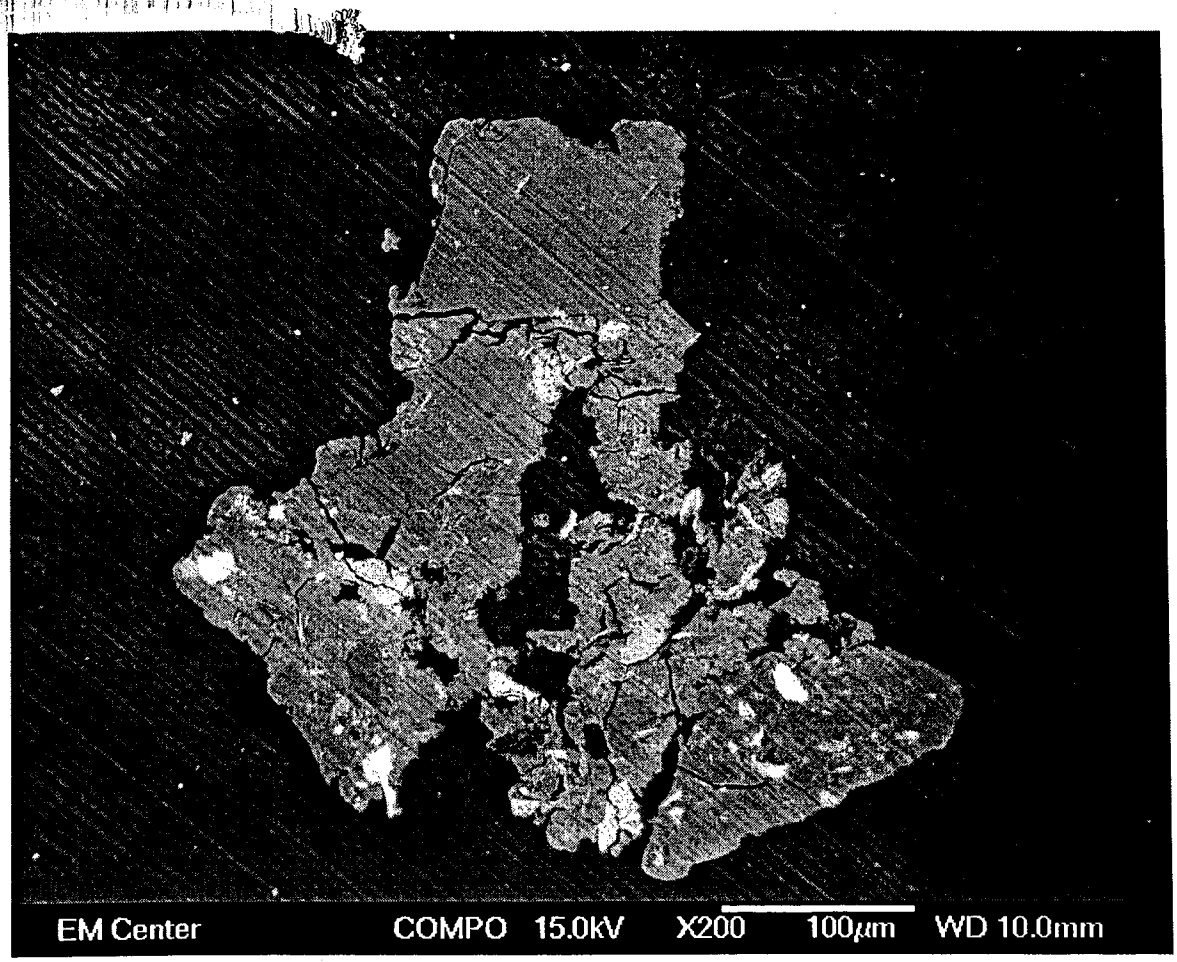

Figure 3.9b. Water treatment residual particle (250 mg L^{-1} P). The light-colored portions on the map indicate the presence of P associated with the particle.

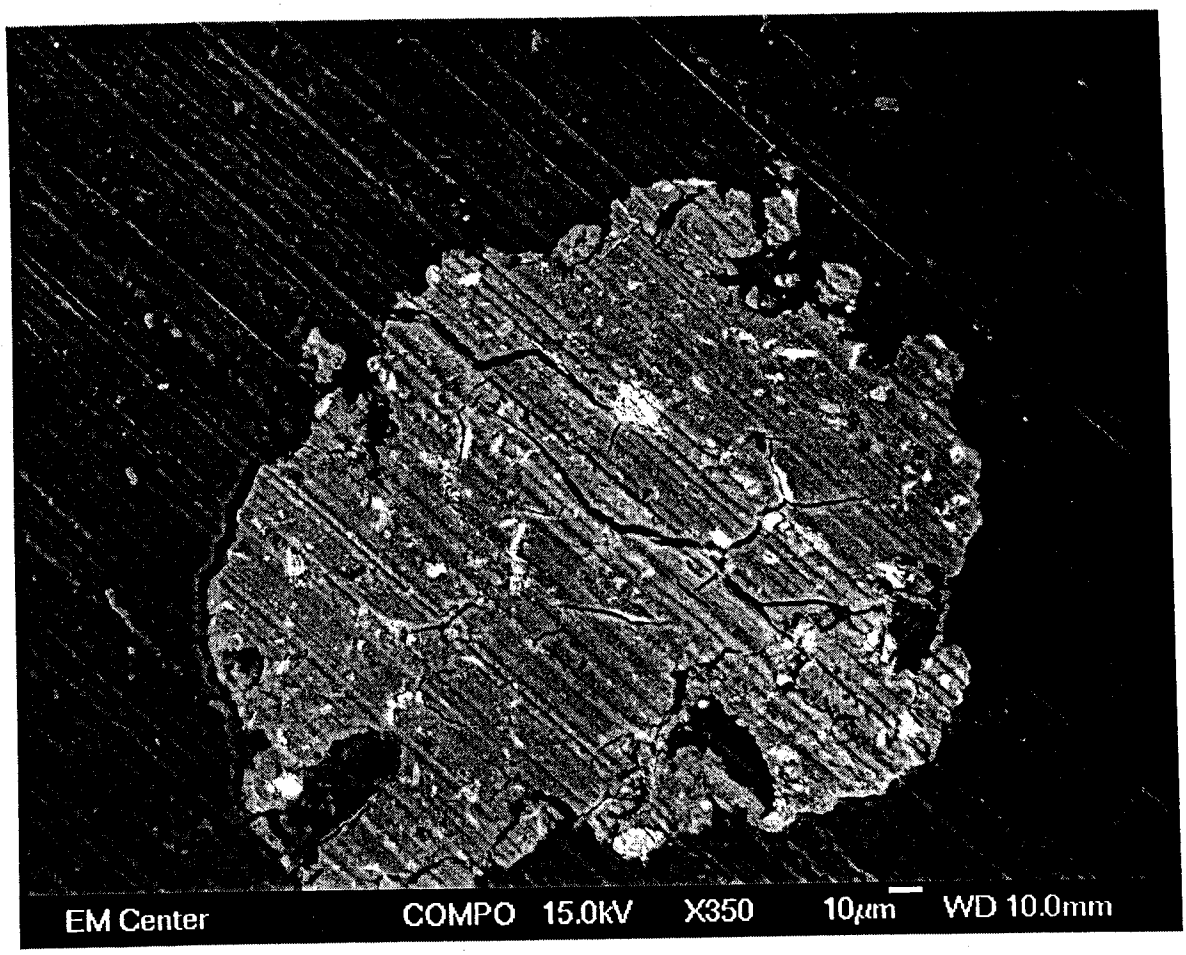

Figure 3.9c. Water treatment residual particle (500 mg L^{-1}). The light-colored portions on the map indicate the presence of P associated with the particle.

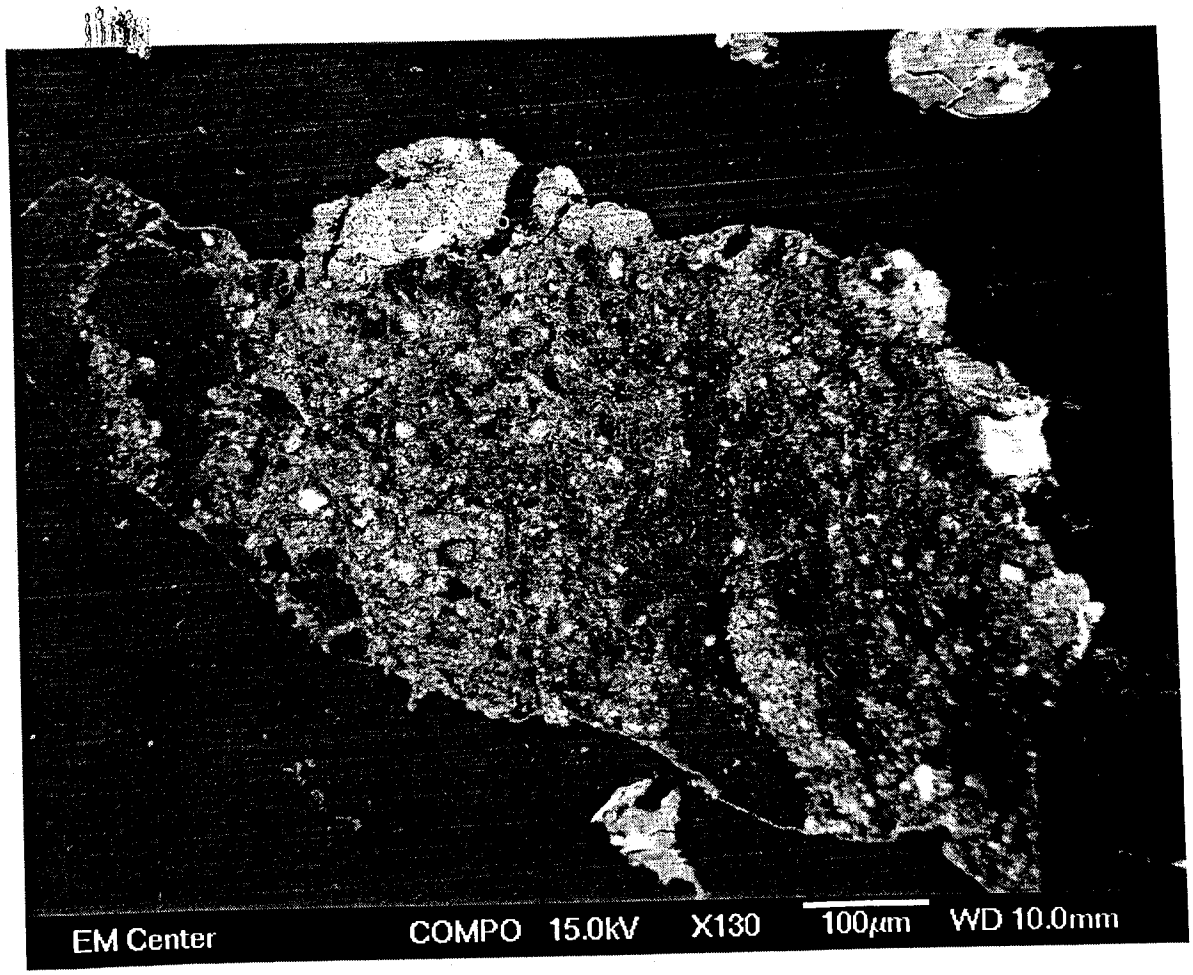

Figure 3.9d. Water treatment residual particle (750 mg L^{-1} P). The light-colored portions on the map indicate the presence of P associated with the particle.

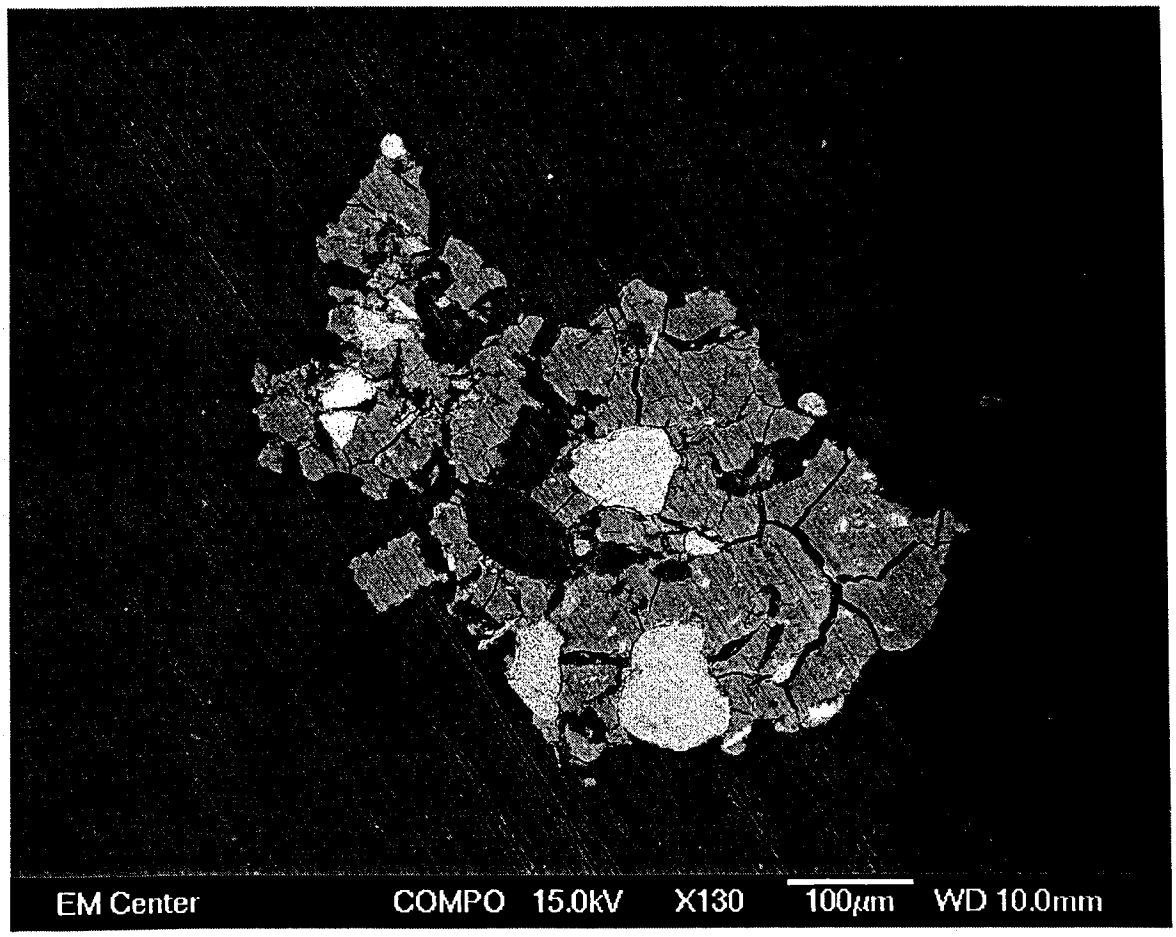

Figure 3.9e. Water treatment residual particle (1000 mg L^{-1}). The light-colored portions on the map indicate the presence of P associated with the particle.

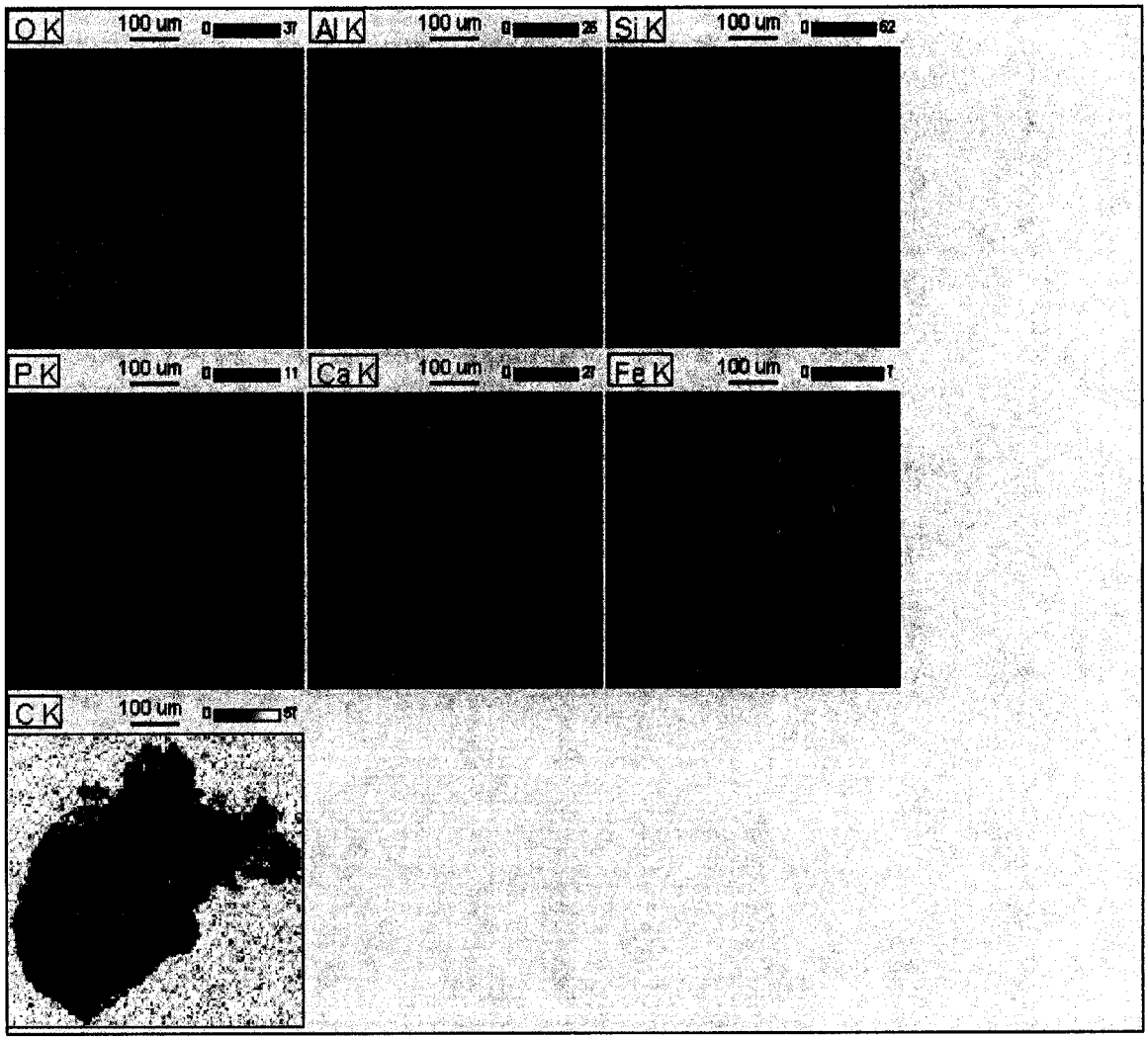

Figure 3.10a. Soil particle (0 mg L^{-1} P). The color intensity identifies the elemental concentration present in the particle.

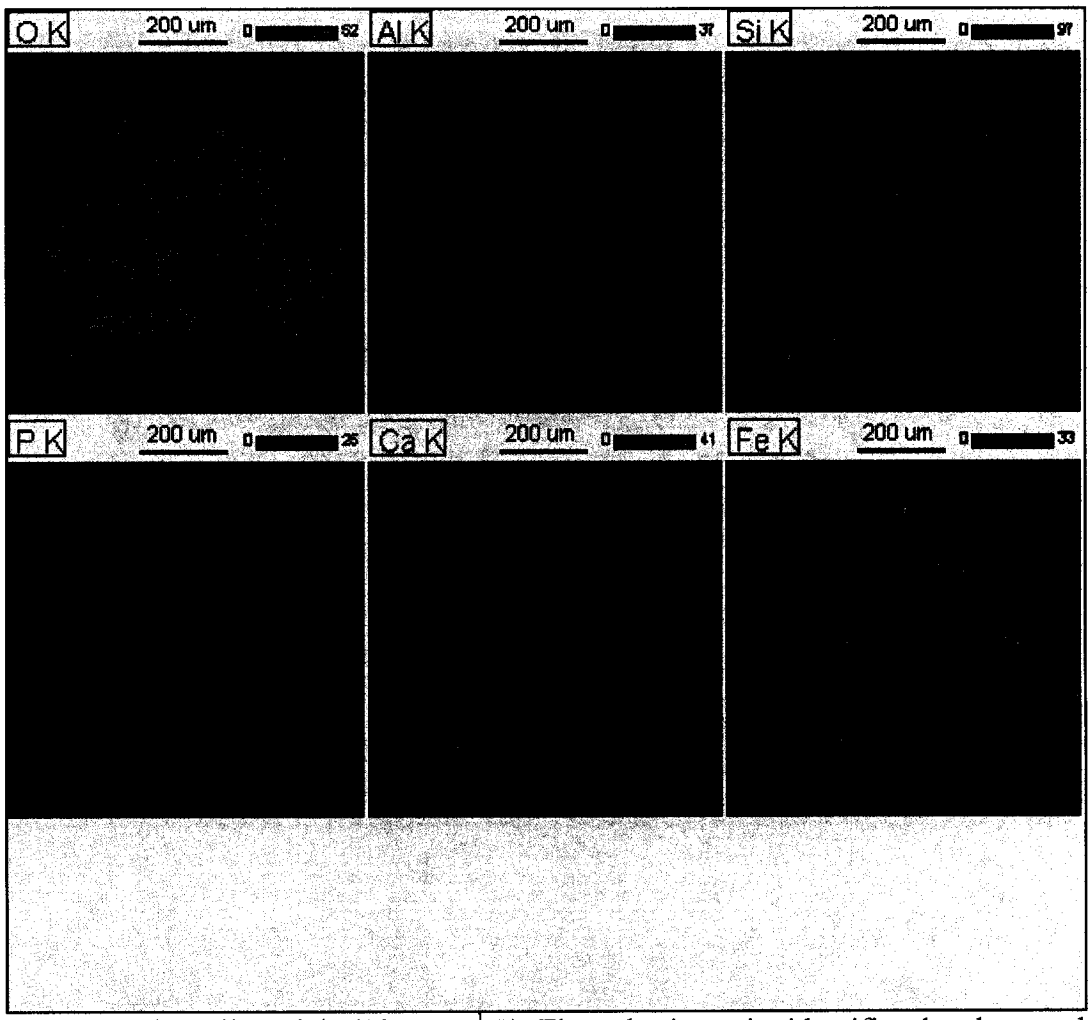

Figure 3.10b. Soil particle (10 mg L^{-1} P). The color intensity identifies the elemental concentration present in the particle.

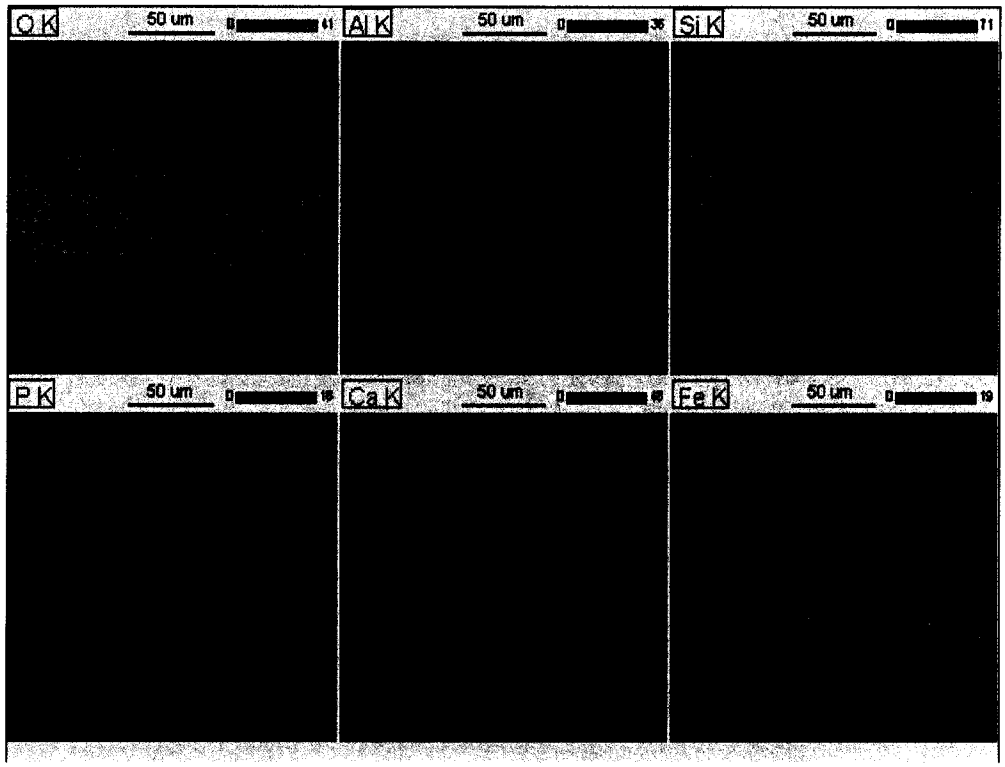

Figure 3.10c. Soil particle (20 mg L^{-1} P). The color intensity identifies the elemental concentration present in the particle.

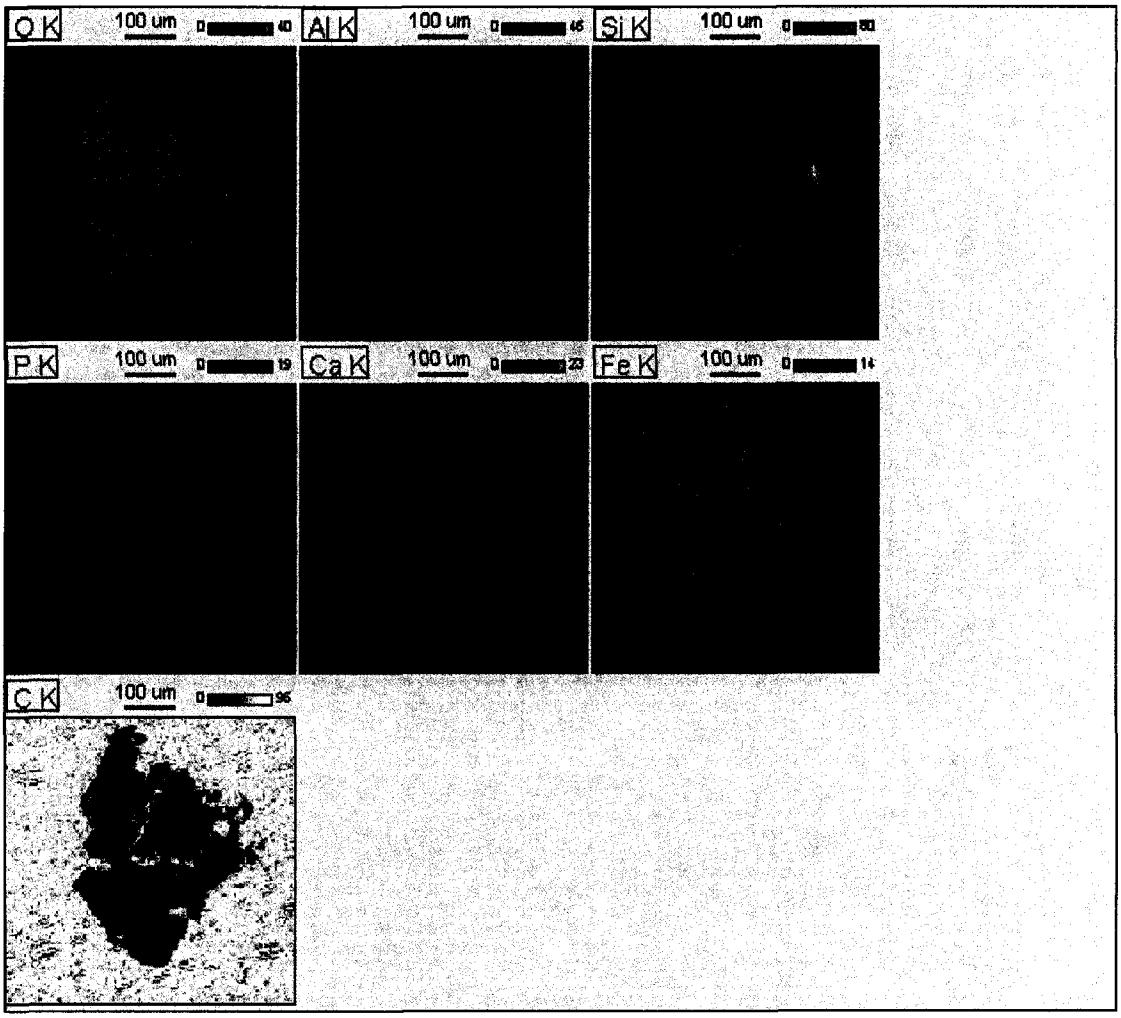

Figure 3.11a. Water treatment residual particle (0 mg L^{-1} P). The color intensity identifies the elemental concentration present in the particle.

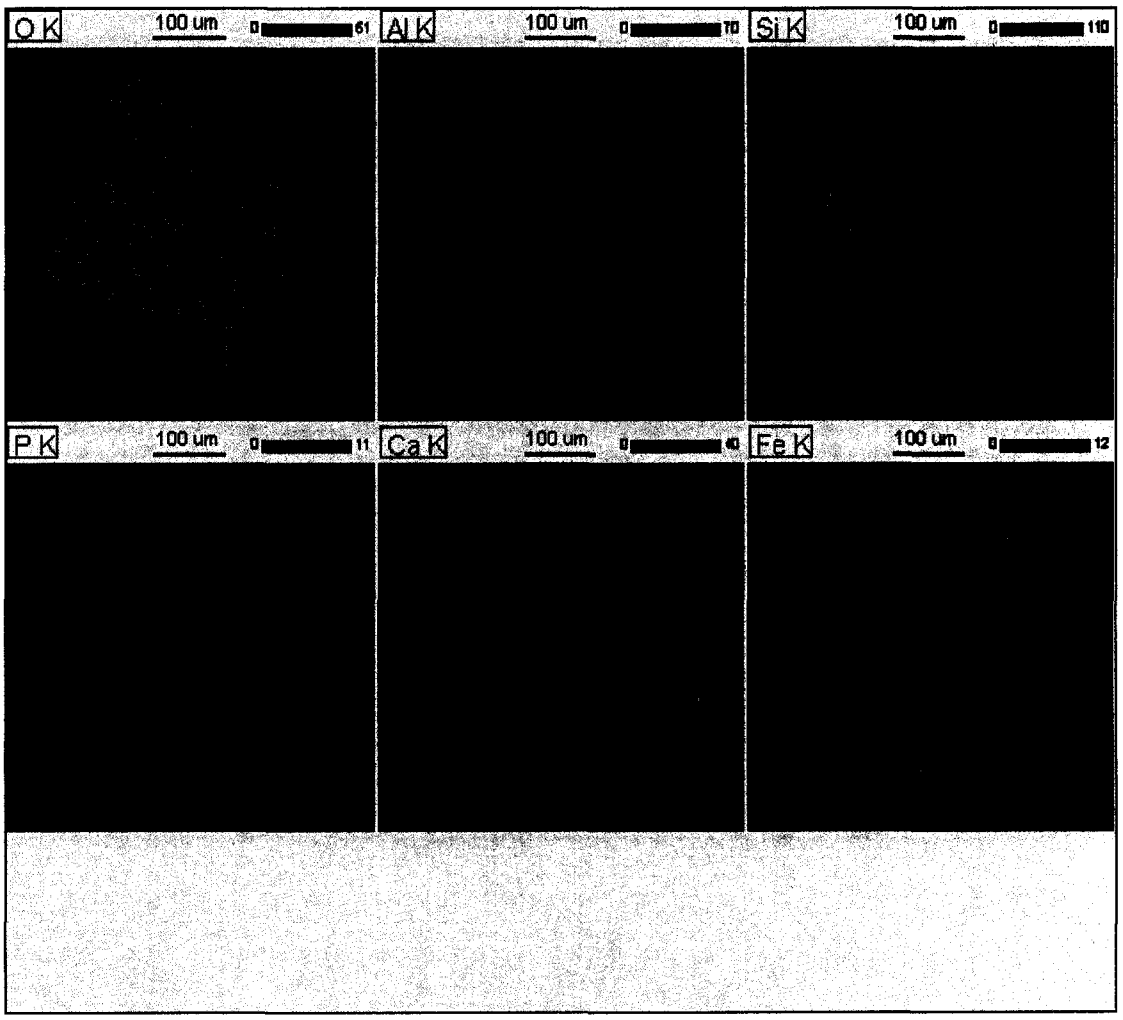

Figure 3.11b. Water treatment residual particle (100 mg L^{-1} P). The color intensity identifies the elemental concentration present in the particle.

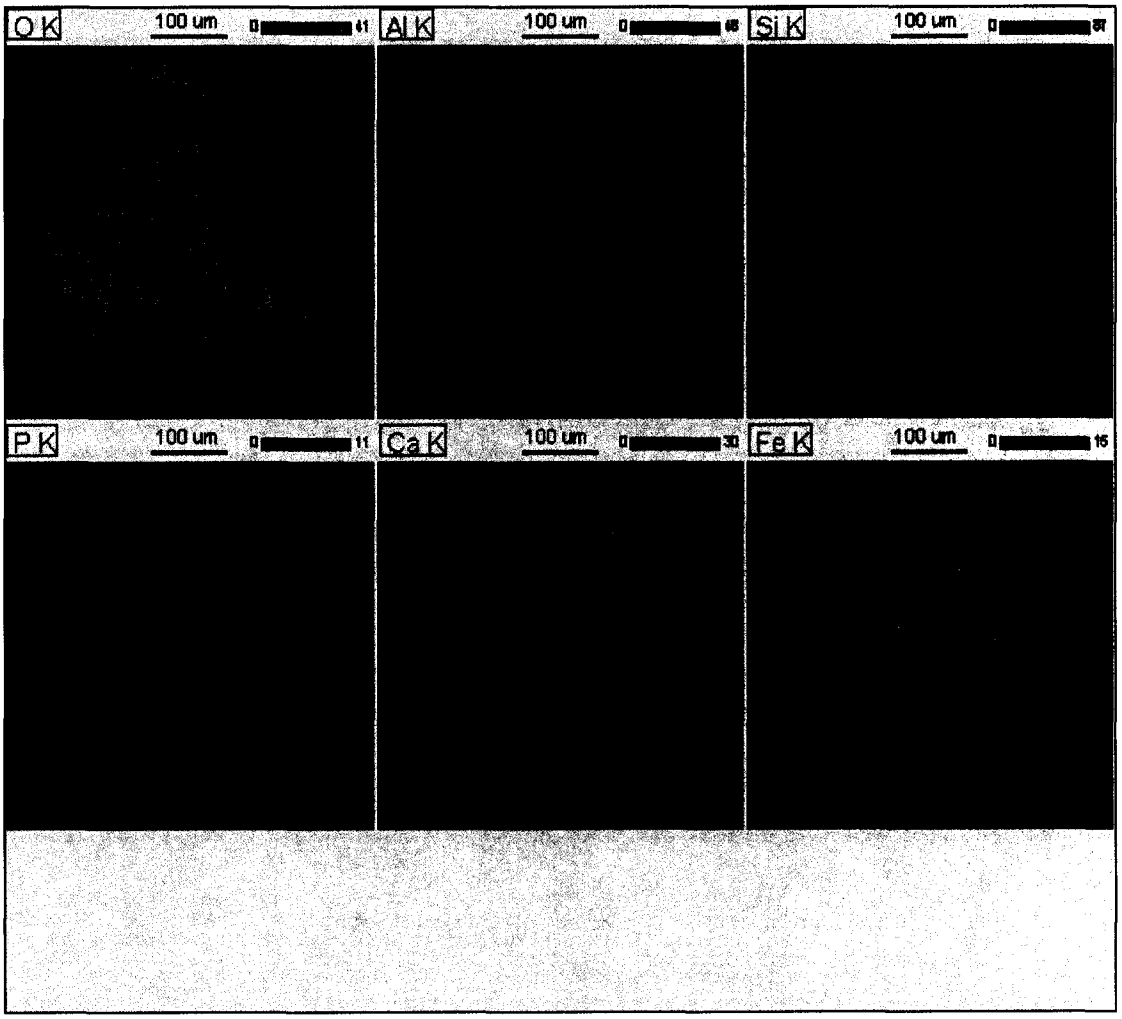

Figure 3.11c. Water treatment residual particle (250 mg L^{-1} P). The color intensity identifies the elemental concentration present in the particle.

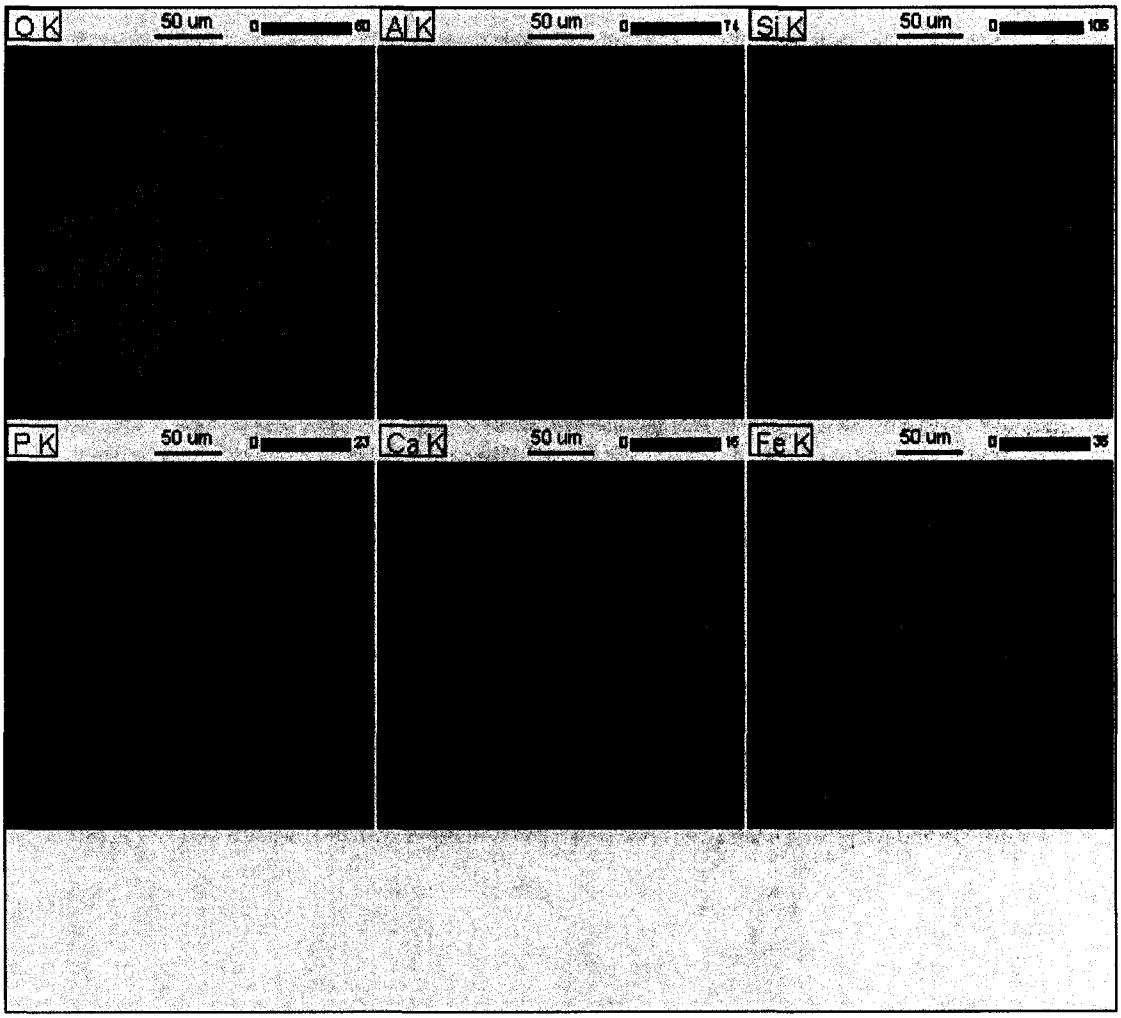

Figure 3.11d. Water treatment residual particle (500 mg L^{-1} P). The color intensity identifies the elemental concentration present in the particle.

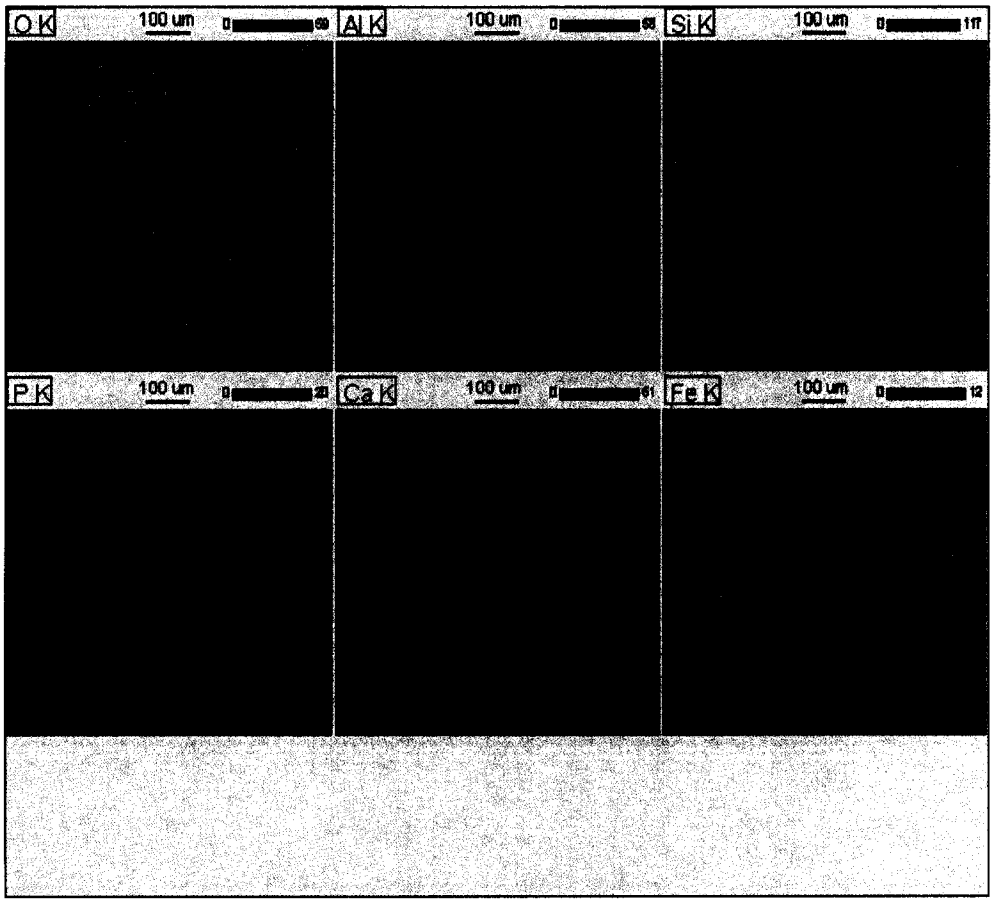

Figure 3.11e. Water treatment residual particle (750 mg L^{-1} P). The color intensity identifies the elemental concentration present in the particle.

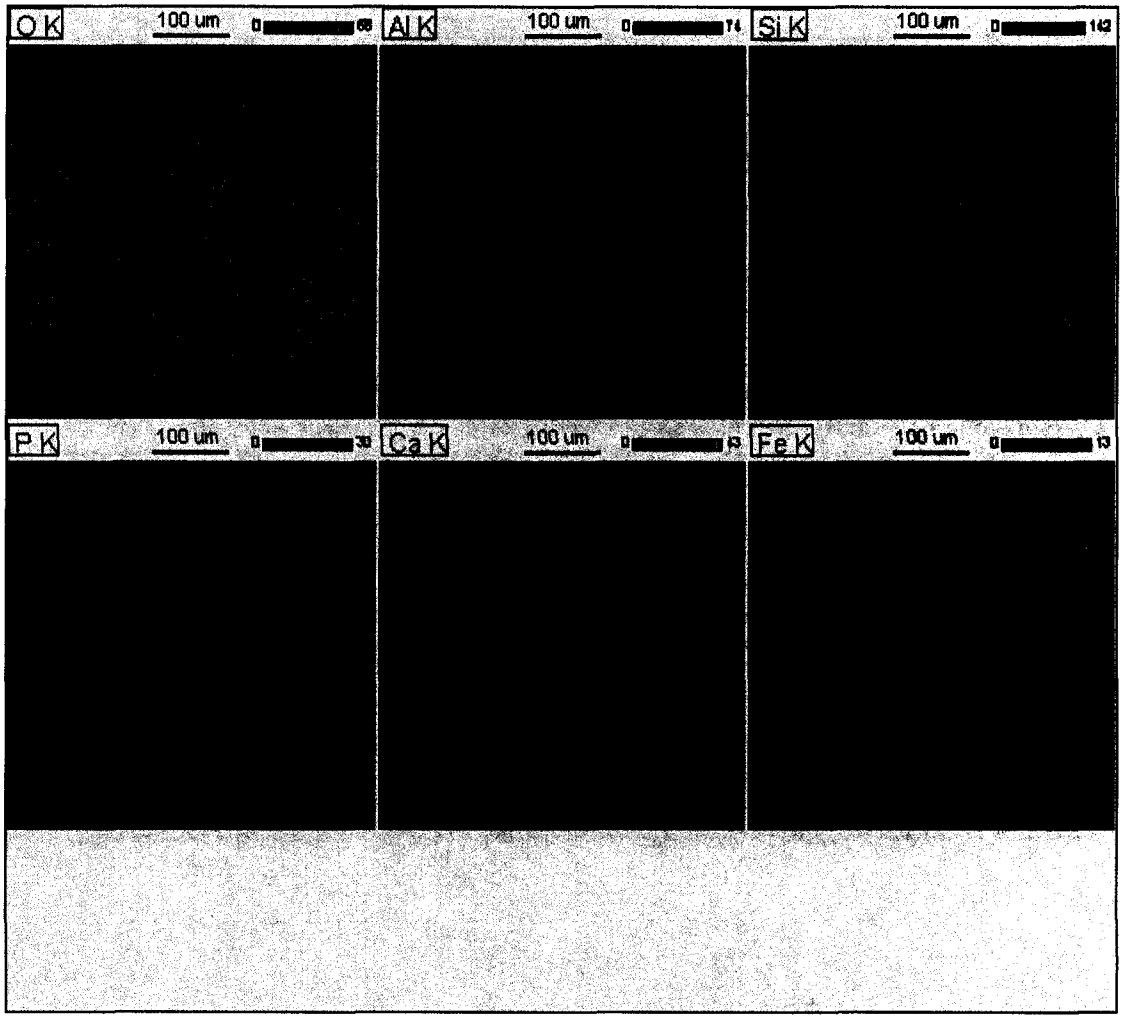

Figure 3.11f. Water treatment residual particle (1000 mg L^{-1} P). The color intensity identifies the elemental concentration present in the particle.

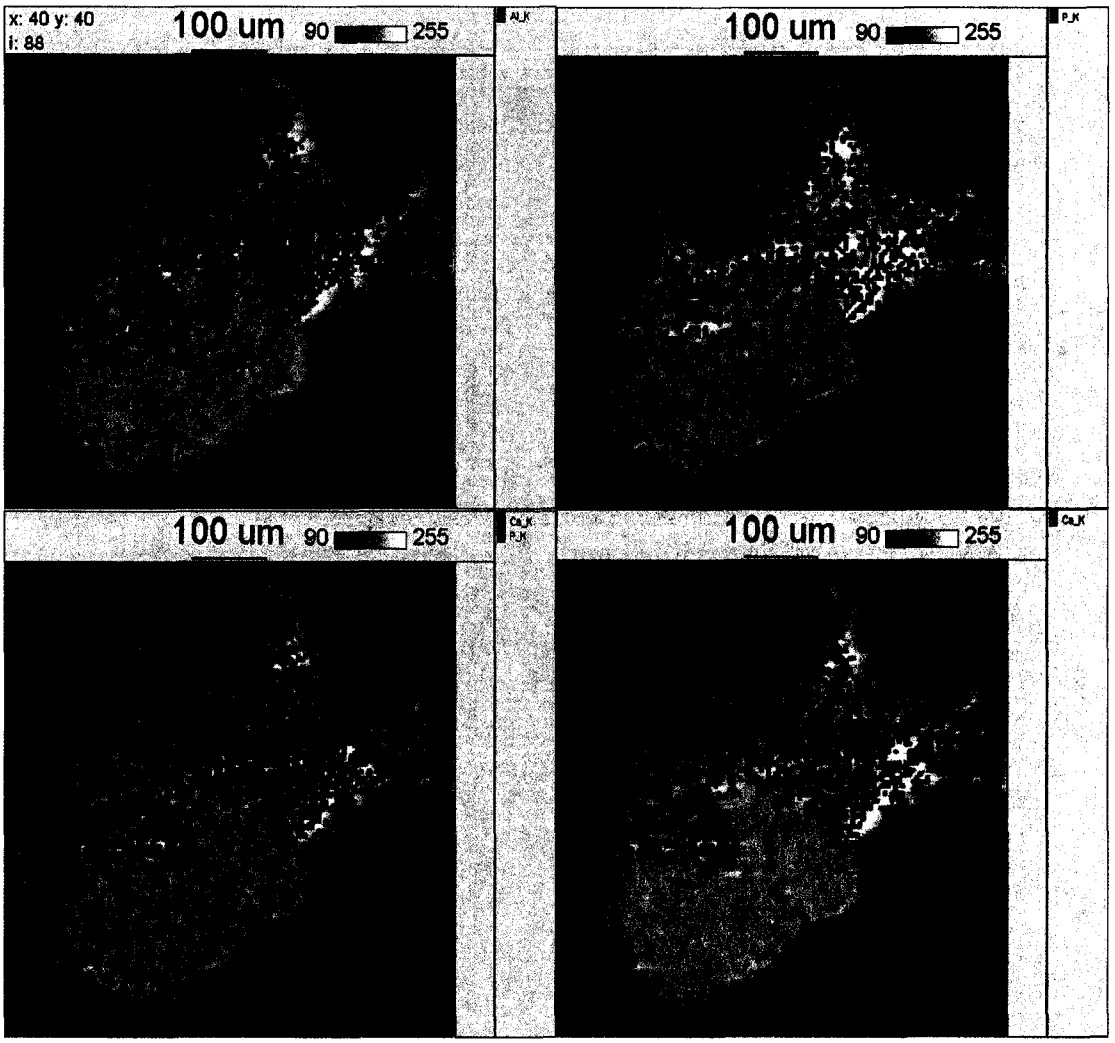

Figure 3.11a1. Soil particle overlay (0 mg L^{-1} P). Both individual and joint element maps are presented. A map that shows a color that cannot be distinguished into its two elemental colors indicates an association between those elements.

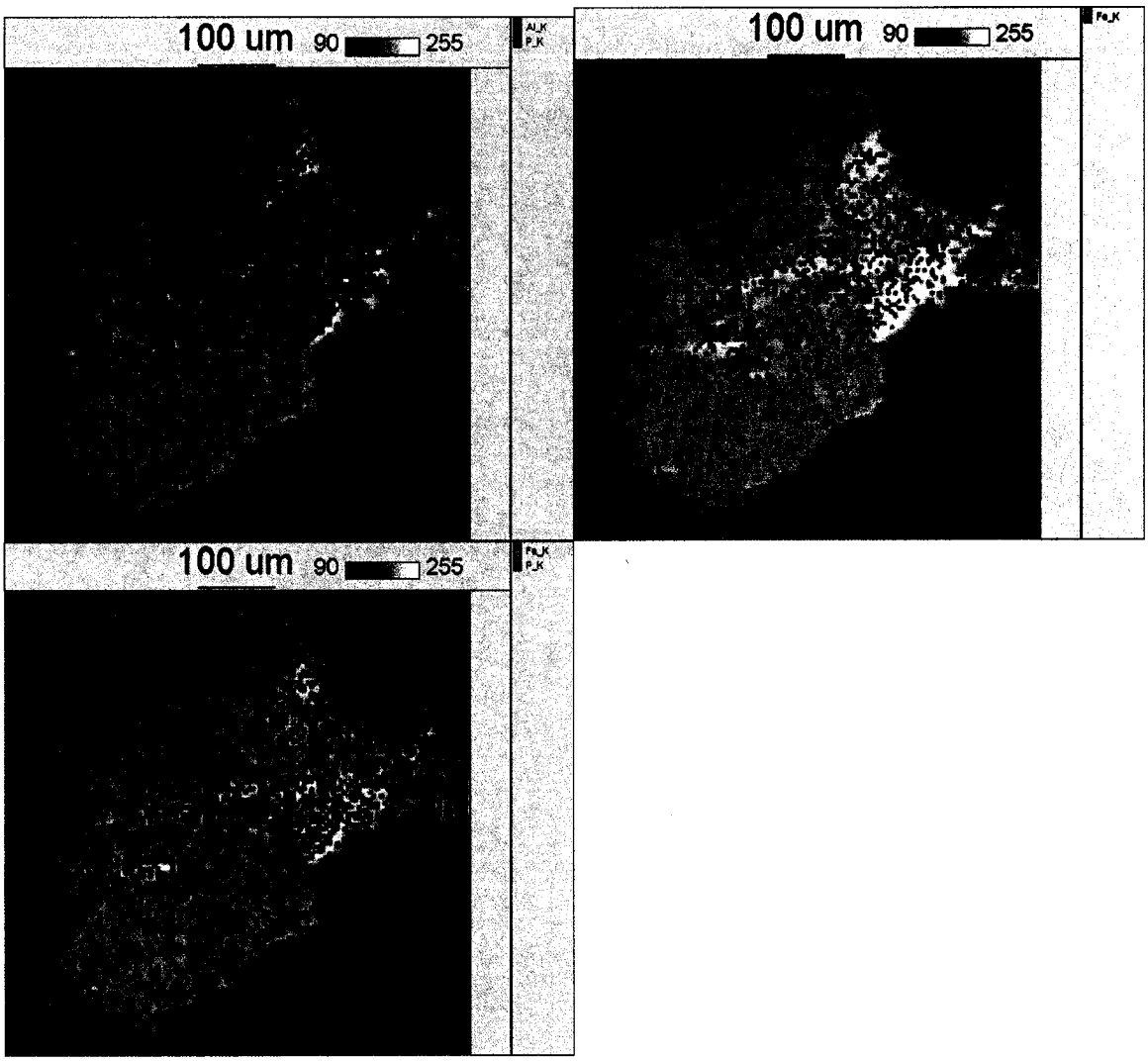

Figure 3.11a2. Soil particle overlay (0 mg L^{-1} P). Both individual and joint element maps are presented. A map that shows a color that cannot be distinguished into its two elemental colors indicates an association between those elements.

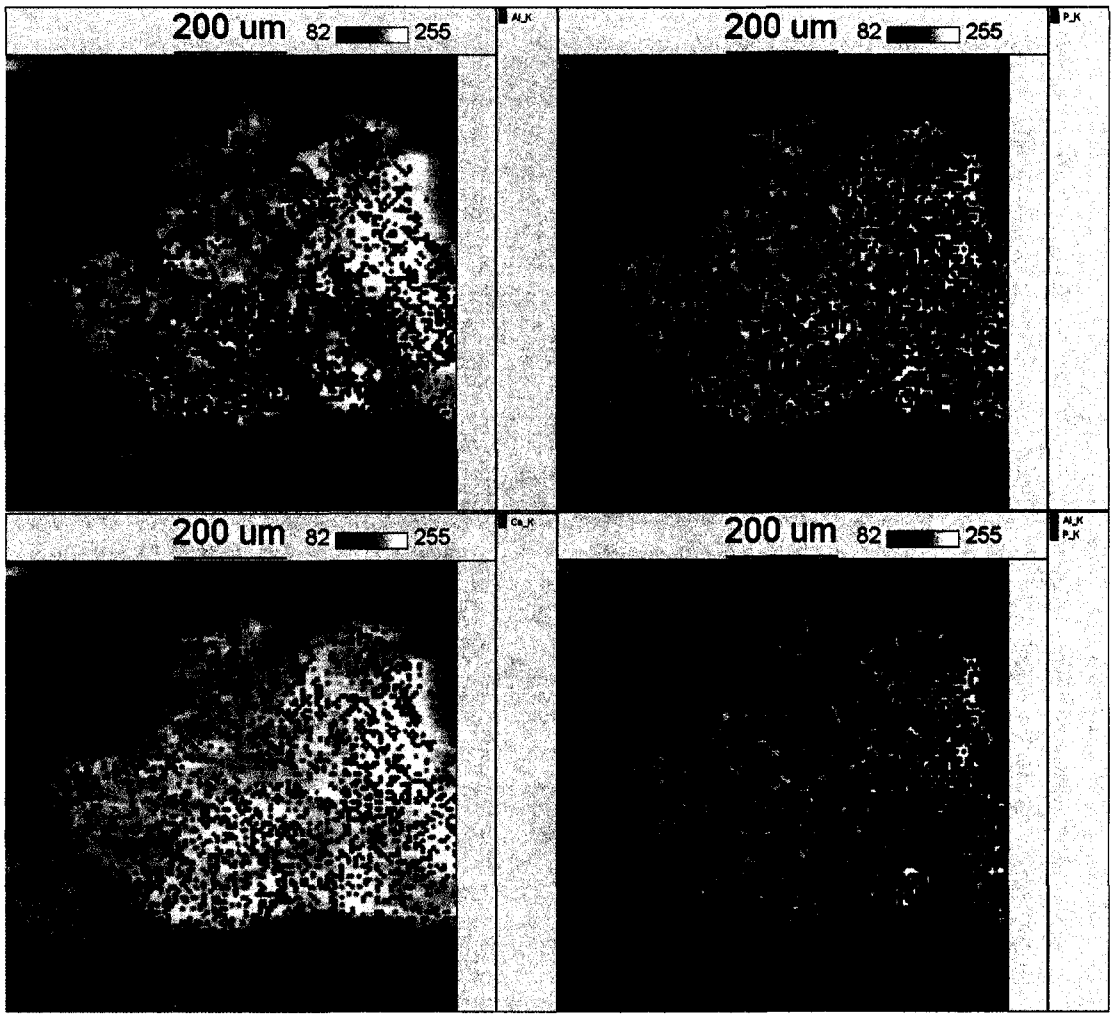

Figure 3.12b1. Soil particle overlay (10 mg L^{-1} P). Both individual and joint element maps are presented. A map that shows a color that cannot be distinguished into its two elemental colors indicates an association between those elements.

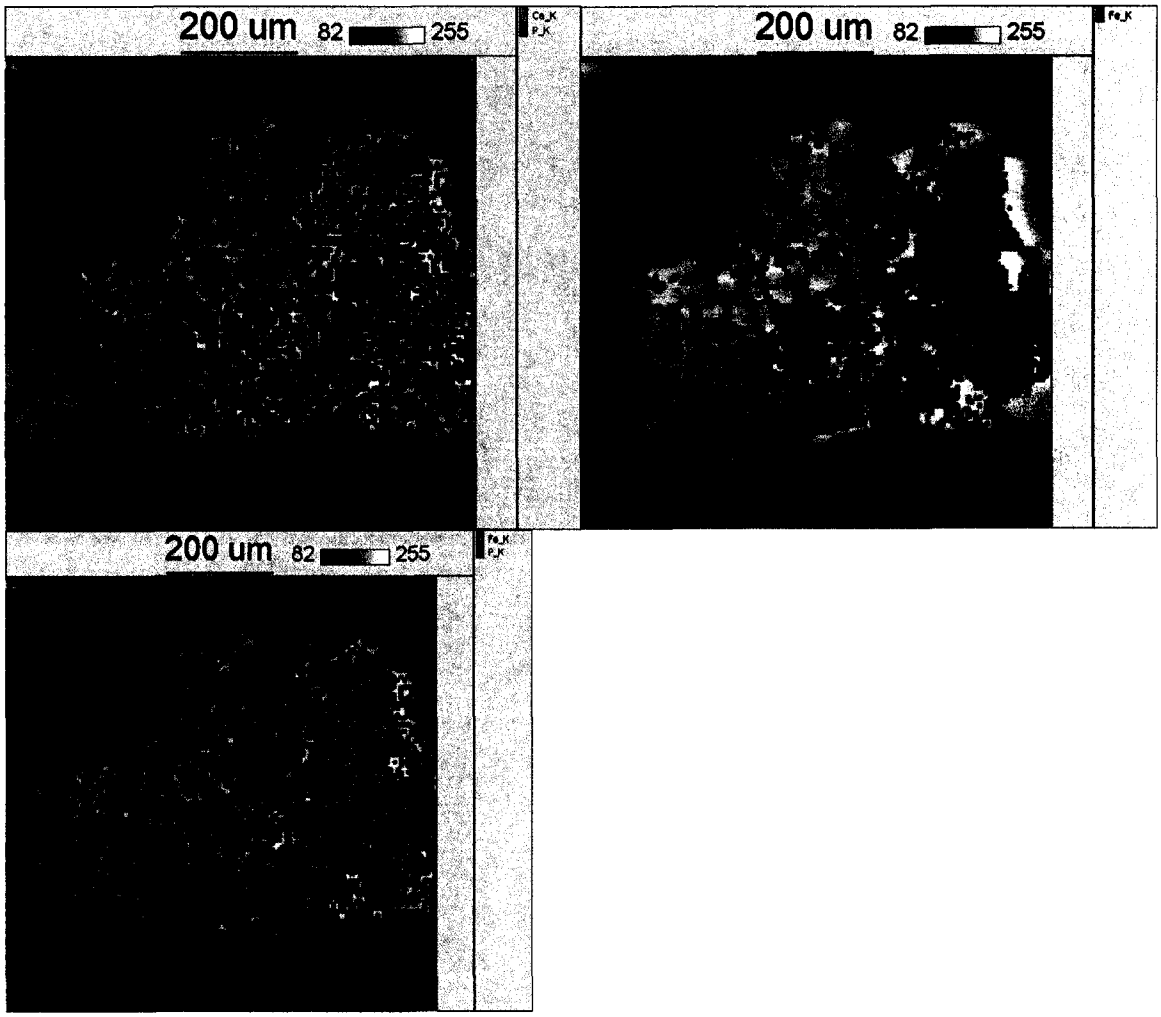

Figure 3.12b2. Soil particle overlay (10 mg L^{-1} P). Both individual and joint element maps are presented. A map that shows a color that cannot be distinguished into its two elemental colors indicates an association between those elements.

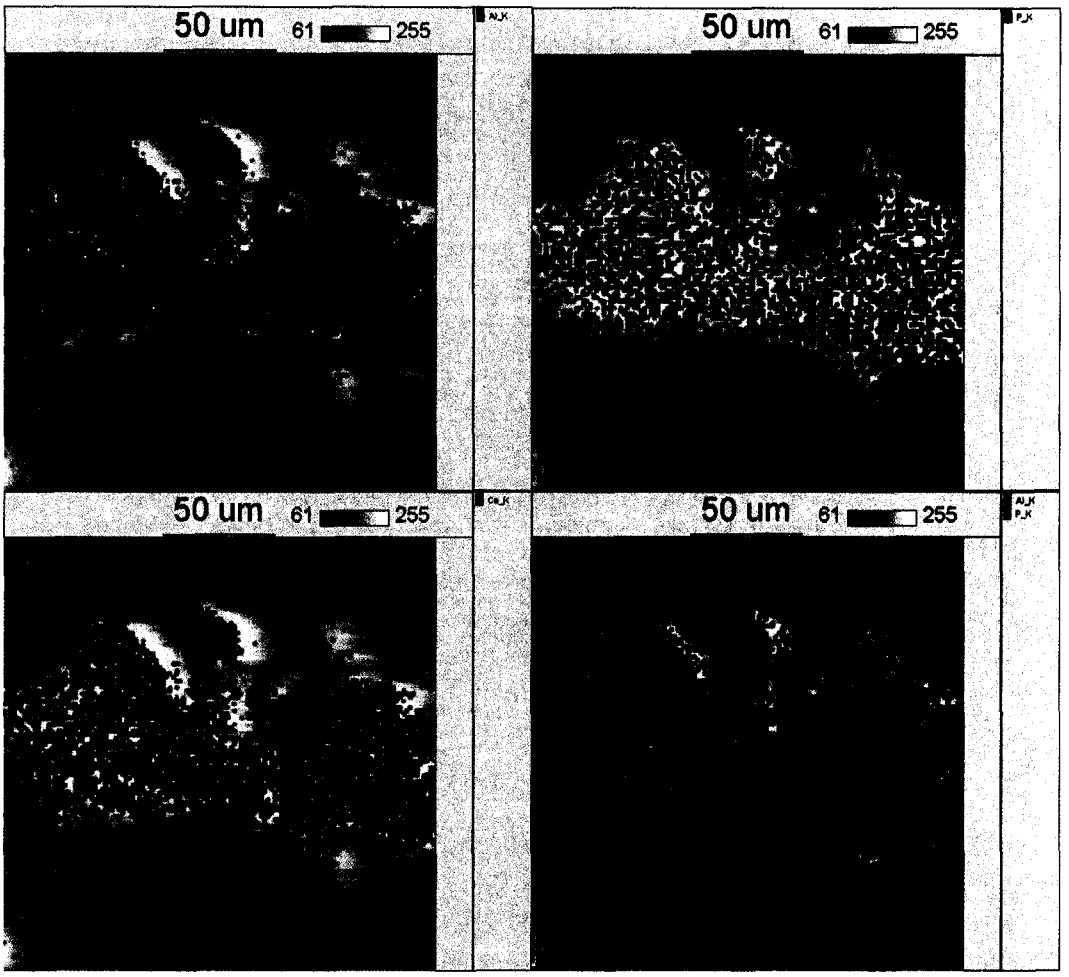

Figure 3.12c1. Soil particle overlay (20 mg L^{-1} P). Both individual and joint element maps are presented. A map that shows a color that cannot be distinguished into its two elemental colors indicates an association between those elements.

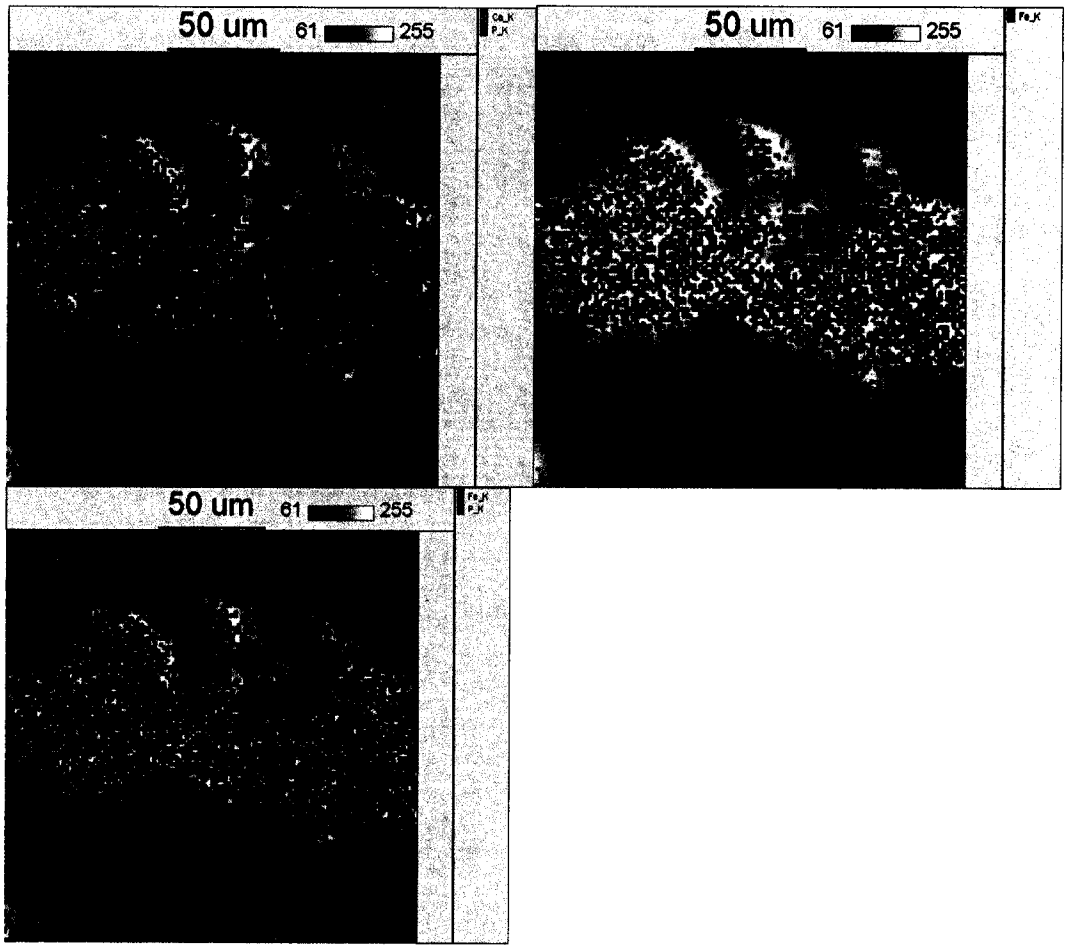

Figure 3.12c2. Soil particle overlay (20 mg L^{-1} P). Both individual and joint element maps are presented. A map that shows a color that cannot be distinguished into its two elemental colors indicates an association between those elements.

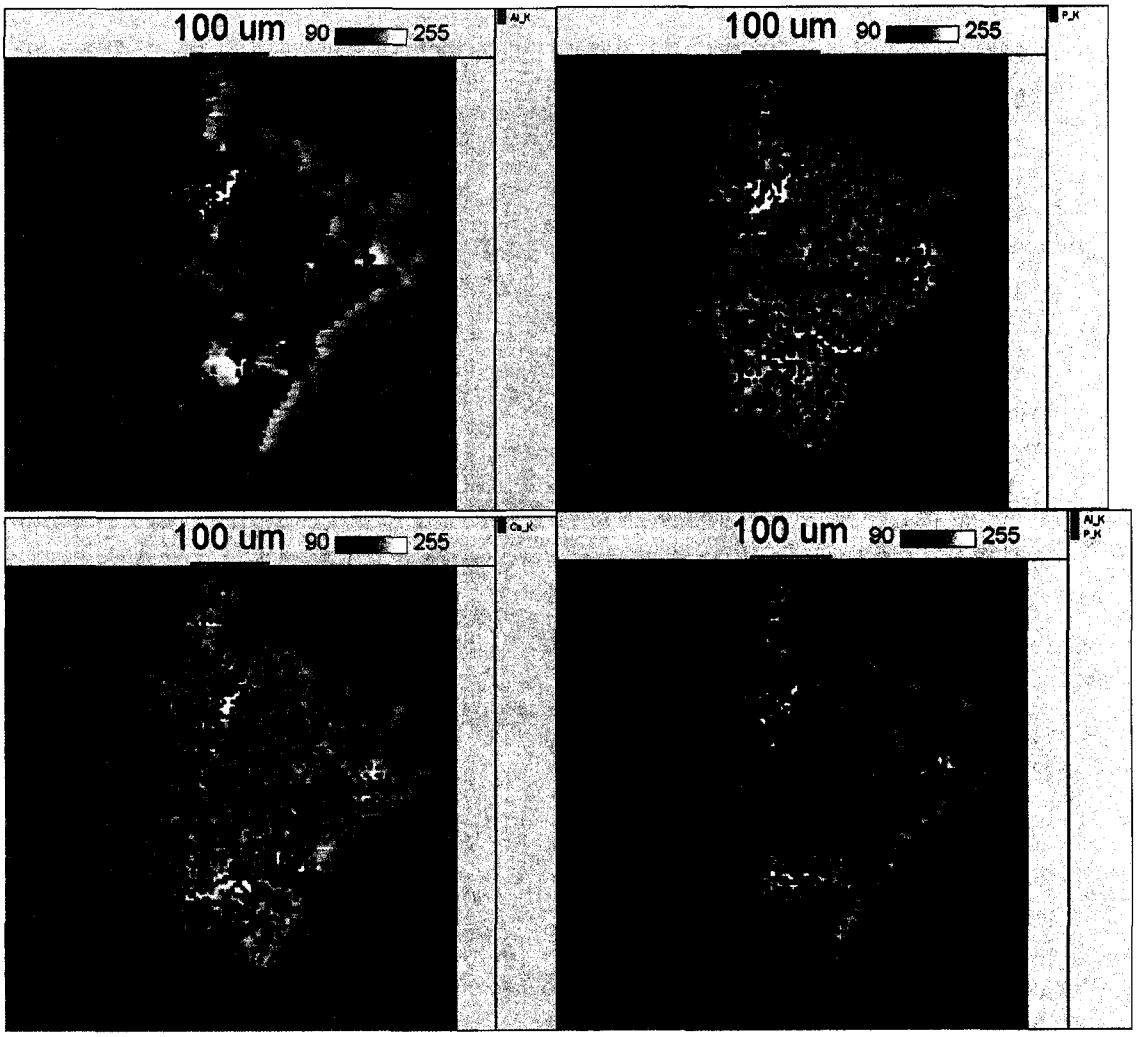

Figure 3.13a1. Water treatment residual particle overlay (0 mg L^{-1} P). Both individual and joint element maps are presented. A map that shows a color that cannot be distinguished into its two elemental colors indicates an association between those elements.

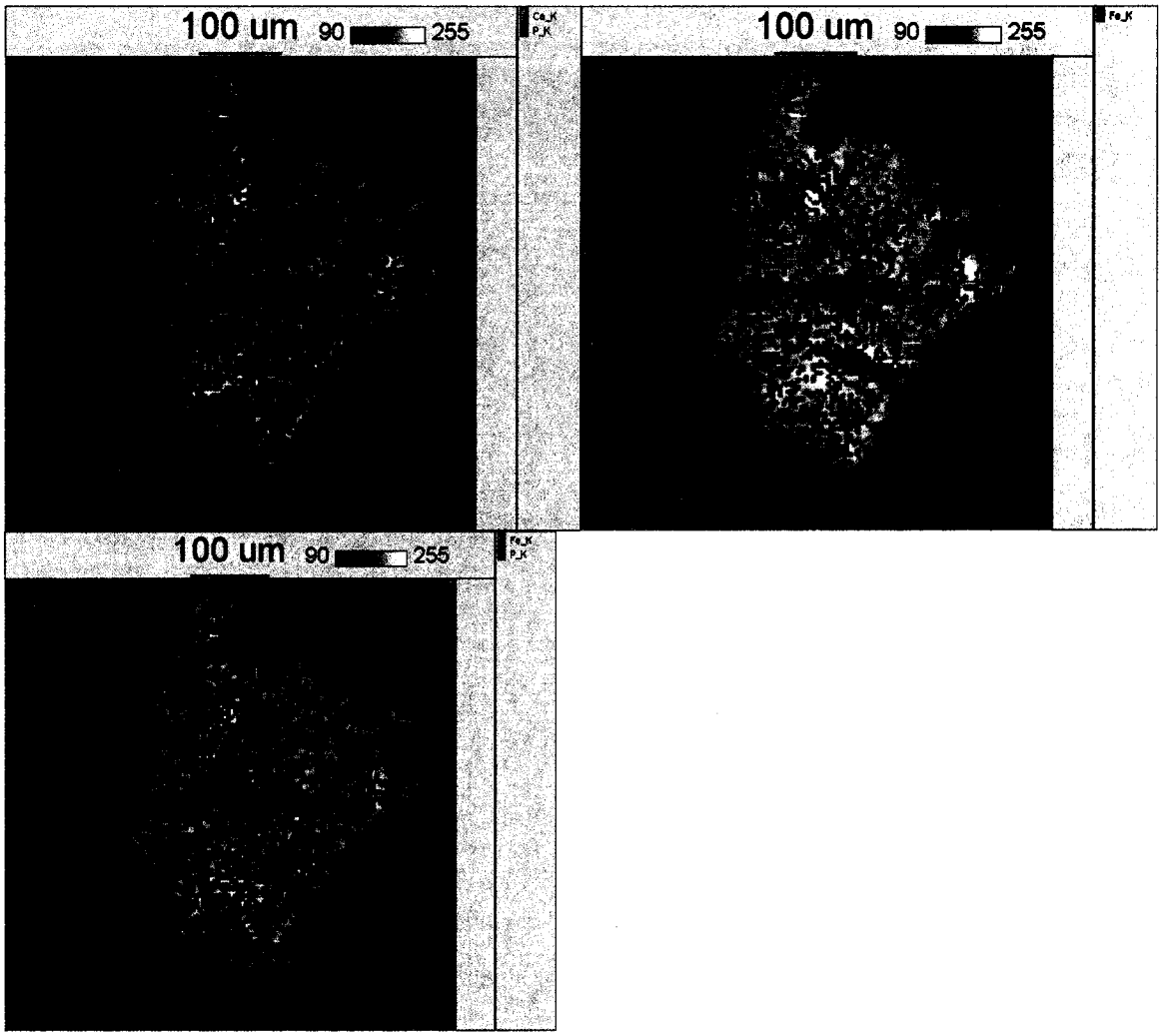

Figure 3.13a2. Water treatment residual particle overlay (0 mg L^{-1} P). Both individual and joint element maps are presented. A map that shows a color that cannot be distinguished into its two elemental colors indicates an association between those elements.

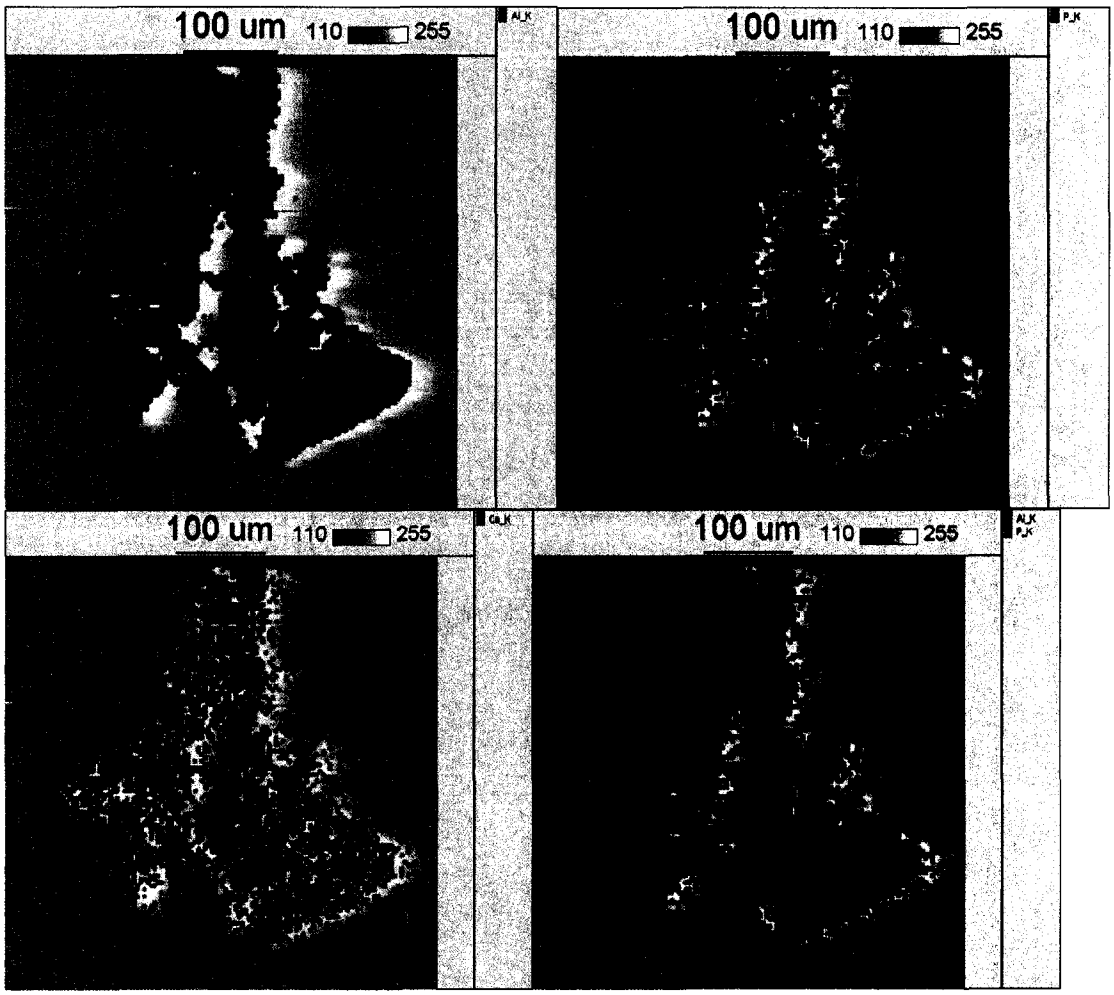

Figure 3.13b1. Water treatment residual particle overlay (250 mg L^{-1} P). Both individual and joint element maps are presented. A map that shows a color that cannot be distinguished into its two elemental colors indicates an association between those elements.

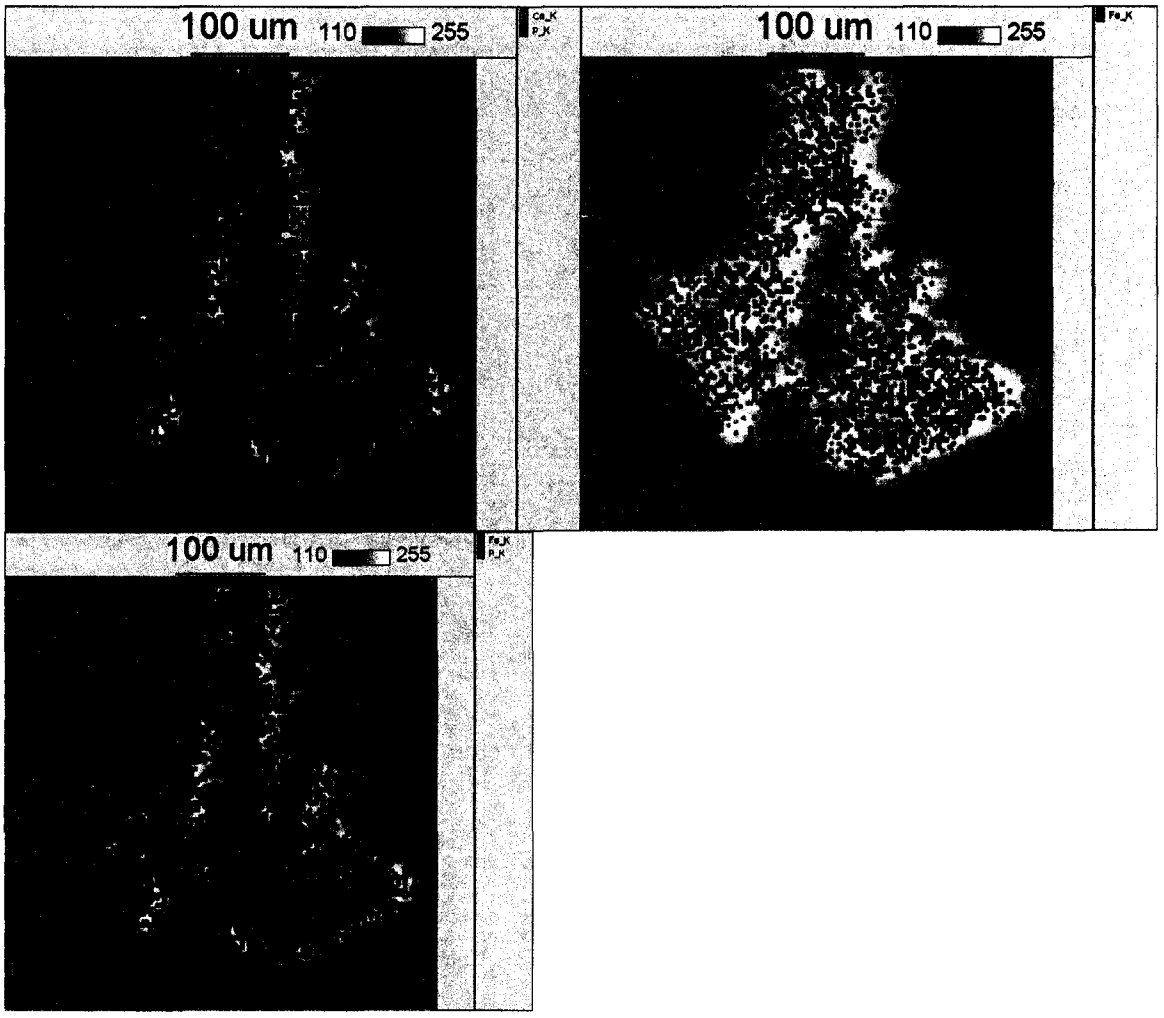

Figure 3.13b2. Water treatment residual particle overlay (250 mg L^{-1} P). Both individual and joint element maps are presented. A map that shows a color that cannot be distinguished into its two elemental colors indicates an association between those elements.

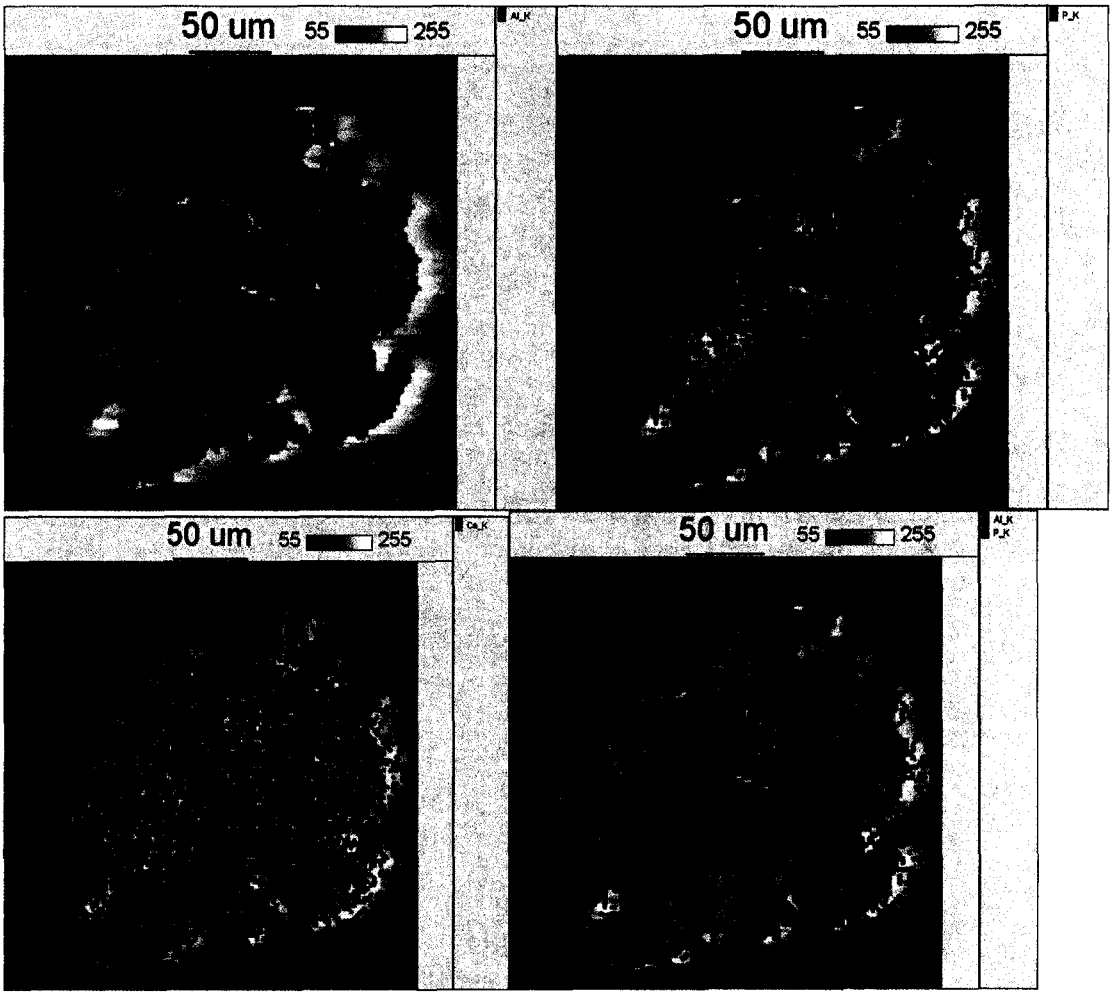

Figure 3.13c1. Water treatment residual overlay (500 mg L^{-1} P). Both individual and joint element maps are presented. A map that shows a color that cannot be distinguished into its two elemental colors indicates an association between those elements.

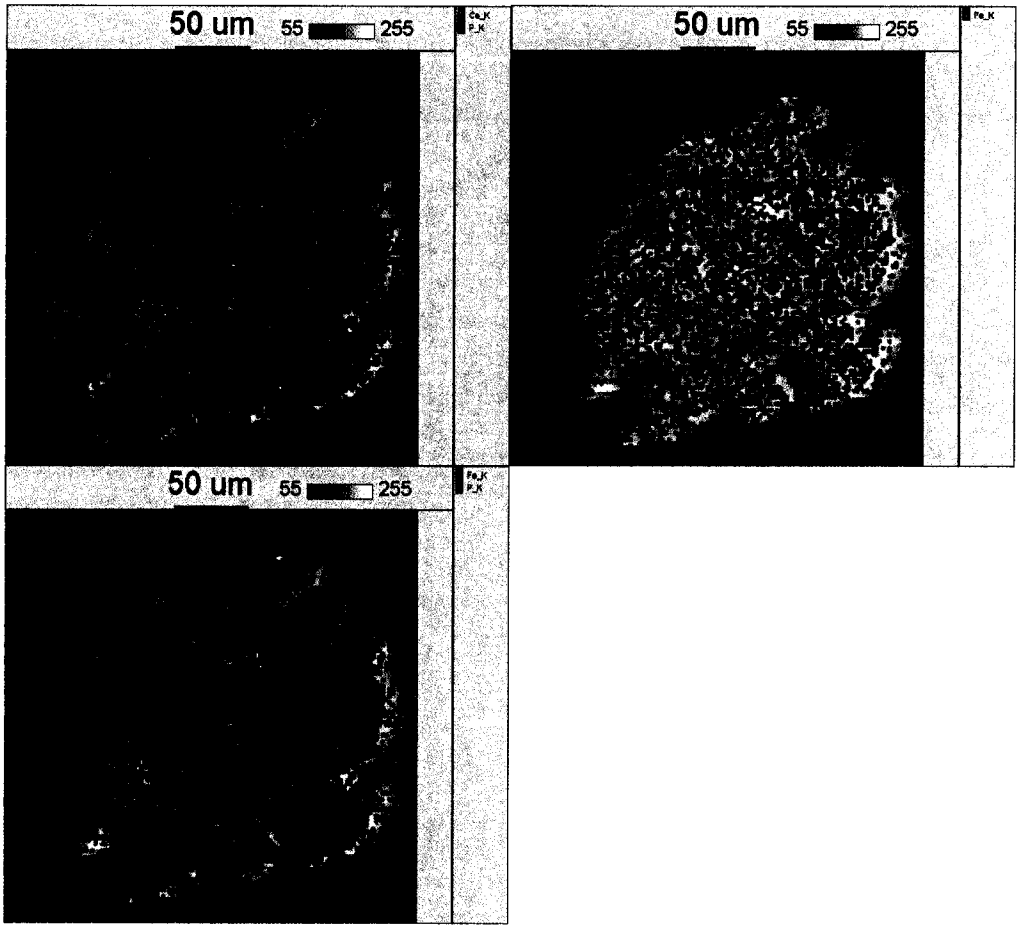

Figure 3.13c2. Water treatment residual overlay (500 mg L^{-1} P). Both individual and joint element maps are presented. A map that shows a color that cannot be distinguished into its two elemental colors indicates an association between those elements.

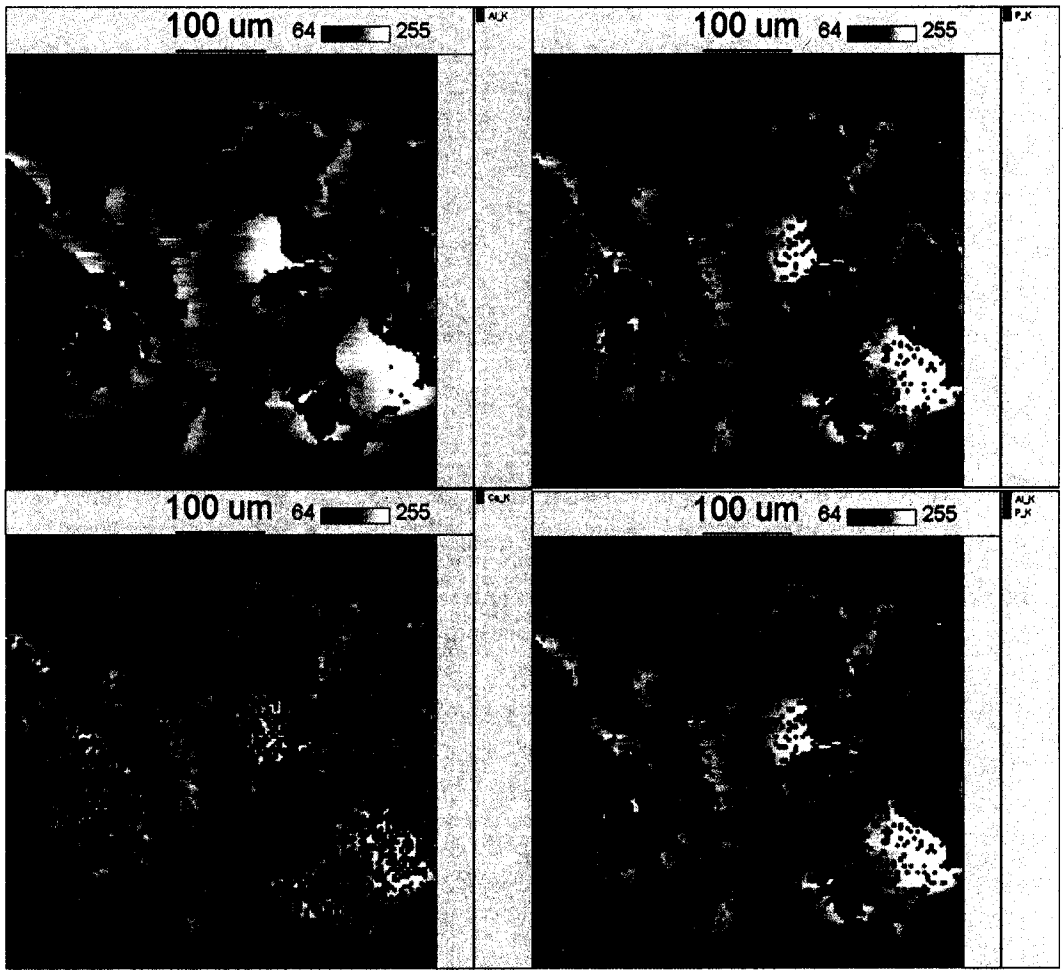

Figure 3.13d1. Water treatment residual overlay (1000 mg L^{-1} P). Both individual and joint element maps are presented. A map that shows a color that cannot be distinguished into its two elemental colors indicates an association between those elements.

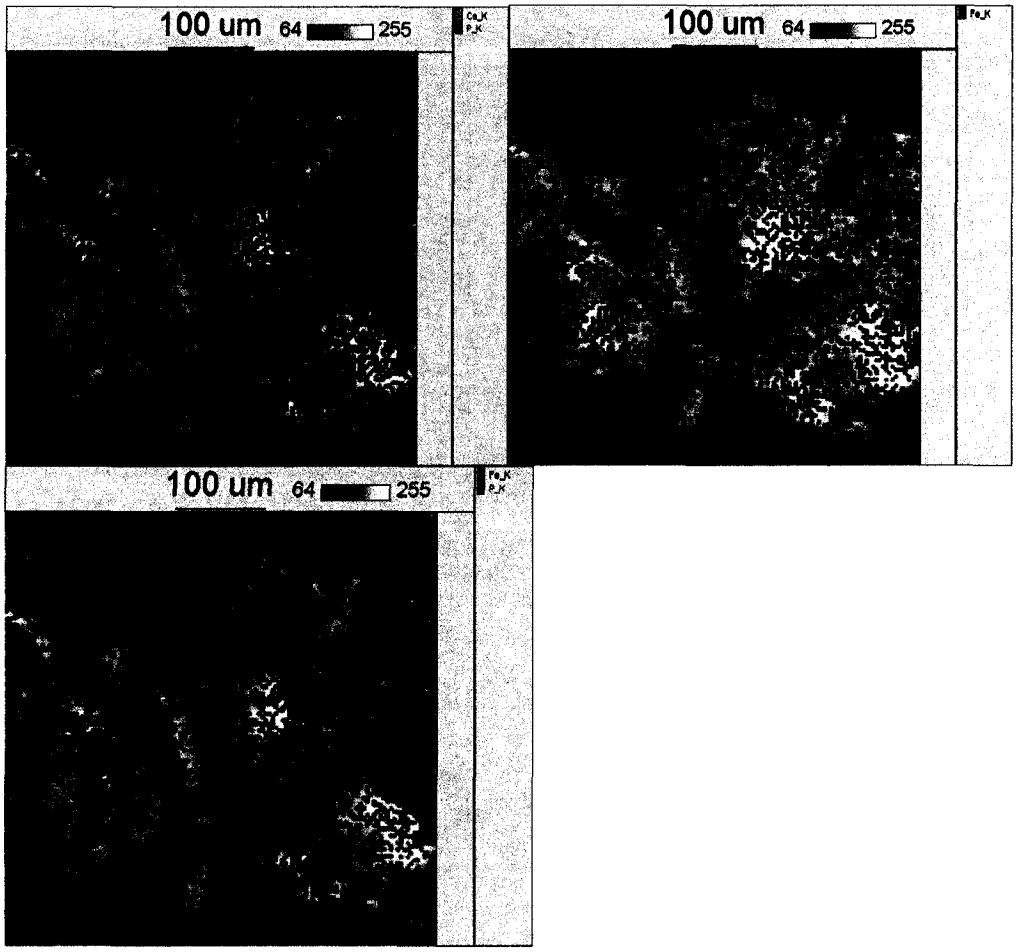

Figure 3.13d2. Water treatment residual overlay (1000 mg L^{-1} P). Both individual and joint element maps are presented. A map that shows a color that cannot be distinguished into its two elemental colors indicates an association between those elements.

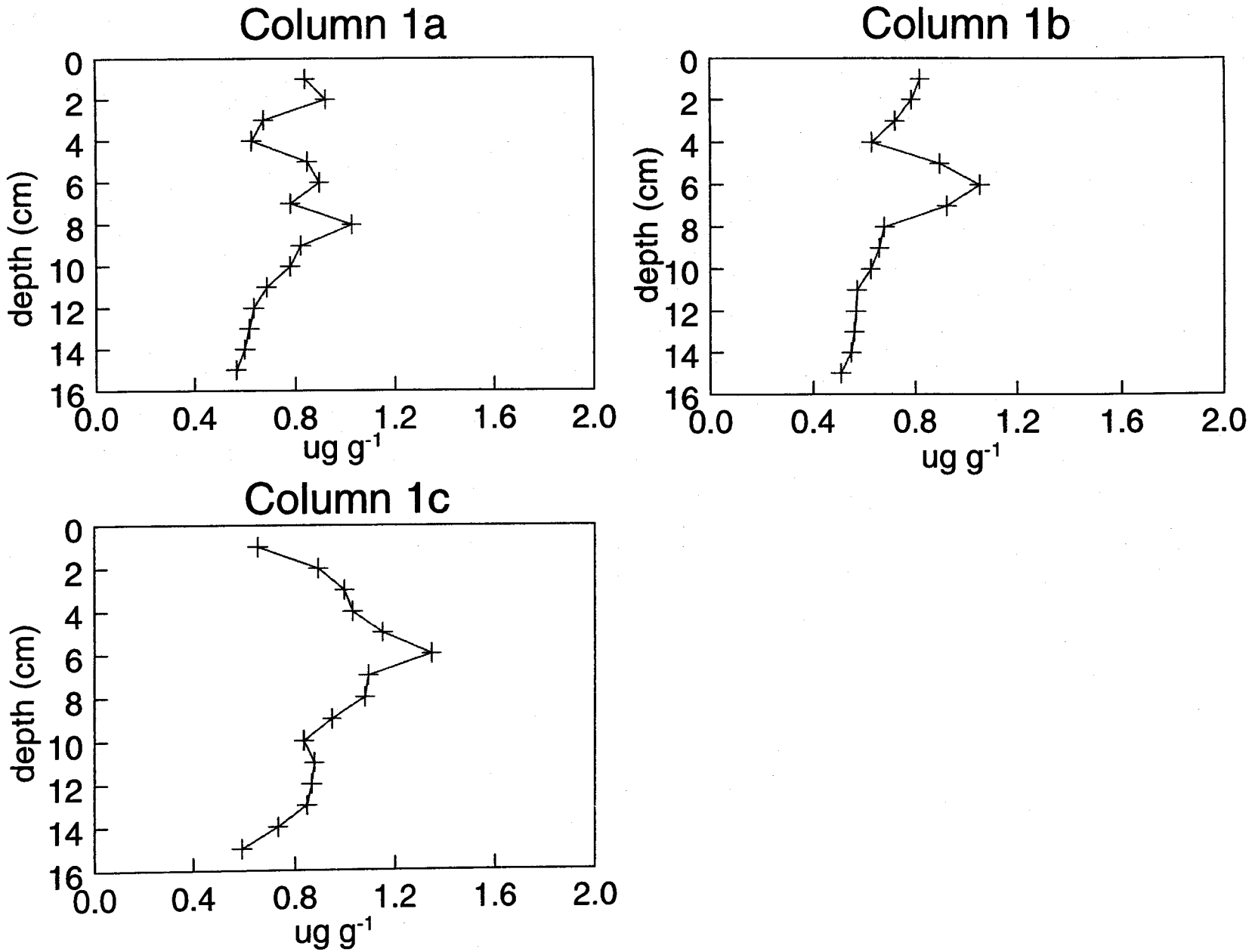

Figure 3.14. Untreated column soil molybdate reactive phosphorus.

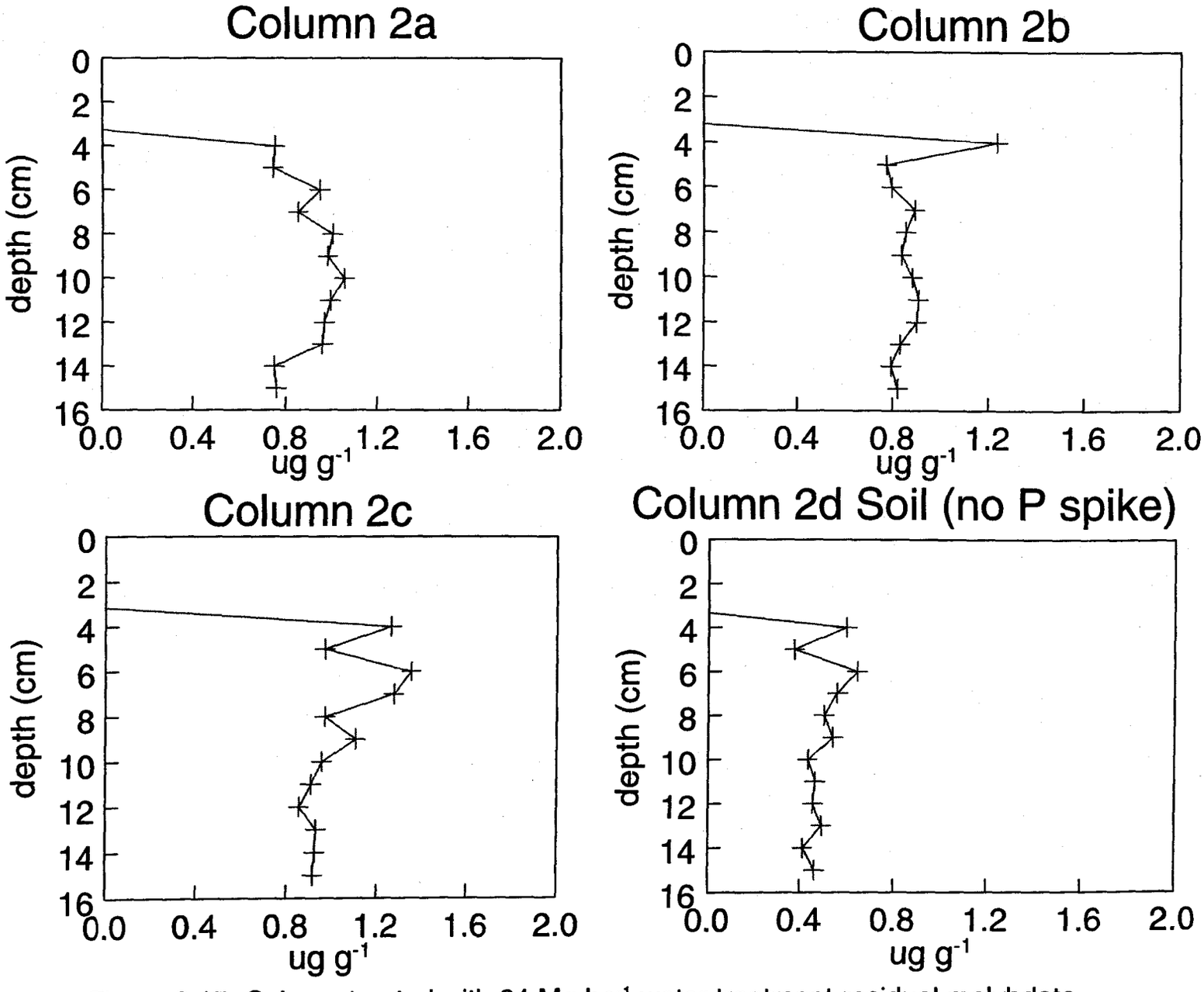

Figure 3.15. Column treated with 64 Mg ha^{-1} water treatment residual molybdate reactive phosphorus concentrations with depth.

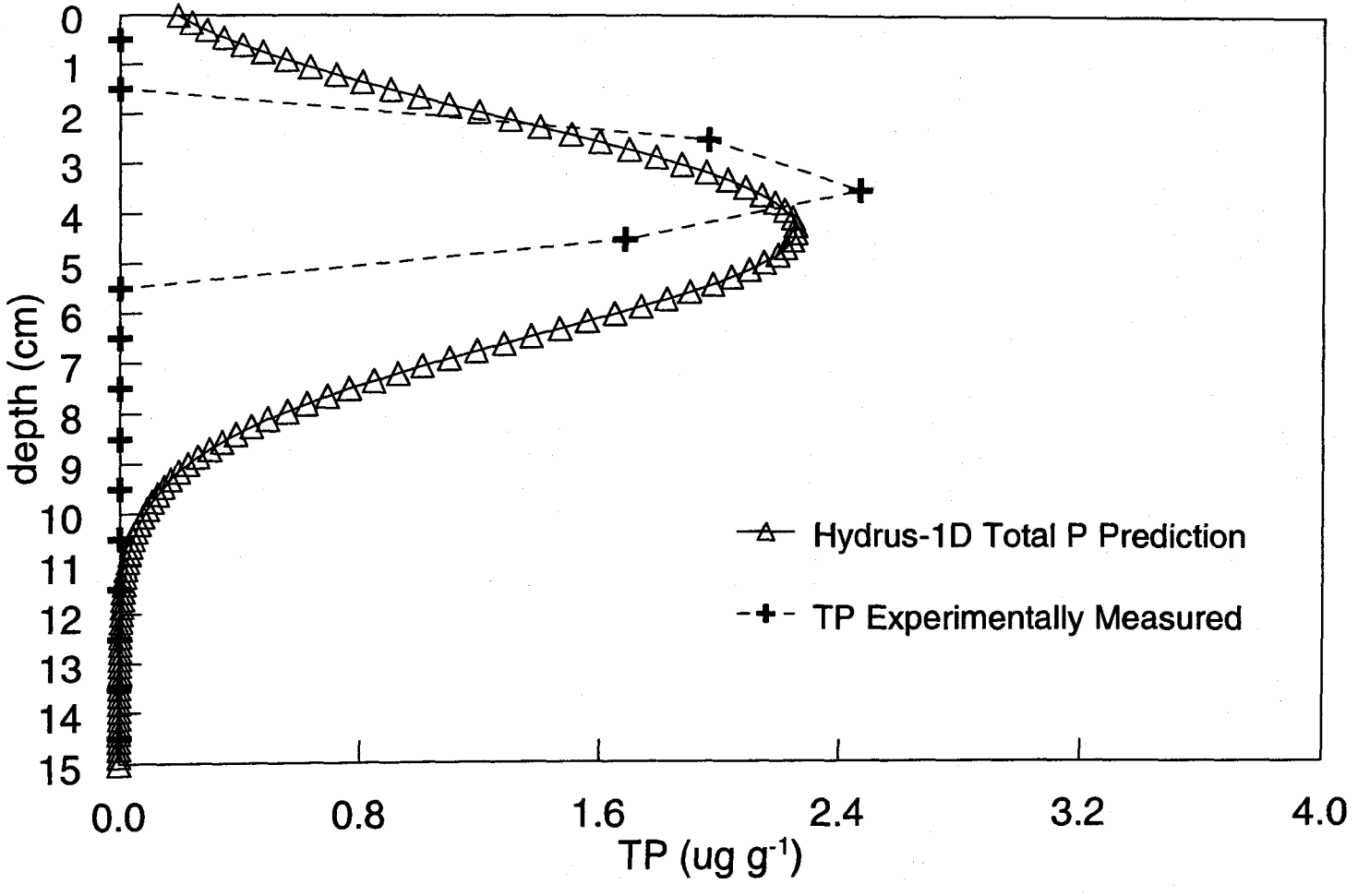

Figure 3.16. Untreated soil column with background total phosphorus concentration removed.

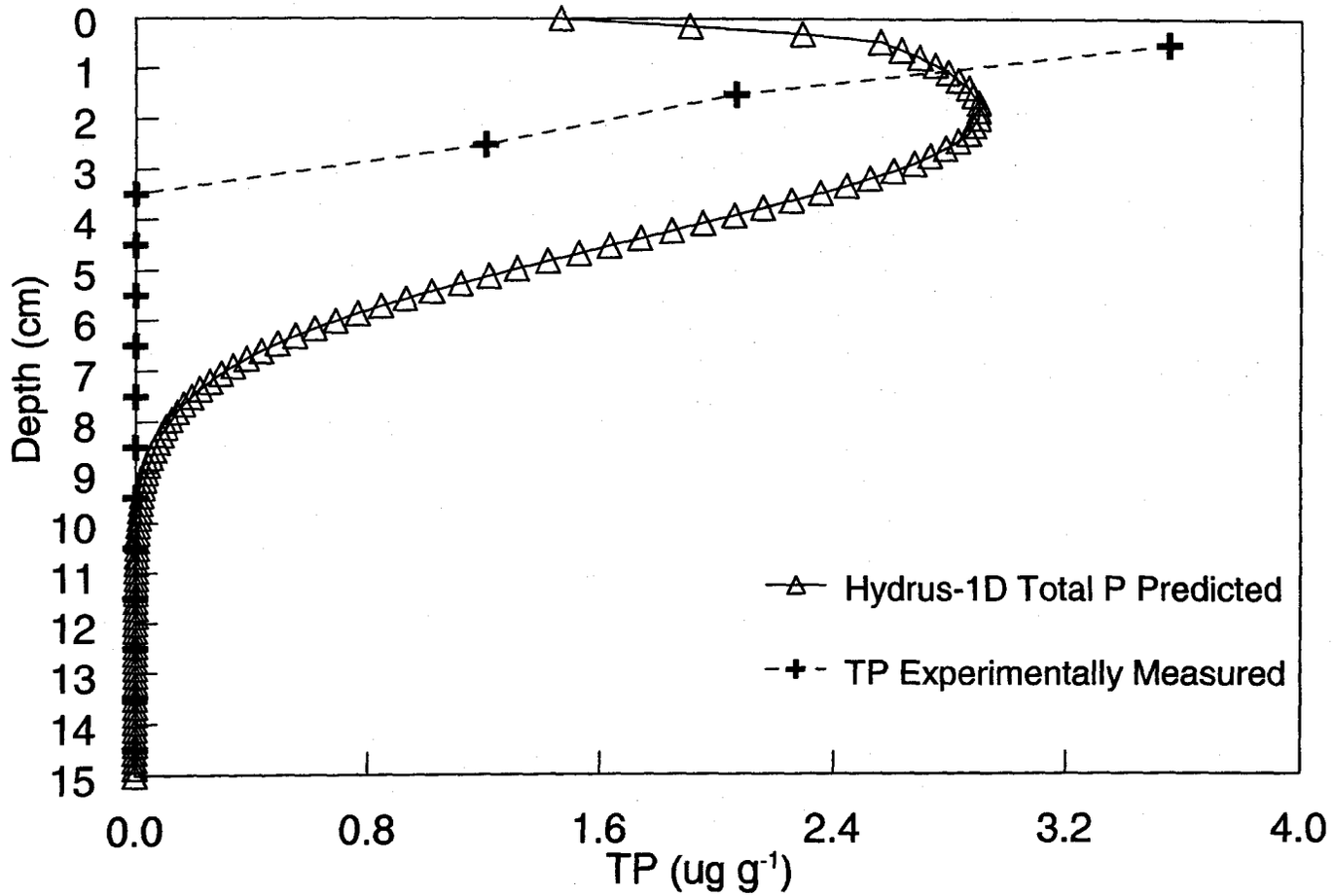

Figure 3.17. Column with 64 Mg ha^{-1} water treatment residual with background total phosphorus concentration removed.

Table 3.1. Molybdate reactive phosphorus in column leachate.
1 pore volume=1040 mL

Column & Hours	mL Leached	P conc (mg L^{-1})	Cumulative Volume Leached (mL)
Soil Col1a-0	3200	0.001558	3200
24	3000	0.002174	6200
48	2900	0.002864	9100
72	2600	0.003014	11700
96	800	0.002544	12500
Soil Col1b-0	250	0.001415	250
24	2000	0.002072	2250
48	2150	0.002784	4400
72	3250	0.002944	7650
96	2100	0.002514	9750
120	2500	0.002126	12250
Soil Col1c-0	1450	0.001628	1450
24	1750	0.002177	3200
48	3100	0.002894	6300
72	2500	0.003054	8800
96	1250	0.002564	10050
120	2300	0.002216	12350
Soil & WTR Col2a-0	1800	0.005715	1800
24	950	5.30E-03	2750
48	2450	0.005174	5200
72	3000	0.001443	8200
96	2250	2.18E-05	10450
120	2250	2.13E-05	12700
144	2150	2.17E-05	14850
Soil & WTR Col2b-0	1550	0.005612	1550
24	2825	0.005401	4375
48	2850	0.005189	7225
72	2750	0.001321	9975
96	2600	2.22E-05	12575
120	2700	2.21E-05	15275
Soil & WTR Col2c-0	1000	0.005428	1500
24	500	0.005445	4000
48	800	0.005294	7925
72	750	0.001619	10100
96	550	2.23E-05	12400
120	400	2.10E-05	12800
144	270	2.01E-05	13070

Chapter IV

Conclusions

The preceding chapters identified the impact of vegetative filter strips (VFSs) and water treatment residuals (WTRs) on surface transport of soluble P. Experiments were conducted to determine i) if a WTR application rate for maximum P sorption could be identified, ii) if WTR applied to the soil surface at a potentially beneficial rate would retain more P and leach less P than the soil alone, iii) if the HYDRUS-1D model can predict total soil and WTR P transport, iv) if electron microprobe analysis using wavelength dispersive spectroscopy (EMPA-WDS) could identify P-Al complexes differently for various soluble P concentrations and, v) if the Opus2Z model could improve the understanding of how VFSs and WTRs impact TP transport in the interaction of surface water and soil water.

The greenhouse experiment incorporated the effects of WTR and VFS on soluble P surface transport while a laboratory column experiment analyzed effluent and soil P concentrations from a vertical standpoint. With model components fit to the conditions under which the column experiment occurred, the HYDRUS-1D model prediction was measured against experimental data. Additional soil and WTR characterizations in conjunction with soluble P provided insight as to what can be expected from their interactions. The EMPA-WDS images elucidated how P associates with a soil particle at varying soluble P concentrations. Finally, a sensitivity analysis of the Opus2Z model was performed to improve the understanding of how VFSs and WTRs impact TP surface transport including the interaction of soil water and surface water. Altogether, greenhouse and laboratory experiments and model simulations provided an understanding of how VFSs and WTRs affect P transport.

The following major conclusions were reached. i) One WTR application rate for maximum P sorption could not be identified, however a continuous broadcast layer of WTR was found to significantly reduce effluent P. This conclusion was based on a greenhouse study in which six WTR application rates (0, 16, 32, 64, 128, and 256 Mg ha^{-1}) were applied in duplicate for an experiment that included VFSs established in constructed greenhouse boxes. Four runoff events occurred with the greenhouse VFS boxes. Molybdate reactive P (MRP) concentrations were measured in surface runoff for approximately one hour. Water treatment residual additions can decrease P runoff concentration compared to soil as evidenced by MRP experimental data. Molybdate reactive P runoff concentrations exhibited a decreasing trend from the control through the highest applied rate of WTR indicating that that a continuous WTR layer above the soil is necessary to significantly reduce runoff P. The 64, 128 and 256 Mg ha^{-1} WTR rates were not significantly different from each other in their MRP runoff concentrations. A likely explanation for this result is the depth of mixing for surface water and soil-water interaction. The effectiveness of WTR is only as pervasive as the depth at which the surface water and soil-water can interact, therefore, allowing P sorption to occur. Overall, the amount of fertilizer applied before the runoff events impacted this experiment more than the P input during the runoff events, as evidenced by no change in STP concentrations and model simulations.

ii) Water treatment residual applied to the soil surface at a potentially beneficial rate significantly retained more P where the WTR was located versus the columns without WTR. Neither treatment had MRP in its effluent. These conclusions were based on a laboratory column experiment to elucidate whether a WTR applied to the surface at

a potentially beneficial rate would retain more P and leach less P than the soil alone. Triplicate columns either had a WTR depth of three cm's or had the soil alone. Due to the WTR K_d of 161 L kg^{-1}, it was likely that the columns treated with WTR would retard P movement. Neither the column with WTR or without WTR had P in the effluent throughout the leaching of 12 pore volumes, as measured by the molybdate blue method. The 15-cm tall columns were divided into three zones for soil MRP analysis. The first zone (0-3 cm) was significantly different (α=0.01) between the two treatments. The second zone (5-9 cm) was not significantly different between treatments (α=0.10). The third zone (11-15 cm) was significantly different (α=0.01) between treatments. The soil with WTR applied on the surface had low MRP in the top 3 cm's and had higher concentrations from 4 to 15 cm. Due to the high K_d of the WTR and minimal propensity for desorption, the P was held tightly in the uppermost layers.

iii) The HYDRUS-1D model predictions for total soil and WTR P transport did not exactly fit the center of tendencies and distribution illustrated by the experimental data. The HYDRUS-1D model was used to determine if total soil and WTR P transport could be predicted. The experimental data from the columns (for both the columns with and without WTR) were used to compare the accuracy of the model predictions. The triplicate data from the columns, per treatment, were averaged when compared to the model predictions. The center of mass of the HYDRUS-1D prediction is deeper than that of the observed P (by about 2 cm for both the columns with and without WTR). The model prediction is also much more dispersed. In comparing positions of observed and predicted P, the model over predicts the P leaching, probably because the model does not account for the sorption-desorption hysteresis (that is, the sorption K_d used in the model

overestimates the ease of P desorption). The difference in area under the observed and predicted profiles is most likely attributed to error in the P measurement and uncertainty in the background concentration for the soil and WTR.

iv) Electron microprobe analysis using wavelength dispersive spectroscopy identified that P-Al complexes images were seemingly different for various soluble P concentrations. The scanning electron microscopy-electron dispersive spectroscopy (SEM-EDS) images show that P complexes to the perimeter of a particle at lower concentrations and to the interior and exterior of a particle at higher P concentrations. Previous research has identified that P was complexing with the Al-fraction of the WTR. With the SEM-EDS images showing that P resides in the interior of a particle at higher soluble P concentrations, it is likely that this P does not become resolubilized as readily as precipitated or sorbed P at the particle surface. The minimal P desorption results from the batch experiment discussed above indicate that since phosphate is tightly bound by Al^{3+}, the P in the interior of a particle most likely will become susceptible to dissolution if the particle's interior becomes exposed. The P adsorption-desorption isotherms from the batch experiments demonstrated that the P sorption process is hysteretic. From the P isotherms and SEM-EDS images, I would speculate that P dissolution kinetics is an extremely slow progression; only minimal P desorption was observed within the time frame of the batch experiment.

v) The Opus2Z model improved the understanding of how VFSs and WTRs impact TP transport in the interaction of surface water and soil water. This model elucidated that the bulk of the TP resided in the top 5-6 mm of WTR depth. Therefore, WTR rates applied to depths greater than 5-6 mm did not retain additional TP. From a

model sensitivity analysis of several components, the S_{max} , film diffusion coefficient, P fertilizer rate, and slope affected TP runoff concentrations. The variations in flow rates resulted in significantly different outflow start times. The Opus2Z model was especially helpful in its ability to simulate total mass leaving the VFS box. Being able to identify the P mass leaving a system would be helpful in determining P's impact on water quality. Although TP runoff concentrations were similar, the variation of the components would not have had the same impact on a water body. To accurately predict P transport, more experiments would be necessary to determine the dependence of P sorption on time. The fact that the experimental P ratio is generally less than 1.0 while the modeled ratio is greater than 1.0 is consistent with the occurrence of P adsorption within the aggregates and the observed sorption hysteresis. The model simulations were based on 24 h P sorption, where surface adsorption of P is likely the dominant process. However, over the time scale between addition of P fertilizer and the onset of the runoff experiments, P initially adsorbed at the surface may have migrated to the particles interior. This would effectively re-open potential sorption sites at the particles surface and allow for additional rapid adsorption to take place once the P influent solution was added.

It may be that there are rate effects in both the P sorption and desorption. From the batch studies, it would appear that P does not desorb within a 24-hour equilibration. The results of the leaching study, however, demonstrated that P desorption from WTR did occur otherwise the applied P would have remained in the upper 1 cm of the columns. Since the greenhouse VFS boxes had extensive times for P equilibration, it is reasonable to conclude that some P desorption and leaching did occur in the boxes allowing for additional sorption capacity at the soil surface.

Determining whether WTR broadcast applied to soils and with VFSs allowed to establish in them has created a possibility for the reduction of overland flow P transport. The combination of these conservation measures provides the opportunity for a beneficial usage of WTRs rather than its disposal in landfills. The WTR contains Al that allows for P to be sorbed from the overland flow solution to the underlying particles. However, the effective depth of interaction between the soil-water and surface water limits the potential for P sorption. The VFSs impede the movement of sediment-laden P as demonstrated by previous literature. The VFSs serve as flow paths for P to become sorbed to additional soil surfaces and could be cropped as a source as of hay.

The images produced by the SEM-EDS are in agreement with previous studies that speculate that P sorbs to the Al in the WTR. The HYDRUS-1D model simulations provided insight as to how well this model predicted vertical TP movement and that impact of surface applied WTR was significant in the reduction of P transport. The Opus2Z model simulation data allowed for the elucidation that a continuous coverage of WTR to a depth of at least 5-6 mm could significantly retard effluent TP transport and that the slope, film diffusion coefficient, and sorption capacity were important components affecting TP effluent concentrations.

The results of the HYDRUS-1D and Opus2Z model simulations differed from the greenhouse and laboratory experimental data possibly due to the models having the same isotherm for both the adsorption and desorption processes. Together soluble and sediment P can be reduced and therefore, VFS with surface application of WTR presents an alternative for nonpoint source P attenuation that can provide benefits to the agricultural producer.

References

Abbozzo, P., A. Boggia, and M. Brunetti. 1996. Environmental quality and hog production. Env. Monit. Assess. 41:171-182.

Ahuja, L.R. and S.A. El-Swaify. 1976. Determining both water characteristics and hydraulic conductivity of a soil core at high water contents from a transient flow experiment. Soil Sci. 121:198-204.

American Society of Civil Engineers and American Water Works Association. 1996. Management of water treatment plant residuals. New York.

American Water Works Association Sludge Disposal Committee. 1987. Committee Report. Research need for alum sludge discharge. J. AWWA. 79:6:99.

Atalay, A. 2001. Variation in phosphorus sorption with soil particle size. Soil and Sed. Contam. 10:317-335.

Bache, B.W. and E.G. Williams. 1971. Phosphate sorption index for soils. 1987. J. Soil Sci. 22:289.

Basta, N.T. and D. Storm. 1997. Use of alum residuals to reduce nutrient runoff from agricultural land treated with animal manures to protect surface water quality. *In*: Water residuals and biosolids management—Approaching the year 2000. Proceedings: Aug 3-6. Philadelphia, PA.

Bengston, L., P. Seuna, A. Lepisto, and R.K. Saxena. 1992. Particle movement of meltwater in a subdrained agricultural basin. J. Hydrol. 135:383-398.

Bennett, J.P. 1974. Concepts of mathematical modeling of sediment yield. Water Resour. Research. 10:485-592.

Bohn, H., B. McNeal, and G. O'Connor. 1985. Soil chemistry. 2nd ed. John Wiley & Sons, New York.

Brooks, R.H. and A.T. Corey. 1966. Properties of porous media affecting fluid flow. J. Irrig. Drainage Div., ASCE Proc. 72(IR2), 61-88.

Bugbee, G.J. and C.R. Frink. 1985. Alum sludge as a soil amendment: Effects on soil properties and plant growth. Conn. Agric. Exp. Stn. Bull. 827.

Burkholder, J.M., E.J. Noga, C.W. Hobbs, H.B. Glasgow, Jr., and S.A. Smith. 1992. New "phantom" dinoflagellates is the causative agent of major estuarine fish kills. Nature 358:407-410.

Burkholder, J.M., M.A. Mallin, H.B. Glasgow, L.M. Larsen, M.R. McIver, G.C. Shank, N. Melia-Deamer, D.S. Briley, J. Springer, B.W. Touchette, and E.K. Hannon. 1997. Impacts to a coastal river and estuary from rupture of a large swine waste holding lagoon. J. Environ. Qual. 26:1451-1466.

Butters, G.L. and P. Duchateau. 2002. Continuous flow method for rapid measurement of soil hydraulic properties: I. experimental considerations. Vadose Zone Journal 1:239-251.

Castro, B. and J. Torrent. 1998. Phosphate sorption by calcareous vertisols and inceptisols as evaluated from extend P-sorption curves. European J. of Soil Sci. 49:661-667.

Carignan, R. and J. Kalff. 1980. Phosphorus sources for aquatic weeds: Water or sediments? Science. 207:987-989.

Chapman, D.C. and R.I. Coombe. 1997. The Watershed Agricultural Program of the New York City Watersheds: People, Pathogens, and Phosphorus. Watershed Agricultural Council.

Daniel, T.C., A.N. Sharpley, J.L. Lemunyon. 1998. Agricultural phosphorus and eutrophication: a symposium overview. J. Environ. Qual. 27:251-257.

Dayton, E.A. and N.T. Basta. 2001. Characterization of drinking water treatment residuals for use as a soil substitute. Water Environ. Res. 73:52-57.

Dillaha, T.A., R.B. Reneau, S. Mostaghimi, and D. Lee. 1989. Vegetative filter strips for agricultural nonpoint source pollution control. Trans. ASAE 32:513-519.

Dillaha, T.A., J.H. Sherrard, D. Lee, S. Mostaghimi, and V.O. Shangoltz. 1988. Evaluation of vegetative filter strips as best management practices for feed lots. J. Water Pollut. Control Fed. 60:1231-1238.

Djodjic, F., L. Bergstrom, B. Ulen, and A. Shirmohammadi. 1999. Mode of transport of surface-applied phosphorus-33 through a clay and a sandy soil. J. Environ. Qual. 28:1273-1282.

Dorioz, J.M., E.A. Cassell, A. Orand, and K.G. Eisenman. 1998. Phosphorus storage, transport, and export dynamics in the Foron River watershed. Hydrol. Process. 12:285-309.

Duda, A.M. and D.S. Finan. 1983. Influence of livestock on nonpoint source nutrient levels of streams. Trans. ASAE. 26:1710-1716.

Durrera, M. and W.P. Robarge. 1999. Soil characteristics and management effects on phosphorus sorption by highland plateau soils of Ethiopia. Soil Sci. Soc. Am. J. 63:1455-1462.

Duxbury, J.M. and J.H. Peverly. 1978. Nitrogen and phosphorus losses from organic soils. J. Environ. Qual. 7:566-570.

Edwards, D.R. and T.C. Daniel. 1993. Runoff quality impacts of swine manure applied to fescue plots. Trans. ASAE. 36:81-86.

Elliott, H.A. and B.A. Dempsey. 1991. Agronomic effects of land application of water treatment sludges. J.Am.Water Works Assoc., 84, 3, 126.

Elliott, H. A., B. A. Dempsey, D.W. Hamilton, and J.R. Wolfe. 1990. Land application of water treatment sludges: Impacts and management. AWWA Research Foundation and American Water Works Association. Denver, CO.

Elliott, H.A. and L.M. Singer. 1988. Effect of water treatment sludge on growth and elemental composition of tomato (*Lycopersicon esculentum*) shoots. Commun. Soil Sci. Plant Anal. 19:345-354.

Erickson, G.E., T.J. Klopfenstein, C.T. Milton, D. Brink, M.W. Orth, and K.M. Whittet. 2002. Phosphorus requirement of finishing feedlot calves. J. Animal Sci. 80:1690-1695.

Fasching, R.A. and J.W. Bauder. 2001. Evaluation of agricultural sediment load reductions using vegetative filter strips of cool season grasses. Water Env. Res. 73:590-596.

Fortenberry, A.D., B. Gartside, and J. Hoelscher. 1994. Land application of water treatment residuals. Misc. Publ. Beaver Water District, Lowell, AR.

Freese, D., S.E.A.T.M. van der Zee, and W.H. van Riemsdijk. 1992. Comparison of different models for phosphate sorption as a function of the iron and aluminum oxides of Soils. J. Soil Sci. 43:729-738.

Gachon, L. 1969. Les methods d'appreciation de la fertilite phosphorique des sols, Bull. Assoc. Fr. Etude. Sol, 4, 17.

Gallimore, L.E., N.T. Basta, D.E. Storm, M.E. Payton, R.H. Huhnke, and M.D. Smolen. 1999. Water treatment residual to reduce nutrients in surface runoff from agricultural Land. J. Environ. Qual. 28:1474-1478.

Galarneau, E. and R. Gehr. 1997. Phosphorus removal from wastewaters: Experimental and theoretical support for alternative mechanisms. Water Res. 31:328-338.

Gaur, A.C. 1969. Studies on the Availability of phosphate in soil as influenced by humic acid. Agrochimica. 14:62-65.

Gburek, W.J. and A.N. Sharpley. 1998. Hydrologic controls on phosphorus loss from upland agricultural watersheds. J. Environ. Qual. 27:267-277.

Gburek, W.J. and H.B. Pionke. 1993. Analyzing the short-term reduction in streamflow pH resulting from acidic precipitation. Hydrol. Sci. J. 38:497-518.

Geertsema, W.S., W.R. Knocke, J.T. Novak, and D.Dove. 1994. Long-term effects on sludge application to land. J. AWWA. 86:11:64.

Grobbelaar, J.U. and W.A. House. 1995. Phosphorus as a limiting resource in inland waters: interaction with nitrogen. *In:* H. Tiessen (ed.) Phosphorus in the Global Environment: Transfers, Cycles and Management. John Wiley & Sons, New York. pp. 255-276.

Haustein, G.K., T.C. Daniel, D.M. Miller, P.A. Moore, Jr., and R.W. McNew. 2000. Aluminum-containing residuals influence high-phosphorus soils and runoff water quality. J. Environ. Qual. 29:1954-1959.

Havis, R.N., R.E. Smith, and D.D. Adrian. 1992. Partitioning solute transport between infiltration and overland flow under rainfall. Water Resour. Res. 28:2569-2580.

He, Z.L., A.K Alva, D.V. Calvert and D.J. Banks. 1999. Effects of leaching solution properties and volume on transport of metals and cations from a riviera fine sand. J. Envron. Sci. Health. 35:981-998.

He, Z.L., Z.X. Zhu, K.N. Yuan, and C.Y. Huang. 1988. Potential phosphate sorptivity value for Langmuir equation and its application for phosphate fertilizer recommendation. Acta Petrol. Sin. 25:397-403.

Heckrath, G., P.C. Brookes, P.R. Poulton, and K.W.T. Goulding. 1995. Phosphorus leaching from soils containing different phosphorus concentrations in the Broadbalk experiment. J. Environ. Qual. 24:904-910.

Heil, D.M. and K.A. Barbarick. 1989. Water treatment sludge influence on the growth of sorghum-sudangrass. J. Environ. Qual. 18:292-298.

Holford, I.R.C. 1979. Evaluation of soil phosphate puffering indices. Aust. J. Soil Res. 17:495-504.

Hsu, P.H. 1964. Adsorption of phosphate by aluminum and iron in soils. Soil Sci. Soc. Am. Proc. 28:474.

Hsu, P.H. 1976. Comparison of iron(III) and aluminum in precipitation of phosphate from solution. Water Res. 10:903.

Ippolito, J.A. 2001. Phosphorus adsorption/desorption of water treatment residuals and biosolids co-application effects. Ph.D. Dissertation. Colorado State Univeristy.

Ippolito, J.A., K.A. Barbarick, D.M. Heil, J.P. Chandler, and E.F. Redente. 2003. Phosphorus retention mechanisms of a water treatment residual. J. Environ. Qual. 32:1857-1864.

Ippolito, J.A., K.A. Barbarick, E.F. Redente. 1999. Co-application effects of water treatment residuals and biosolids on two range grasses. J. Environ. Qual. 28:1644-1650.

King, L.D., J.C. Burns, and P.W. Westerman. 1990. Long-term swine lagoon effluent applications on coastal bermudagrass. II. effect on nutrient accumulation in soil. J. Environ. Qual. 19:756-760.

Kumar, V. 1994. Identification of residual P compounds in fertilized soils using density fractionation, x-ray diffraction, scanning and transmission electron microscopy. Fert. Res. 32:133-149.

Kuo, S. 1996. Phosphorus. *In:* Methods of soil analysis. Part 3. Chemical Methods. D.L. Sparks et al., Ed. Soil Science Society of America, Inc. American Society of Agronomy.

Lemunyon, J.L. and R.G. Gilbert. 1993. The concept and need for a phosphorus assessment tool. J. Prod. Agric. 6:483-486.

Lindsay, W.L. 1979. Chemical equilibria in soils. John Wiley & Sons, New York.

Magette, W.L., R.B. Brinsfield, R.E. Palmer, and J.D. Wood. 1986. Vegetated filter strips for nonpoint source pollution control – nutrient considerations. *In:* Proceedings from summer meeting ASAE. San Luis Obispo, CA.

Magette, W.L., R.B. Brinsfield, R.E. Palmer, and J.D. Wood. 1989. Nutrient and sediment removal by vegetated filter strips. Trans. ASAE 32:663–667.

Mansell, R.S., H.M. Selim, P. Kanchanasut, J.M. Davidson, and J.G.A. Fiskell. 1977. Experimental and simulated transport of phosphorus through sandy soils. Water Resour. Res. 13: 189-194.

Mansell, R.S., S.A. Blooom, and B. Burgoa. 1991. Phosphorus transport with water flow in acid, sandy soils. *In:* B.Jacob and M.Y. Corapciogla (eds.) Transport Process in Porous Media. Kluwer Academic Publ. Dorecht, the Netherlands. 271-314.

Miller, M.H. 1979. Contribution of nitrogen and phosphorus to subsurface drainage water from intensively cropped mineral and organic soils in Ontario. J.Environ. Qual. 8:42-48.

Moore, P.A., Jr., and D.M. Miller. 1994. Decreasing phosphorus solubility in poultry litter with aluminum, calcium, and iron amendments. J. Environ. Qual. 23:325-330.

Murphy, J. and J.P. Riley. 1962. A modified single solution method for the determination of phosphate in natural waters. Anal. Chim. Acta. 27:31-36.

Nair, V.D., D.A. Graetz, and K.R. Reddy. 1998. Dairy manure influences on phosphorus retention capacity of Spodosols. J. Environ. Qual. 27:522-527.

Novak, J.T., W.R., Knocke, W. Geertsema, D.Dove, A. Taylor, and R. Mutter. 1995. Long-term impacts on water quality and forest soils. *In*: An assessment of cropland application of water treatment residuals. Am. Water Works Assoc. Res. Found., Am. Water Works Assoc., Denver, CO.

Nurnberg, G.K. and R.H. Peters. 1984. Biological availability of soluble reactive phosphorus in anoxic and oxic freshwaters. Can. J. Fish. Aquat. Sci. 41:757-765.

Parlange, J.Y. and R.E. Smith. 1978. Ponding time for variable rainfall rates. Can. J. Soil Sci. 56:121-123.

Parry, R. 1998. Agricultural phosphorus and water quality: a U.S. Enivornmental Protection Agency Perspective. J. Environ. Qual. 27:258-261.

Peters, J.M. and N.T. Basta. 1996. Reduction of excessive bioavailable phosphorus in soils by using municipal and industrial wastes. J. Environ. Qual. 25:1236-1241.

Pierzynski, G.M. (ed.). 2000. Methods for phosphorus analysis for soils, sediments, residuals and waters. Southern Cooperative Series Bulletin No. 396.

Pierzynski, G.M., T.J. Logan, S.J. Traina and J.M. Bigham. 1990a. Phosphorus chemistry and mineralogy in excessively fertilized soils: Quantitative analysis of phosphorus-rich particles. Soil Sci. Soc. Am. J. 54:1576-1583.

Pierzynski, G.M., T.J. Logan, S.J. Traina and J.M. Bigham. 1990b. Phosphorus chemistry and mineralogy in excessively fertilized soils: Descriptions of phosphorus-rich particles. Soil Sci. Soc. Am. J. 54:1583-1589.

Pote, D.H., T.C. Daniel, A.N. Sharpley, P.A. Moore, Jr., D.R. Edwards, and D.J. Nichols. 1996. Relating extractable soil phosphorus to phosphorus losses in runoff. Soil Sci. Soc. Am. J. 60:855-859.

Pote, D.H., T.C. Daniel, D.J. Nichols, A.N. Sharpley, P.A. Moore, D.M. Miller, and D.R. Edwards. 1999. Relationship between phosphorus levels in three ultisols and phosphorus concentrations in runoff. J. Environ. Qual. 28:170-175.

Reddy, M.D., I.K. Murthy, K.A. Reddy, and A. Venkatachari. 1980. Consumptive-use and daily evapo-transpiration of corn under different levels of nitrogen and moisture regimes. Plant and Soil. 56:143-147.

Rengasamy, P., J. M. Oades, and T.W. Hancock. 1980. Improvement of soil structure and plant growth by addition of alum sludge. Commun. Soil Sci. Plant Anal. 11:533-545.

Rhoades, J.D. 1982a. Soluble salts. *In:* A.L. Page, R.H. Miller, and D.R. Keeney (eds.). Methods of Soil Analysis, Part 2. Chemical and biological properties. 2nd ed. American Society of Agronomy, Madison. WI. pp. 1167-180.

Rhoades, J.D. 1982b. Soluble salts. *In:* A.L. Page, R.H. Miller, and D.R. Keeney (eds.). Methods of soil analysis, Part 2. Chemical and biological properties. 2nd ed. American Society of Agronomy, Madison. WI. pp. 149-157.

Richards, L.A. 1931. Capillary conduction of liquids in porous mediums. Physics. 1:318-333.

SAS Institute. 2003. SAS User Manual/Softaware Version 8e. Cary, NC.

Samadi, A. and R.J. Gilkes. 1999. Phosphorus transformations and their relationships with calcareous soil properties of southern western Australia. Soil Sci. Soc. Am. J. 63:809-815.

Satchell, M. 1996. Hog heaven-and-hell. U.S. News and World Report 120 (3):55-59.

Satchell, M. 1997. The cell from hell. U.S. News and World Report 123 (4):26-28.

Sawhney, B.L. 1973. Electron microprobe analysis of phosphates in soils and sediments. Soil Sci. Soc. Am. Proc. 37:658-660.

Schmitt, T.J., M.G. Dosskey, and K.D. Hoagland. 1999. Filter strip performance and processes for different vegetation, widths, and contaminants. J. Environ. Qual. 28:1479-1489.

Self, J. R. and J. B. Rodriguez. 1998. Soil and plant chemical analysis. Version 4. Soil, Water, and Plant Testing Laboratory, Dept. of Soil and Crop Sciences, Colorado State University.

Selim, H.M. and M.C. Amacher. 1997. Reactivity and transport of heavy metals in soils. CRC Press, San Diego, CA.

SERA17. 2001. National research project for simulating rainfall-surface runoff studies.

Schackellette, H.T. and J.G. Boerngen. 1984. Element concentration in soil and other surficial materials of the conterminous United States. U.S. Geological Survey. Professional Pater 1270. U.S. Gov. Printing Office, Washington, D.C.

Sharpley, A.N. 1995. Dependence of runoff phosphorus on extractable soil phosphorus. J. Environ. Qual. 24:920-926.

Sharpley, A.N. A.N. Paul, and J.A. Withers. 1994. The environmentally-sound management of agricultural phosphorus. Fert. Res. 39:133-146.

Sharpley, A.N. and J.K Syers. 1979. Loss of nitrogen and phosphorus in tile drainage as influenced by urea application and grazing animals. New Zealand J. Agric. Res. 22:127-131.

Shreve, B.R. , P.A. Moore, Jr., T.C. Daniel, D. R. Edwards, and D.M. Miller. 1995. Reduction of phosphorus in runoff from field-applied poultry litter using chemical amendments. J. Environ. Qual. 24:106-111.

Sims, J.T. 1992. Environmental management of phosphorus in agricultural and municipal wastes. *In:* F.J. Sikora (ed.) Future Directions for Agricultural Phosphorus Research. TVA Bulletin Y-224. Agricultural Research Department, National Fertility and Environmental Research Center, Muscle Shoals, AL.

Sims, J.T. (ed.). 1997. Soil testing for phosphorus: Environmental Uses and Implications. A publication of SERA-IEG 17 USDA-CREES Regional Committee: Minimizing Agricultural Phosphorus Losses for Protection of the Water Resource.

Sims, J.T. and B.G. Ellis. 1983. Changes in phosphorus adsorption associated with aging of aluminum hydroxide suspensions. Soil Sci. Soc. Am. J. 47:912-916.

Sims, J.T., R.R. Simard, and B.C. Joern. 1998. Phosphorus loss in agricultural drainage: historical perspective and current research. J. Environ. Qual. 24:267-276.

Simunek, J., M. Sejna and M. Th. Van Genuchten. 1998. The HYDRUS-1D software package for simulating the movement of water, heat, and multiple solutes in variably saturated media, software Version 7.0, manual Version 2.0, U.S. Salinity Laboratory, USDA, ARS, Riverside, CA.

Skene, T.M., J.M. Oades, and G. Kilmore. 1995. Water-treatment sludge-a potential plant-growth medium. Soil Use Manag. 11:29-33.

Smith, R.E. 1992. Opus: An integrated simulation model for transport of nonpoint-source pollutants at the field scale. Vol 1, Model Documentation. United States Department of Agriculture ARS-98.

Sparks, D.L. 1996. Environmental soil chemistry. 1st ed. Academic Press, New York.

Stumm, W. and J.J. Morgan. 1981. Aquatic Chemistry. John Wiley & Sons, New York.

Tate, K.W., G.A. Nader, D.J. Lewis, E.R. Atwill, and J.M. Connor. 2000. Evaluation of buffers to improve the quality of runoff from irrigated pastures. J. Soil and Water Conserv. 55:473-478.

Tisdale, S.L., W.L. Nelson, and J.D. Beaton. 1985. Soil Fertility and Fertilizers. 4th ed., MacMillan Publishing Company, New York.

Tunesi, S., V. Poggi, and C. Gessa. 1999. Phosphate adsorption and precipitation in calcareous soils: the role of calcium ions in solution and carbonate minerals. Nutr. Cyc. Agro. 53:219-227.

USDA-SCS. 1994. A Phosphorus Assessment Tool. Engineering Technical Note, Series 1901. South National Technical Center, Fort Worth, TX.

USEPA. 2001. Environmental Assessment of Proposed Revisions to the National Pollutant Discharge Elimination System Regulation and the Effluent Guidelines for Concentrated Animal Feeding Operations. EPA-821-B-01-001. Office of Water (4303)m Washington, DC.

van Genuchten, M. Th. 1980. A closed form equation for predicting hydraulic conductivity of unsaturated soils. Soil Sci. Soc. Am. J. 44:892-898.

Vyas, K.K. 1964. Availability and uptake of phosphorus by wheat under different moisture and organic matter levels. Curr. Sci. 33:756-757.

Young, R.A., T. Huntrods, and W. Anderson. 1980. Effectiveness of vegetative filter strips in controlling pollution from feedlot runoff. J. Environ. Qual. 9:483-487.

Table A1. Molybdate reactive phosphorus (MRP) concentration of the manifold output:input ratio per runoff event for the vegetative filter strip (VFS) experiment at various water treatment residual application rates. Replicate VFS box MRP values were averaged.

WTR rate 0 Mg ha^{-1}					WTR rate 16 Mg ha^{-1}				
time (min)	Runoff Event 1	Runoff Event 2	Runoff Event 3	Runoff Event 4	time (min)	Runoff Event 1	Runoff Event 2	Runoff Event 3	Runoff Event 4
0	0.96	0.83	0.72	0.97	0	0.72	1.08	1.03	0.92
0.5	0.92	0.76	0.69	0.93	0.5	0.64	1.05	0.93	0.90
1	0.91	0.94	0.65	0.93	1	0.65	0.94	1.01	0.89
1.5	0.91	0.78	0.57	0.92	1.5	0.77	0.75	0.98	0.92
2	0.87	0.91	0.65	0.90	2	0.68	0.78	0.98	0.87
2.5	0.92	1.02	0.74	1.00	2.5	0.69	1.06	0.98	0.92
3	1.00	0.73	0.69	0.92	3	0.69	0.97	0.99	0.94
3.5	0.98	0.92	0.69	0.93	3.5	0.69	1.01	0.95	0.94
4	0.98	1.02	0.85	0.96	4	0.70	0.98	1.00	0.93
4.5	0.98	1.03	0.74	0.98	4.5	0.75	0.94	1.01	0.88
5	0.92	0.95	0.73	1.00	6.5	0.69	1.02	0.94	0.89
7	0.87	0.85	0.75	0.93	8.5	0.78	0.96	1.00	0.86
9	0.89	0.95	0.79	0.89	10.5	0.75	0.93	0.98	0.93
11	0.92	1.05	0.72	0.94	12.5	0.85	0.99	1.01	0.97
13	0.82	0.82	0.72	0.98	14.5	0.66	0.88	1.10	0.93
15	0.86	0.84	0.95	0.94	16.5	0.94	0.89	0.93	0.95
17	0.95	0.90	0.94	0.97	18.5	0.75	0.83	1.04	0.95
19	1.06	0.81	0.97	0.97	20.5	0.75		1.08	0.93
21	1.06	0.97	0.94	0.99	22.5	0.79		1.05	0.97
23	1.03	0.84	0.84	0.98	24.5	0.82		1.03	0.97
25	0.96	0.95	0.70	0.93	26.5	0.98		1.02	0.96
27	0.95	1.06	0.76	0.95	28.5	0.80		1.01	0.95
29	0.92	1.01	0.77	0.96	30.5	0.83		1.07	0.94
31	0.94	0.90	0.76	0.96	32.5	0.92		0.99	0.98
33	1.05	1.03	0.84	0.96	34.5	0.85		1.00	0.98
35	1.08	0.99	0.82	0.95	39.5	0.89		1.08	0.97
40		0.90	0.76	0.97	44.5	0.87		0.91	0.98
45		0.92	0.76	0.97	49.5	0.92		0.97	0.99
50		0.91	0.75	0.93	54.5	0.88		0.98	0.99
55		0.97	0.69	0.97				0.99	0.99
60		0.99	0.96	0.93				0.98	1.03
input solution (mg P L^{-1})	9.80	10.10	9.90	10.00		9.80	10.10	9.90	10.00

Table A1. Molybdate reactive phosphorus concentration of the manifold output:input ratio ratio per runoff event for the vegetative filter strip (VFS) experiment at various water treatment residual application rates. Replicate VFS box MRP values were averaged.

WTR rate 32 Mg ha^{-1}					WTR rate 64 Mg ha^{-1}				
time (min)	Runoff Event 1	Runoff Event 2	Runoff Event 3	Runoff Event 4	time (min)	Runoff Event 1	Runoff Event 2	Runoff Event 3	Runoff Event 4
0	0.82	0.77	0.60	0.93	0	0.76	0.70	0.58	0.83
0.5	0.82	0.79	0.70	0.89	0.5	0.81	0.86	0.65	0.84
1	0.93	0.64	0.74	0.88	1	0.80	0.80	0.69	0.84
1.5	0.72	0.69	0.78	0.90	1.5	0.84	0.81	0.63	0.85
2	0.74	0.73	0.74	0.90	2	0.83	0.83	0.66	0.88
2.5	0.93	0.77	0.80	0.94	2.5	0.88	0.80	0.67	0.84
3	0.67	0.87	0.80	0.95	3	0.88	0.91	0.72	0.81
3.5	0.86	1.14	0.74	0.89	3.5	0.88	0.85	0.69	0.88
4	0.77	0.86	0.74	0.89	4	0.88	0.88	0.71	0.82
4.5	0.68	0.76	0.73	0.96	4.5	0.82	0.92	0.72	0.89
5	0.71	0.88	0.78	0.91	5	0.89	0.89	0.75	0.84
7	0.78	0.88	0.81	0.91	7	0.91	0.83	0.70	0.89
9	0.91	0.91	0.72	0.99	9	0.84	0.87	0.61	0.91
11	0.97	0.90	0.76	0.97	11	0.91	0.87	0.73	0.90
13	1.00	0.92	0.80	0.96	13	0.85	0.93	0.74	0.88
15	0.94	0.92	0.76	0.92	15	0.88	0.92	0.75	0.88
17	1.00	0.91	0.78	0.98	17	0.90	0.87	0.75	0.88
19	0.89	0.96	0.89	0.95	19	0.90	0.89	0.69	0.92
21	1.00	0.92	0.83	0.98	21	0.88	0.94	0.79	0.90
23	0.82	0.90	0.87	0.98	23	0.91	0.95	0.79	0.91
25	0.94	0.93	0.81	1.01	25	0.92	0.93	0.78	0.92
27	0.97	0.95	0.90	1.00	27	0.91	0.96	0.76	0.88
29	1.01	1.03	0.87	1.00	29	0.91	0.91	0.74	0.91
31	1.06	0.96	0.90	0.94	31	0.94	0.95	0.78	0.90
33	1.02	1.01	0.88	0.97	33	0.95	0.90	0.79	0.92
35	1.01	0.92	0.83	0.97	35	0.87	0.91	0.72	0.91
40	0.94	1.10	0.78	0.98	40	0.93	0.85	0.80	0.92
45	1.02	1.00	0.87	0.92	45		0.94	0.75	0.93
50	1.04	0.85	0.84	0.94	50		0.99	0.77	
55		1.02	0.88		55		0.95	0.81	
60		0.87	0.92		60		1.03	0.79	
					65		0.99		
					70		1.00		
					75		1.00		
input solution (mg P L^{-1})	9.80	10.10	9.90	10.00		9.80	10.10	9.90	10.00

Table A1. Molybdate reactive phosphorus concentration of the manifold output:input ratio ratio per runoff event for the vegetative filter strip (VFS) experiment at various water treatment residual application rates. Replicate VFS box MRP values were averaged.

WTR rate 128 Mg ha^{-1}					WTR rate 256 Mg ha^{-1}					
time (min)	Runoff Event 1	Runoff Event 2	Runoff Event 3	Runoff Event 4	time (min)	Runoff Event 1	time (min)	Runoff Event 2	Runoff Event 3	Runoff Event 4
0	0.74	0.81	0.66	0.90	0	0.60	0	0.88	0.93	0.84
0.5	0.70	0.74	0.74	0.94	2	0.67	0.5	0.88	0.88	0.87
1	0.68	0.77	0.63	0.92	4	0.80	1	0.93	0.99	0.84
1.5	0.76	0.69	0.71	0.93	6.5	0.82	1.5	0.88	0.88	0.86
2	0.71	0.76	0.66	0.92	8.5	0.83	2	0.89	0.88	0.88
2.5	0.91	0.70	0.64	0.93	10.5	0.78	2.5	0.85	0.96	0.92
3	0.89	0.73	0.71	0.99	12.5	0.80	3	0.88	0.88	0.92
3.5	0.81	0.76	0.68	0.92	14.5	0.71	3.5	0.81	0.84	0.9
4	0.83	0.74	0.69	0.96	16.5	0.73	4	0.81	0.83	0.89
4.5	0.76	0.73	0.72	0.96	18.5	0.75	4.5	0.84	0.92	0.87
5	0.76	0.74	0.70	0.99	20.5	0.81	5	0.9	0.89	0.85
7	0.77	0.75	0.72	1.02	22.5	0.79	7	0.87	0.84	0.91
9	0.81	0.81	0.65	1.02	24.5	0.77	9	0.96	0.88	0.91
11	0.77	0.81	0.75	0.98	26.5	0.76	11	0.91	0.82	0.93
13	0.81	0.81	0.77	1.04	32.5	0.81	13	0.93	0.88	0.89
15	0.77	0.82	0.76	1.08	37.5	0.77	15	0.96	0.91	0.94
17	0.82	0.82	0.78	1.10	42.5	0.75	17	0.97	0.92	0.94
19	0.82	0.87	0.75	1.06	47.5	0.76	19	0.86	0.81	0.89
21	0.79	0.81	0.72	0.96			21	0.88	0.92	0.89
23	0.87	0.84	0.75	1.05			23	1.04	0.92	0.95
25	0.81	0.84	0.77	1.04			25	0.94	0.89	0.95
27	0.84	0.86	0.76	0.99			27	1.15	0.88	0.92
29	0.86	0.75	0.78	1.04			29	1.03	0.92	0.96
31	0.83	0.85	0.79	1.01			31	1.04	0.89	0.92
33	0.87	0.87	0.79	0.97			33	0.92	0.93	0.94
35	0.90	0.91	0.75	1.07			35	0.97	0.85	0.92
40		0.88	0.74	0.93			40	0.96	0.92	0.98
45		0.91	0.82	0.93			45	0.96	0.94	0.92
50		0.86	0.79	0.95			50	0.93	0.91	0.92
55		0.88	0.76	0.98			55	0.9	0.93	0.92
60		0.93	0.70				60	1.05	0.98	0.83
65		0.92					65	1.13	0.93	
70		0.90					70	1.11	0.87	
							75	1.09		
							80	1.05		
input solution (mg P L^{-1})	9.80	10.10	9.90	10.00		9.80		10.10	9.90	10.00

Table A2. Vegetative filter strip (VFS) plant basal count for the 2 m by 0.5 m box. The plant basal count was measured every 2 cm for the 2 m length of the VFS box.

Water treatment residual application rate (mg ha^{-1})	Replicate	Plant basal count
0	1	30
0	2	27
0	1	27
0	2	40
16	1	30
16	2	33
16	1	31
16	2	28
32	1	28
32	2	29
32	1	30
32	2	31
64	1	35
64	2	32
64	1	31
64	2	36
128	1	34
128	2	32
128	1	29
128	2	33
256	1	27
256	2	31
256	1	26
256	2	30

Table A3. Greenhouse Vegetative Filter Strip Experiment Chronology

Time Frame	Activity
week 1	soil put into VFS boxes most of the WTR was applied to soil surface in their appropriate rates* soil allowed to settle in boxes
week 2	soil allowed to settle in boxes
week 3	VFS seeds were scattered to box surfaces remaining WTR was applied for completion of WTR rate required VFS boxes watered with soluble fertilizer in irrigation water approximately 2
week 4	times per week**
week 5	VFS boxes watered with soluble fertilizer in irrigation water approximately 2 times per week**
week 6	VFS boxes watered with soluble fertilizer in irrigation water approximately 2 times per week**
week 7	VFS boxes watered with soluble fertilizer in irrigation water approximately 2 times per week**
week 8	VFS boxes watered with soluble fertilizer in irrigation water approximately 2 times per week**
week 9	VFS boxes watered with soluble fertilizer in irrigation water approximately 2 times per week**
week 10	VFS boxes watered with soluble fertilizer in irrigation water approximately 2 times per week**
week 11	VFS boxes watered with soluble fertilizer in irrigation water approximately 2 times per week**
week 12	with the grasses established and maintained at a 15 cm height, the boxes were irrigated to maintain the plants and allow for additional soil settling
week 13	with the grasses established and maintained at a 15 cm height, the boxes were irrigated to maintain the plants and allow for additional soil settling
week 14	with the grasses established and maintained at a 15 cm height, the boxes were irrigated to maintain the plants and allow for additional soil settling
week 15	with the grasses established and maintained at a 15 cm height, the boxes were irrigated to maintain the plants and allow for additional soil settling
week 16	with the grasses established and maintained at a 15 cm height, the boxes were irrigated to maintain the plants and allow for additional soil settling
week 17	with the grasses established and maintained at a 15 cm height, the boxes were irrigated to maintain the plants and allow for additional soil settling
week 18	with the grasses established and maintained at a 15 cm height, the boxes were irrigated to maintain the plants and allow for additional soil settling
week 19	with the grasses established and maintained at a 15 cm height, the boxes were irrigated to maintain the plants and allow for additional soil settling
week 20	with the grasses established and maintained at a 15 cm height, the boxes were irrigated to maintain the plants and allow for additional soil settling

*not all the WTR for each rate was applied because the seeds would need to be covered to become established

** VFS boxes were irrigated until water leached underneath the boxes and runoff occurred at the end of the boxes (Chapter 2 contains total fertilizer applied)

Table A3. Greenhouse Vegetative Filter Strip Experiment Chronology

Time Frame	Activity
week 21	pre-runoff event soil and grass sampling, storage tank water sampled, runoff event 1 occurred for each WTR box, post-runoff event soil sampling
week 22	storage tank water sampled, runoff event 2 occurred for each WTR box, post-runoff event soil sampling
week 23	storage tank water sampled, runoff event 3 occurred for each WTR box, post-runoff event soil sampling
week 24	storage tank water sampled, runoff event 4 occurred for each WTR box, post-runoff event soil sampling